MR Jan. 1944

NATIONAL ADVISORY COMMITTEE FOR AERONAUTICS

WARTIME REPORT

ORIGINALLY ISSUED
January 1944 as
Memorandum Report

HIGH-SPEED AERODYNAMIC CHARACTERISTICS OF A FOUR-ENGINE BOMBER AIRPLANE AS DETERMINED FROM TESTS OF A 0.075-SCALE MODEL

By Robert H. Barnes

Ames Aeronautical Laboratory
Moffett Field, California

WASHINGTON

NATIONAL ADVISORY COMMITTEE FOR AERONAUTICS

MEMORANDUM REPORT

for the

Air Materiel Command, U. S. Army Air Forces

HIGH-SPEED AERODYNAMIC CHARACTERISTICS OF A FOUR-ENGINE BOMBER AIRPLANE AS DETERMINED FROM TESTS OF A 0.075-SCALE MODEL

By Robert H. Barnes

SUMMARY

Tests of the airplane model reported herein included investigations to determine the longitudinal stability and control, and the effects of various constituent parts or their modification on longitudinal stability and control, critical speed, and distribution of wing load. The changes in the model, made in attempts to improve longitudinal control and to increase critical speed, were addition of auxilliary control flaps on the lower surface of the wing, revision of windshield, increase in dimensions of outboard nacelles, and alteration in profile of wing leading edge. Deflection of the landing flaps a small amount was also tried as a means for improving the longitudinal control.

The results of the tests indicated:

1. Additional lift for recovery from high-speed dives may be obtained either by deflecting the landing flaps about 10° or by adding auxilliary control flaps.

2. None of the modifications tested increased the critical speed of the model.

3. In order to fly level at any altitude above 32,000 feet, the critical speed of the airplane will be exceeded.

INTRODUCTION

Tests of a 0.075-scale model of a four-engine bomber airplane were carried out in the Ames 16-foot high-speed wind tunnel at the request of the Army Air Forces.

The purposes of the tests were:

1. To investigate the longitudinal stability and proposed methods for improving longitudinal control at supercritical speeds

2. To find means of increasing the critical speed

3. To obtain data showing distribution of loads on the tail and wing

This report shows the results of force tests, pressure-distribution measurements, and wake surveys.

APPARATUS AND METHOD

Figure 1 is a three-view drawing of the model in its standard form. The principal dimensions and areas were as follows:

Model scale = 0.075 full scale
Wing area = 9.65 square feet
Wing span = 10.592 feet
Mean aerodynamic chord = 0.965 feet
Aspect ratio = 11.62
Taper ratio = 2.28
Tail length = 3.859 feet
Tail area (including elevators) = 1.896 square feet

The coordinates of the wing section are given in figure 2. The thickness ratio varied from 22 percent at the root to 9 percent at the tip. Pressure orifices were provided at ten stations on the wing, as shown in figure 3. The stabilizer section was symmetrical from 20 percent chord to the trailing edge. Forward of 20 percent chord, the mean camber line curved upward. The thickness ratio was 12 percent.

In addition to tests of the model in its standard form (fig. 1) tests were made to determine the effects of the following modifications:

1. Addition of auxiliary control flaps on the lower surface of the wing (figs. 4 to 6)

2. Revision of windshield (fig. 7)

3. Increase in dimensions of outboard nacelles with and without extensions of the wing trailing edge (fig. 8)

4. Alterations in profile of wing leading edge on partial or entire span (figs. 9 and 10)

The model was mounted on a three-strut support system as shown in figure 11.

The forces were measured by automatic balancing and recording scales. The static pressures were measured on multiple-tube manometers and were recorded photographically. Measurements of wake momentum were made by means of the rake of total-pressure tubes shown in figure 12.

SYMBOLS

The following symbols are used in this report:

q	dynamic pressure ($\frac{1}{2}\rho V^2$), pounds per square foot
V	velocity, feet per second
ρ	mass density, slugs per cubic foot
S	wing area, square feet
M.A.C.	mean aerodynamic chord, feet
α	corrected angle of attack
$\Delta\alpha$	angle-of-attack correction due to tunnel-wall effects and flow inclination
C_L	lift coefficient $\left(\frac{\text{lift}}{qS}\right)$
$C_{D_{gross}}$	drag coefficient $\left(\frac{\text{measured drag}}{qS} + \Delta C_D\right)$
ΔC_D	drag-coefficient correction due to tunnel-wall effects and flow inclination
$C_{m_{c/4}}$	pitching-moment coefficient about quarter point of the mean aerodynamic chord $\left(\frac{\text{pitching moment}}{qS \text{ M.A.C.}} + \Delta C_m\right)$

ΔC_m pitching-moment-coefficient correction due to tunnel-wall effects

S pressure coefficient $\left(\frac{\text{total pressure} - \text{local static pressure}}{q}\right)$

$\Delta H/q$ $\left(\frac{\text{total pressure in free stream} - \text{total pressure in wake}}{q}\right)$

M Mach number $\left(\frac{\text{free-stream velocity}}{\text{velocity of sound}}\right)$

RESULTS AND DISCUSSION

Correction of data.- The data were obtained for a speed range corresponding to Mach numbers from 0.22 to 0.775, and at angles of attack from -4° to 10°. Corrections were applied for the tunnel-wall effects and flow inclination. Tares were not evaluated because the main interest was in comparative values. The tunnel-wall corrections were computed by the method outlined in reference 1. The values of the flow inclination were determined by comparing the results of tests with the model mounted inverted and upright and were as follows:

Mach number	Flow inclination	
	Radians	Degrees
0.22 to 0.60	0.0027	0.15
.625	.0039	.22
.65	.0054	.31
.675	.0080	.46
.70	.0112	.64
.725	.0165	.95
.75	.0222	1.27
.775	.0280	1.61

The total corrections applied were as follows:

$\Delta\alpha = 0.353\ C_L + (\text{flow inclination in degrees})$

$\Delta C_D = 0.00616\ C_L^2 + C_L\ (\text{flow inclination in radians})$

$\Delta C_m = 0.0063\ C_L$

Longitudinal stability and control.- The variation of drag coefficient, angle of attack, and pitching-moment coefficient with the lift coefficient is shown in figures 13 and 14. Figure 13 is for the wing, nacelles, and fuselage; figure 14 is for the complete model, wing, nacelles, fuselage, and tail. Figure 15 shows the variation of the pitching-moment coefficient with Mach number at constant values of the lift coefficient for the complete model. These data provide a basis for the study of the longitudinal stability and control of the airplane.

The essential requirement for recovery from dives is to obtain enough lift to change the flight path. Ordinarily, such lift is derived from increasing the angle of attack by deflecting the elevators. However, if the elevators become difficult to move, unstable, or ineffective, it will be extremely difficult, if not impossible, to recover from a dive by this means. In such cases it would be advantageous if the desired lift could be obtained in some other way. Tests were made with the landing flaps deflected 10° to ascertain their utility for this purpose. The results are shown in figures 16 to 18.

Figure 16 shows that, for constant lift coefficient, landing flap deflection increases the pitching-moment coefficient. This would have the effect of shifting the pitching-moment curves of figure 14 along the $C_{m_{c/4}}$ axis in the positive direction an amount equal to the increment, and thus of increasing the lift coefficient corresponding to zero pitching-moment coefficient. It can be seen then, that if the airplane were initially balanced ($C_m = 0$) and if the control surfaces remained fixed, it would be balanced at a greater lift coefficient after the flaps were deflected. For example, at a Mach number of 0.75 the model balances at a lift coefficient of 0.37 with the flaps retracted and at 0.58 with the flaps deflected 10°, an increase of 0.21. Thus it appears that small landing flap deflections will result in extra lift needed for recovery from dives.

Tests were also made of auxiliary control flaps, having various chords, spans, chordwise locations, and deflections, to determine their usefulness for recovery from dives. The results are shown in figures 19 to 33. The effects of varying the chord and chordwise location are shown in figures 19 to 21 for flaps extending from the fuselage to the inboard nacelle and for a deflection of 45°. It is seen from figure 19 that for the small tapered flaps the forward position produces the greatest increment of pitching-moment coefficient for small lift coefficients and for Mach numbers

greater than approximately 0.6. With increasing lift coefficient, the increment due to these flaps becomes less, especially at low Mach numbers. Nevertheless, in the range of Mach numbers in which the flaps are most likely to be used, the forward position of the small tapered flap is the more effective. Figure 19 also shows that for the intermediate position the larger chord flaps are the most effective, approximately in proportion to the chord. It does not necessarily follow that this relationship will hold for still larger chords.

Figures 22 to 24(b) consist of a family of curves for two flaps which extend out to 60 percent of the wing span. The curves of figure 22 show, as do those of figure 19, that in general the forward flap location is better than the others. A comparison of figures 22 and 25 shows that increasing the flap span from 60 percent of the wing span to 97 percent does not appreciably increase the lift coefficient for balance. This comparison is shown more clearly by figure 28, which presents the characteristics of the model with three auxiliary flaps of varying span. It is seen that the optimum flap span is about 60 percent of the wing span, and that increase of the flap span beyond this does not provide enough additional lift to warrant it.

The effects of varying the flap deflection are shown by figures 31 to 33. A deflection of 22.5° is seen to be detrimental in all cases; whereas a deflection of 45° is beneficial. Although these data are for the small span flaps, it seems reasonable to assume that similar results would be obtained with larger span flaps.

Surveys of the wake in the region of the tail (see stations, fig. 3) were made for the wing with no auxiliary flaps, and for the wing with the small tapered 0.16 span flaps at the rear spar (fig. 5). During these surveys, the turrets and sighting domes (fig. 11) were in place, but it is believed that their effect on the wake was negligible. The results of the surveys are shown in figures 34 and 35.

Critical Mach number.– The pressure distribution over the wing is presented in figures 36(a) to 36(g) and 37(a) to 37(g) for the nacelles-off and nacelles-on conditions, respectively. In these figures, wherever the peak-pressure coefficient exceeded the critical value, the curve from that peak value to the next value which was less than the critical was drawn with a dotted line. This procedure was followed because the exact point of recovery, which is usually abrupt when passing from supersonic to subsonic local speeds, is not known.

Figures 38 and 39 show, for constant lift coefficients, the maximum pressure coefficients for the upper surface of the wing as functions of Mach number. Figure 38 is for station 35.64 on the bare wing, and figure 39 for station 25.45 when the nacelles are mounted. With the nacelles on, the maximum local velocities measured were at station 25.45. However, for the nacelles-off condition, the data for station 25.45 indicated that the maximum local velocity was at a chordwise location beyond the pressure orifices provided. Consequently, for nacelles off, the data of station 35.64 were used; it being assumed that since the stations were not far apart, there would be no significant difference between them in the chordwise distribution and magnitude of the local velocities on the bare wing. Figure 40 shows the variation with lift coefficient of the critical Mach number for these two stations. It is seen from this figure that for lift coefficients less than 0.44, the critical Mach number at the wing-nacelle juncture was increased by the nacelles. However, it was found that the nacelles had an insignificant effect on the local velocities at station 35.64. Consequently, the critical speed of the wing as a whole would be unchanged by the nacelles for lift coefficients less than 0.44. For greater lift coefficients, the critical Mach number of the wing was decreased by the addition of the nacelles. It must be remembered that the critical Mach number may have been lower at some point on the model where the pressures were not measured. Referring again to figure 40 it is seen that, in order to fly level at any speed whatsoever at altitudes above approximately 32,000 feet with a wing loading of 61.25 pounds per square foot, the critical speed of the airplane will be exceeded.

It is seen in figure 38, for wing station 35.64, that the maximum pressure coefficients continued to increase with Mach number until their critical values had been exceeded by 0.3 or more and until the corresponding critical Mach numbers had been exceeded by 0.06 or more. As the Mach number was further increased, the pressure coefficients decreased. In this range, the pressure coefficients correspond approximately to those derived for a local static pressure of 45 percent of the atmospheric pressure. A curve for such pressure coefficients is given. The pressures at station 25.45 (fig. 39), however, reached values as low as 35 percent of atmospheric pressure, but general agreement was lacking.

Figure 41 presents the pressure-distribution data for the leading-edge portion of the upper surface of the wing and for various cooling-flap deflections. The data are given for one station only (outboard juncture of inboard nacelle with wing)

as all the wing–nacelle junctures showed similar characteristics. In general, opening the cooling flaps decreased the pressure coefficients and consequently increased the critical Mach number. The first 2° of opening had the greatest effect and the effectiveness decreased for larger openings. This reduction in pressure coefficient was probably due to the formation of a region of separation next to the nacelles.

The effect of the cooling flaps on the minimum drag coefficient is shown in figure 42. At subcritical Mach numbers, the drag coefficient increased with flap opening, being doubled at 20°. At higher speeds, however, the drag coefficient was minimum for a flap opening of approximately 2°. At a Mach number of 0.775 the drag was the same for openings of 0° and of 10°, but was smaller for intermediate positions. At these higher speeds the drag was presumably decreased because of the greater critical speeds, which would result from lowering the maximum pressure coefficients, as shown in figure 41.

Pressure-distribution measurements were made on a revised windshield to determine its critical Mach number. The results, as presented in figure 43, show that the critical Mach number of this windshield is greater than that of the wing and nacelles. Force measurements showed no appreciable effect from the revised windshield. The data are therefore omitted.

The Army Air Forces requested that tests be made with larger outboard nacelles which are interchangeable with the inboard nacelles. In conjunction with these tests, the effect of a wing trailing–edge extension similar to that between the fuselage and inboard nacelles was determined. The results are presented in figures 44 to 46(c). The large outboard nacelles, as compared with the standard nacelles, decreased the pitching–moment coefficient for equal lift coefficients by approximately 0.01, and decreased the lift coefficient for equal angles of attack by approximately 0.02. However, when the trailing–edge extensions were added, the pitching–moment coefficient was essentially the same as with the small nacelles and the lift coefficient was increased. The addition of the nacelles, both with and without the trailing–edge extensions, changed the drag coefficient negligibly. It may therefore be assumed that the critical Mach number was practically unchanged.

In an attempt to increase the critical Mach number and decrease the drag at high angles of attack, the wing leading edge was modified, as shown in figures 9 and 10. Results of tests are shown in figures 47 to 54. The pitching–moment data, presented in

figure 47, indicate that no advantage is to be gained from any of these modifications, since the Mach number at which the pitching-moment coefficient begins to decrease is in no case greater. From the standpoint of drag, shown in figures 48(a) to 48(d), the extreme leading-edge droop was definitely detrimental throughout the Mach number range and none of the other leading-edge modifications decreased the drag except at Mach numbers above the critical. Figures 49 to 54 show typical pressure distributions for several angles of attack and Mach numbers. From these data it is seen that any increase of critical Mach number at high angles of attack which might be gained is so small as to be unimportant; whereas the critical Mach number at moderate angles of attack would definitely be decreased.

Loads on surfaces.- Owing to the fact that pressure orifices were not provided over the rear portion of the wing at enough wing stations, it was not possible to determine accurately the wing load distribution. However, a study of figures 36(a) to 36(g) and 37(a) to 37(g) does reveal some information regarding the variation of the load distribution with Mach number.

As the Mach number increases, the wing begins to lose lift over the inboard portion first. Inasmuch as the inboard sections of the wing are the thicker, it is to be expected that the compressibility effects would occur on these portions of the wing first.

Likewise a comparison of figures 36(a) and 37(a), for example, shows the effect of the nacelles on the local velocities. The nacelles increased the local velocities over the forward portion of the upper surface of the wing, but decreased them over the remaining portion. On the lower surface the nacelles caused increased local velocities, but did not change the character of the pressure distribution as they did on the upper surface. At low angles of attack the peak velocities on the upper surface were actually reduced by the presence of the nacelles. With increasing angle of attack, however, the maximum local velocities became pronounced and soon exceeded those for the wing without nacelles. The effect is seen in figure 40 by the reduction of the critical Mach number. Critical Mach number is defined as the free-stream Mach number at which the maximum local velocity over the wing is equal to the local velocity of sound.

CONCLUSIONS

The results of the tests indicate that:

1. Lowering the landing flaps 10° will provide additional lift for recovery from high-speed dives.

2. Auxiliary control flaps will provide additional lift. The optimum arrangement appears to consist of flaps on the lower surface at the forward spar of the wing, having a span 60 percent of the wing span and a deflection of 45°.

3. Addition of the nacelles lowers the critical speed for lift coefficients greater than 0.44.

4. The critical speed of the airplane will be exceeded in order to fly level at any speed whatsoever above approximately 32,000 feet altitude with a wing loading of 61.25 pounds per square foot.

5. Opening the cooling flaps decreases the pressure peaks at the wing-nacelle junctures. Deflections up to 2° do not materially increase the low-speed drag coefficient, and actually decrease the drag at high Mach numbers.

6. The critical Mach number of the revised windshield is greater than that of the wing and nacelles.

7. The large outboard nacelles in place of the standard outboard nacelles make no appreciable difference in the characteristics of the model.

8. The modified wing leading edges would not increase the critical Mach number appreciably at high angles of attack, while at low angles of attack they would decrease the critical Mach number.

Ames Aeronautical Laboratory,
National Advisory Committee for Aeronautics,
Moffett Field, Calif.

REFERENCE

1. Silverstein, Abe, and White, James A.: Wind-Tunnel Interference with Particular Reference to Off-Center Positions of the Wing and to the Downwash at the Tail. NACA Rep. No. 547, 1935.

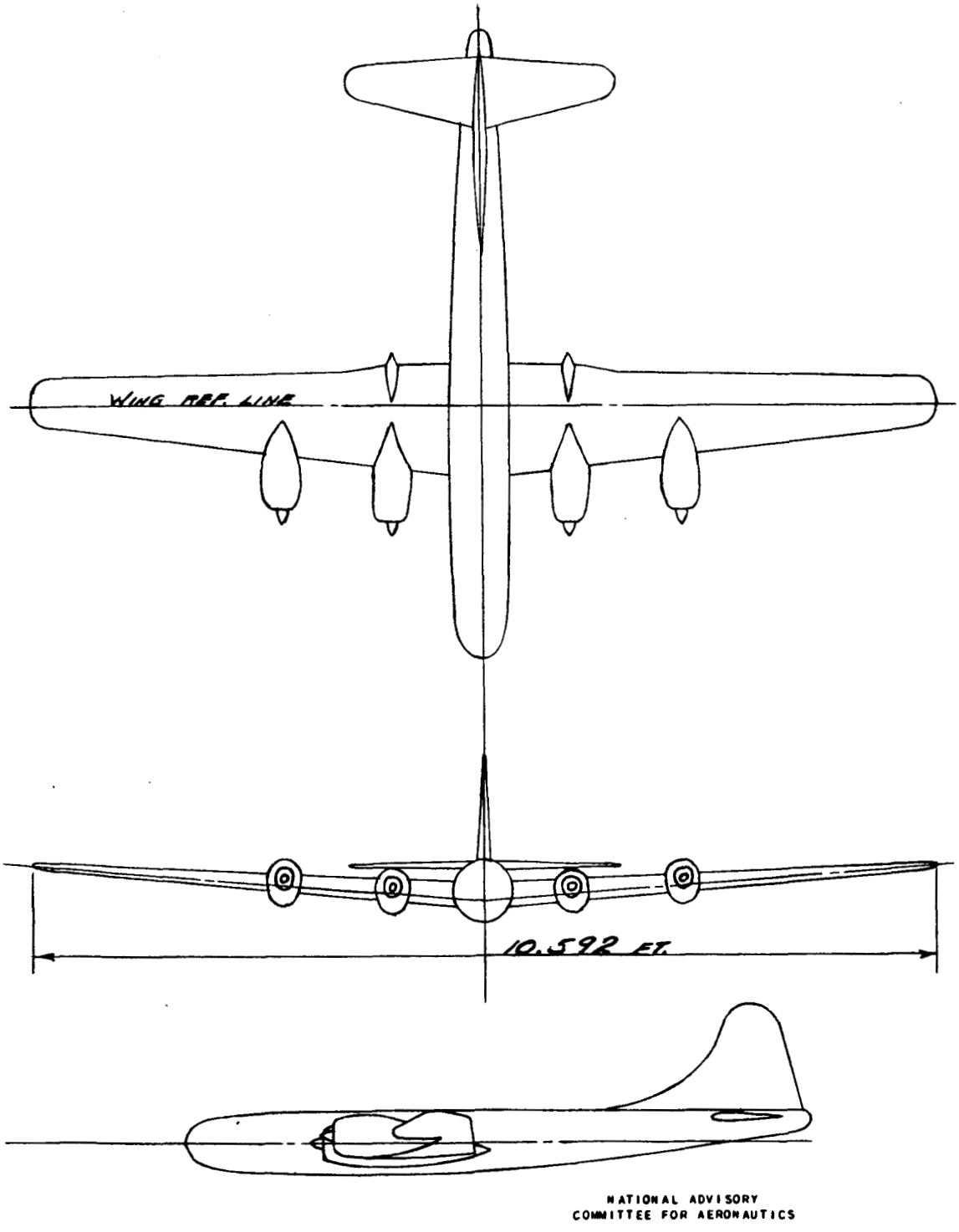

FIGURE 1.- THREE-VIEW DRAWING OF THE MODEL.

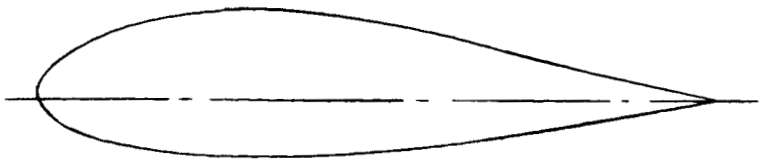

ROOT SECTION

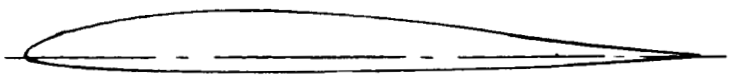

TIP SECTION

COORDINATES IN PERCENT CHORD

	ROOT SECTION		TIP SECTION	
STA.	UPPER ORD.	LOWER ORD	UPPER ORD	LOWER ORD.
0	1.82	0	0.36	0
0.5	2.94	1.11	1.08	0.54
0.75	3.33	1.48	1.30	0.67
1.25	3.98	2.09	1.65	0.84
2.5	5.24	3.19	2.33	1.13
5.0	7.00	4.54	3.29	1.45
7.5	8.33	5.45	4.03	1.62
10	9.42	6.14	4.63	1.74
15	11.10	7.17	5.58	1.90
20	12.31	7.90	6.27	2.00
25	13.07	8.36	6.72	2.05
30	13.44	8.57	6.93	2.07
40	13.15	8.46	6.76	2.09
50	11.82	7.85	5.95	2.10
60	9.76	6.89	4.77	2.04
70	7.26	5.62	3.40	1.88
80	4.66	4.09	2.04	1.54
90	2.18	2.26	0.85	0.95
95	1.04	1.18	0.38	0.54
100	0	0	0	0

NATIONAL ADVISORY
COMMITTEE FOR AERONAUTICS

FIGURE 2.- COORDINATES OF THE WING SECTION.

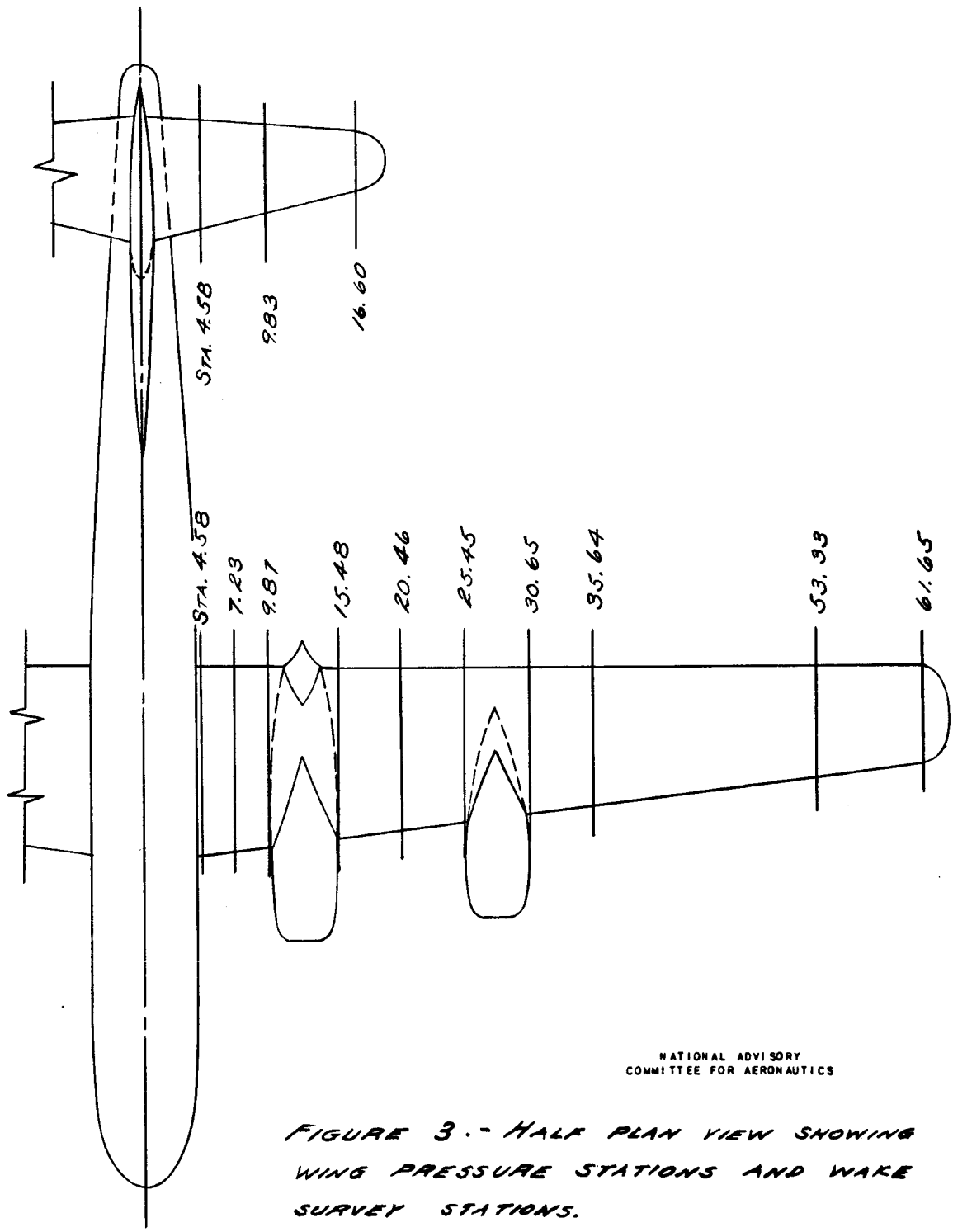

NATIONAL ADVISORY
COMMITTEE FOR AERONAUTICS

FIGURE 3.- HALF PLAN VIEW SHOWING WING PRESSURE STATIONS AND WAKE SURVEY STATIONS.

WING STATION	FLAP CHORD	X
4.58	0.54"	6.89"
9.87	0.49	6.79
15.48	0.47	6.71
25.45	0.45	5.79
30.65	0.40	5.19
38.25	0.37	4.45

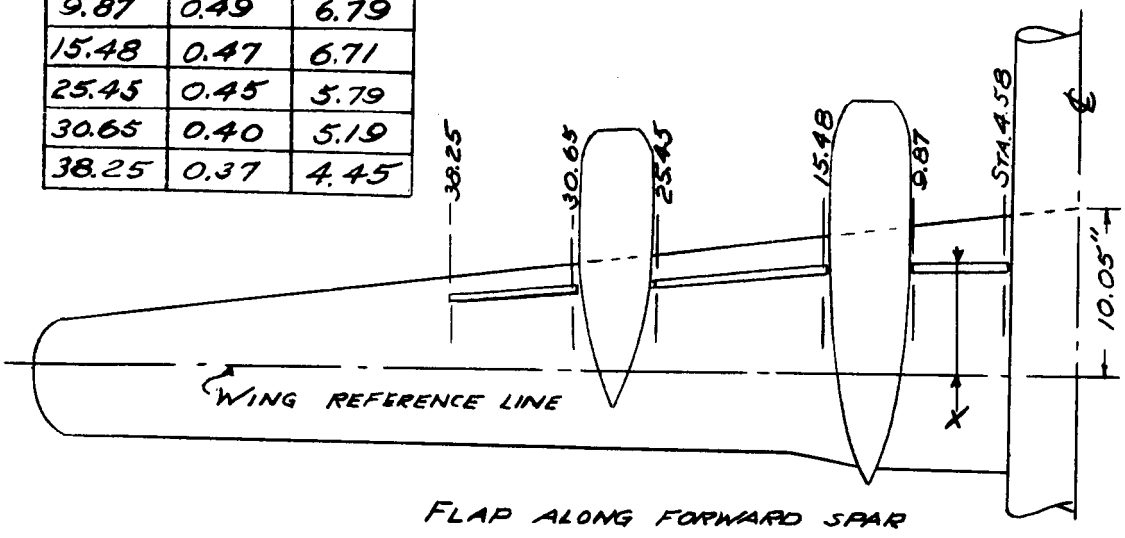

FLAP ALONG FORWARD SPAR

WING STATION	FLAP CHORD	X
4.58	0.56"	2.66"
9.87	0.52	2.61
15.48	0.50	2.66
25.45	0.46	2.62
30.65	0.44	2.03
38.25	0.42	2.03
40.0	0.40	-0.05
61.65	0.26	-0.06

NATIONAL ADVISORY
COMMITTEE FOR AERONAUTICS

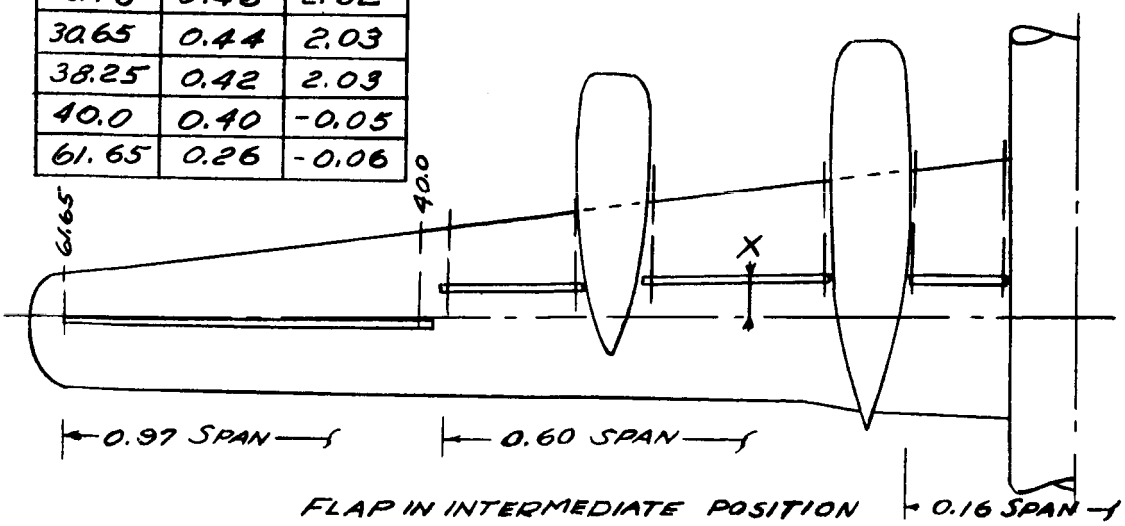

FLAP IN INTERMEDIATE POSITION

FIGURE 4. - LOCATION AND DIMENSIONS OF 45° SMALL TAPERED FLAP ALONG FORWARD SPAR AND IN INTERMEDIATE POSITION.

WING STATION	FLAP CHORD	X
4.58	0.56"	-0.54"
9.87	0.52"	-0.51"

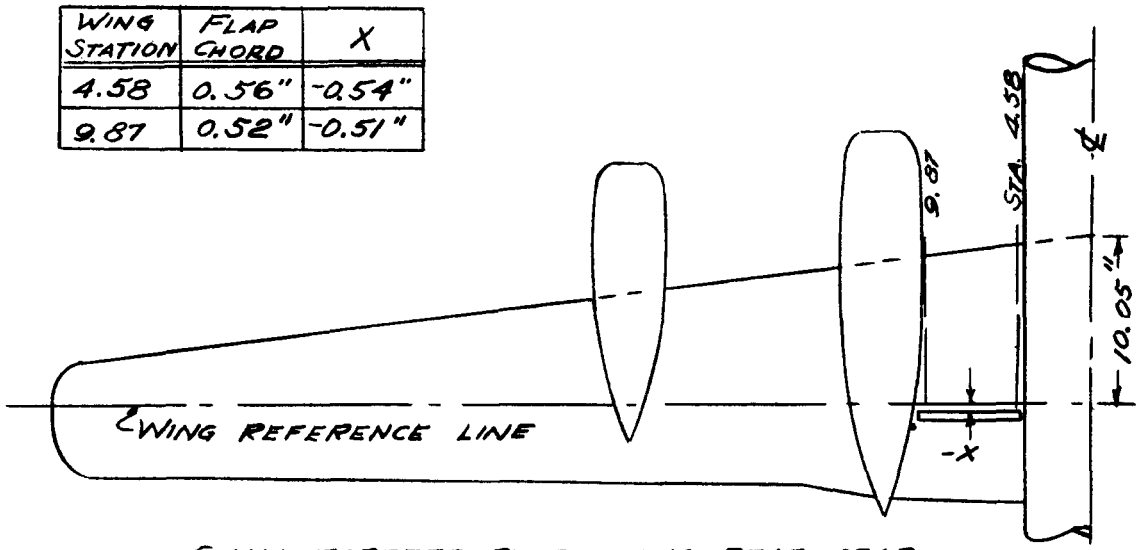

SMALL TAPERED FLAP ALONG REAR SPAR

WING STATION	FLAP CHORD	X
4.58	1.12"	-0.31
9.87	1.02	-0.32
15.48	0.93	-0.33
25.45	0.69	-0.33
30.65	0.63	-0.32
38.25	0.50	-0.31

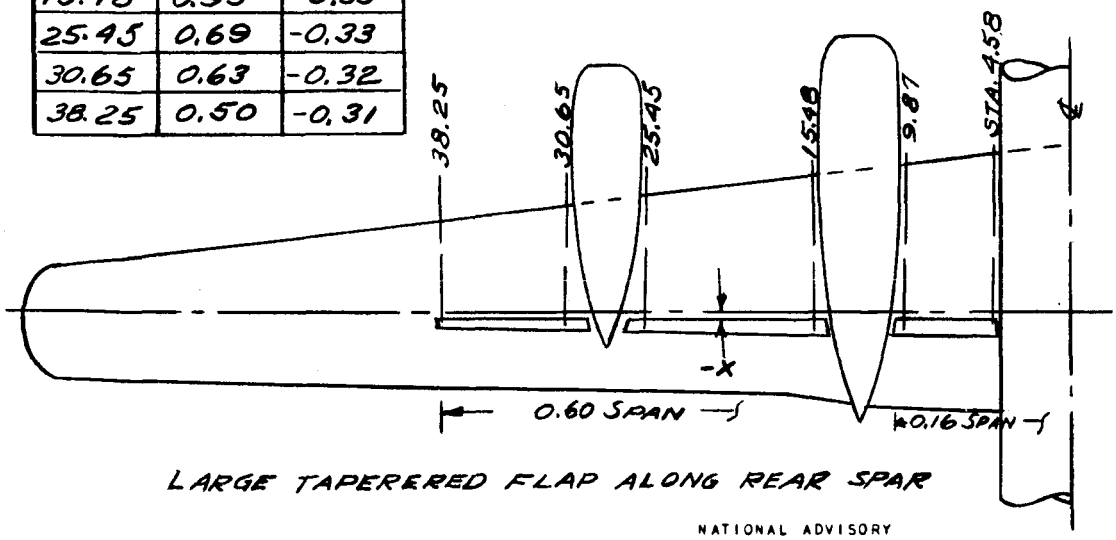

LARGE TAPERERED FLAP ALONG REAR SPAR

NATIONAL ADVISORY
COMMITTEE FOR AERONAUTICS

FIGURE 5. - LOCATION AND DIMENSIONS OF 45° LARGE AND SMALL TAPERED FLAPS ALONG REAR SPAR.

WING STATION	FLAP CHORD	X
4.58	1.16"	2.96"
9.87	1.16	2.92
15.48	1.15	3.02
25.45	1.15	3.00
30.65	1.15	2.41
38.25	1.15	2.41
40.0	0.90	0.28
61.65	0.52	0.02

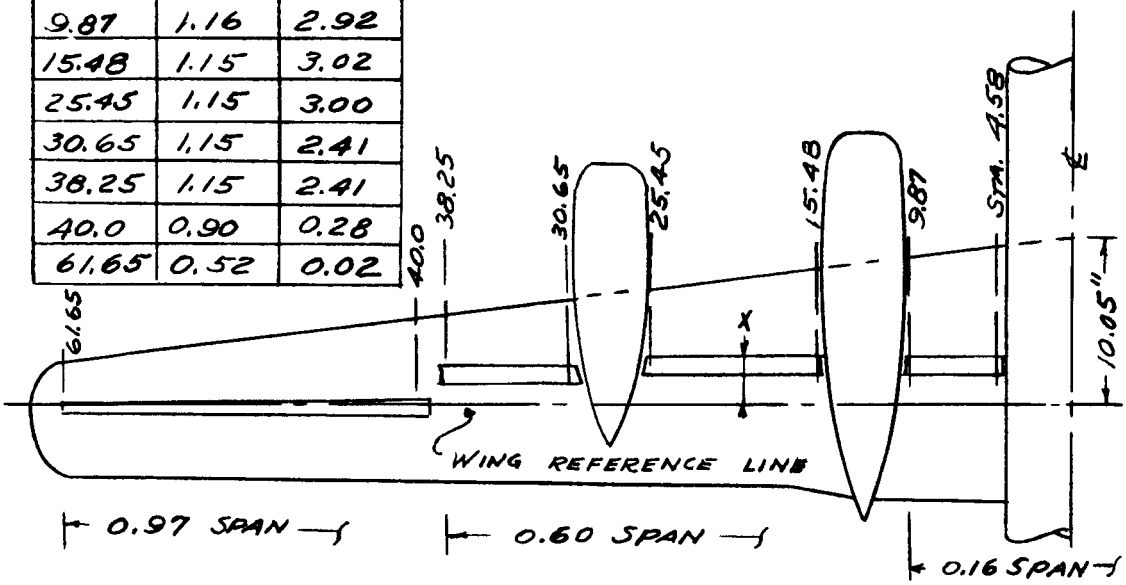

45° CONSTANT - CHORD FLAP, INTERMEDIATE POSITION

WING STATION	FLAP CHORD	X
4.58	0.53"	-0.51"
9.87	0.51"	-0.51

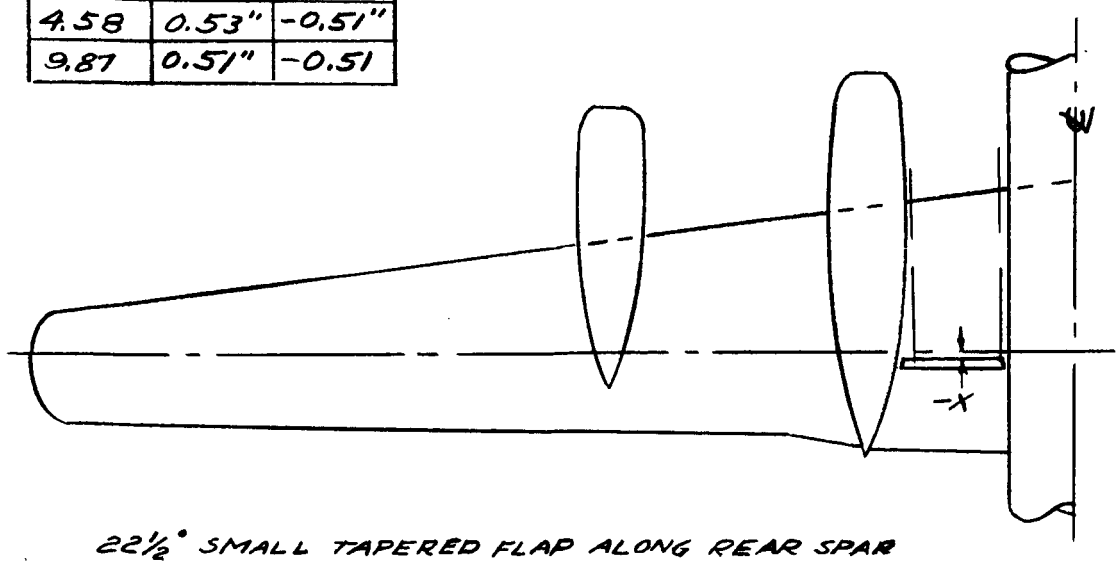

22½° SMALL TAPERED FLAP ALONG REAR SPAR

NATIONAL ADVISORY
COMMITTEE FOR AERONAUTICS

FIGURE 6. - LOCATION AND DIMENSIONS OF 45° CONSTANT-CHORD FLAP AND 22½° SMALL TAPERED FLAP.

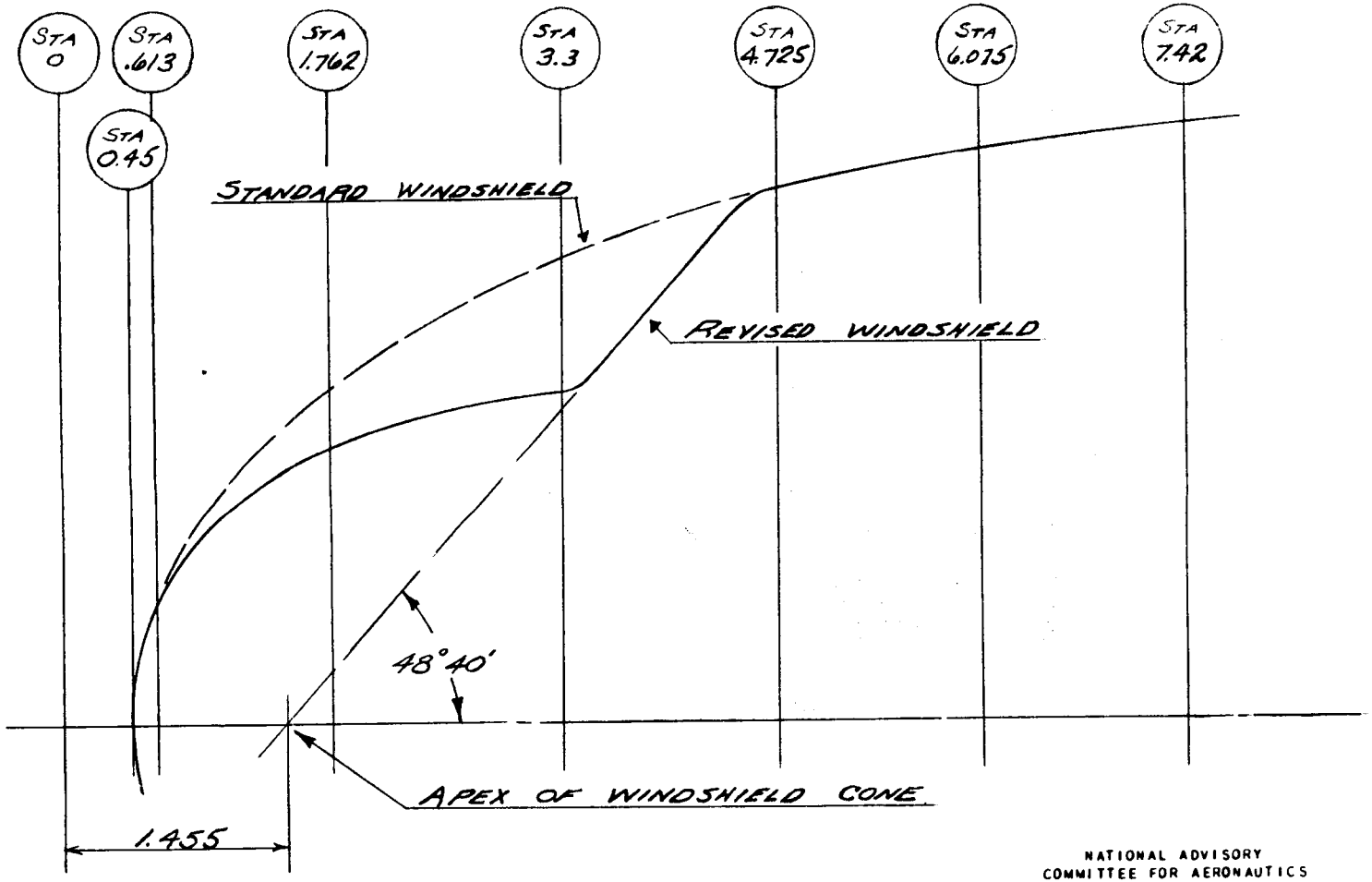

FIGURE 7. - SIDE VIEW OF FUSELAGE SHOWING STANDARD AND REVISED WINDSHIELDS. ALL DIMENSIONS ARE INCHES MODEL - SCALE.

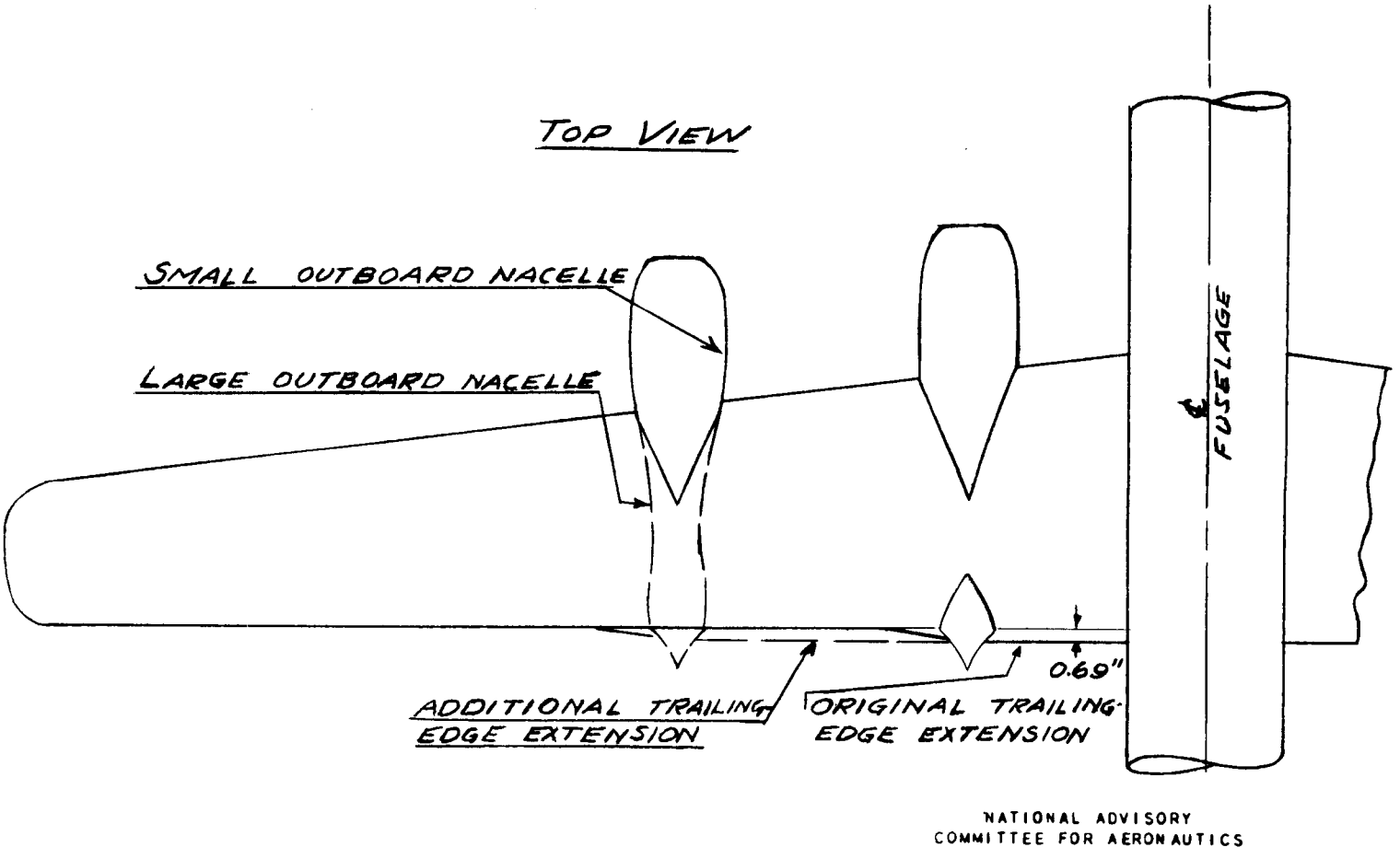

FIGURE 8. - LARGE OUTBOARD NACELLE AND ADDITIONAL TRAILING-EDGE EXTENSION.

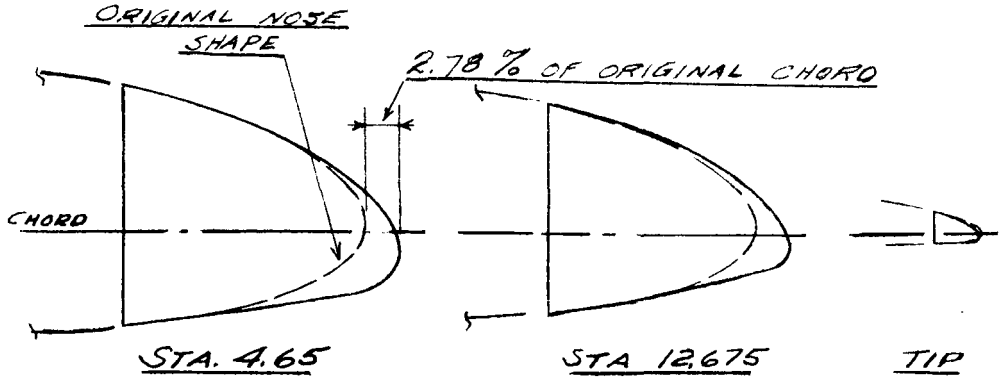

NATIONAL ADVISORY
COMMITTEE FOR AERONAUTICS

SECTION AT WING STATION 4.65			SECTION AT WING STATION 12.675					TIP SECTION		
				INB'D SECTION		OUTB'D SECTION				
STA.	UPPER ORD.	LOWER ORD	STA	UPPER ORD.	LOWER ORD	UPPER ORD	LOWER ORD.	STA	UPPER ORD.	LOWER ORD.
-2.78	—	1.51	-2.59	—	1.06	—	1.13	0.15	—	0.55
-2.62	-0.51	2.54	-2.43	-0.27	1.77	-0.20	1.88	0.28	-0.10	0.96
-2.47	-0.02	2.92	-2.27	0.15	2.10	0.19	2.14	0.40	0.12	1.09
-2.15	0.69	3.41	-1.96	0.70	2.53	0.80	2.49	0.64	0.44	1.24
-1.83	1.22	3.73	-1.64	1.12	2.85	1.26	2.74	0.89	0.72	1.32
-1.19	2.05	4.22	-1.02	1.81	3.25	2.01	3.09	1.38	1.18	1.38
0.41	3.57	4.88	0.56	3.29	3.87	3.49	3.56	2.61	2.07	1.43
3.61	5.89	5.38	3.71	5.61	4.55	5.89	4.13	5.08	3.22	1.53
6.80	7.64	5.83	6.85	7.47	5.15	7.60		7.54	4.01	1.64
10.0	9.13	6.29	10.0	8.93	5.72	8.95		10.0	4.63	1.74
15.0	10.92	7.00						15.0	5.58	1.90

NOTE: 1. ALL DIMENSIONS GIVEN IN PERCENT OF ORIGINAL WING CHORD.

2. THERE IS A CHANGE OF SECTION AT STATION 12.675.

3. WHEN USING THE MODERATELY DROOPED LEADING EDGE ON ONLY PART OF THE SPAN, A TRANSITION SECTION WAS USED FROM WING STATION 28.05 TO STATION 38.25, AND THE BASIC WING SECTION WAS USED OUTBOARD OF WING STATION 38.25.

FIGURE 9. - DIMENSIONS OF MODERATELY CAMBERED LEADING-EDGE MODIFICATION.

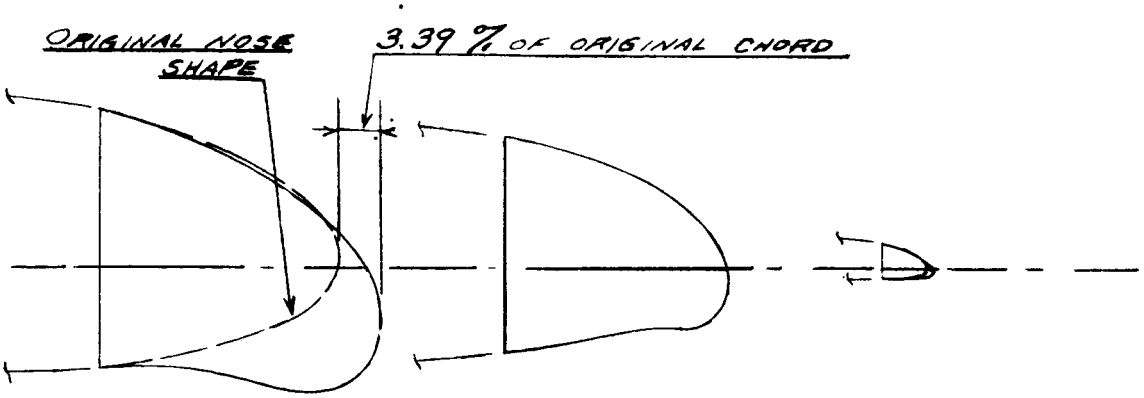

ROOT SECTION			SECTION AT WING STATION 12.675			TIP SECTION		
STA.	UPPER ORD	LOWER ORD	STA.	UPPER ORD.	LOWER ORD	STA	UPPER ORD.	LOWER ORD.
-3.39	—	3.96	-0.38	—	0.83	-0.29	—	0.62
-3.22	-2.39	5.40	-0.25	0.37	1.84	-0.16	-0.15	1.05
-3.05	-1.77	6.02	-0.12	0.86	2.30	-0.03	0.05	1.20
-2.72	-0.87	6.83	0.14	1.54	2.91	0.22	0.40	1.40
-2.38	-0.20	7.40	0.40	2.04	3.32	0.48	0.68	1.53
-1.71	0.87	8.20	0.92	2.84	3.94	0.99	1.16	1.68
-0.04	2.84	9.22	2.22	4.36	4.79	2.28	2.07	1.74
3.31	5.54	9.43	4.81	6.34	4.91	4.85	3.25	1.61
6.65	7.62	8.67	7.41	7.81	5.05	7.43	4.02	1.61
10.0	9.23	7.99	10.0	8.95		10.0	4.63	
15.0	11.05	7.46						
20.0	12.31							

NOTE: 1. ALL DIMENSIONS GIVEN IN PERCENT OF ORIGINAL WING CHORD.
2. STRAIGHT LINE ELEMENTS JOIN ROOT SECTION WITH STATION 12.675 AND STATION 12.675 WITH TIP SECTION.
3. THIS MODIFICATION USED ON COMPLETE SPAN ONLY.

NATIONAL ADVISORY COMMITTEE FOR AERONAUTICS

FIGURE 10.- DIMENSIONS OF EXTREMELY CAMBERED LEADING-EDGE MODIFICATION.

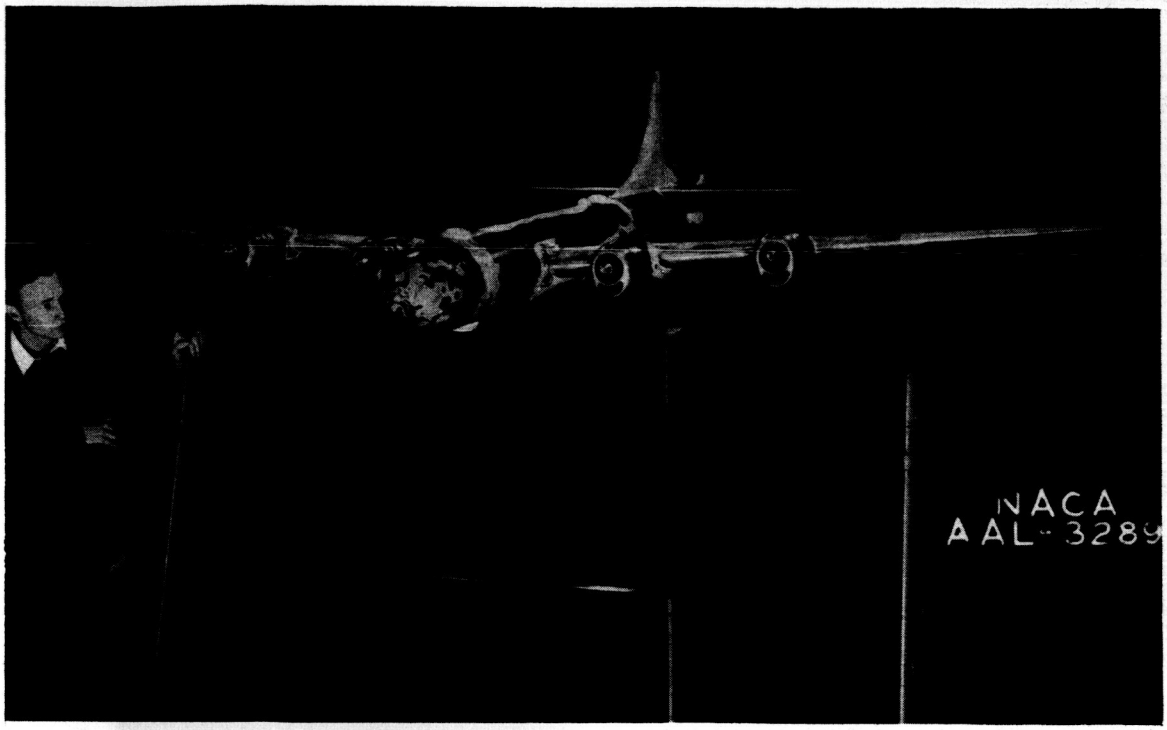

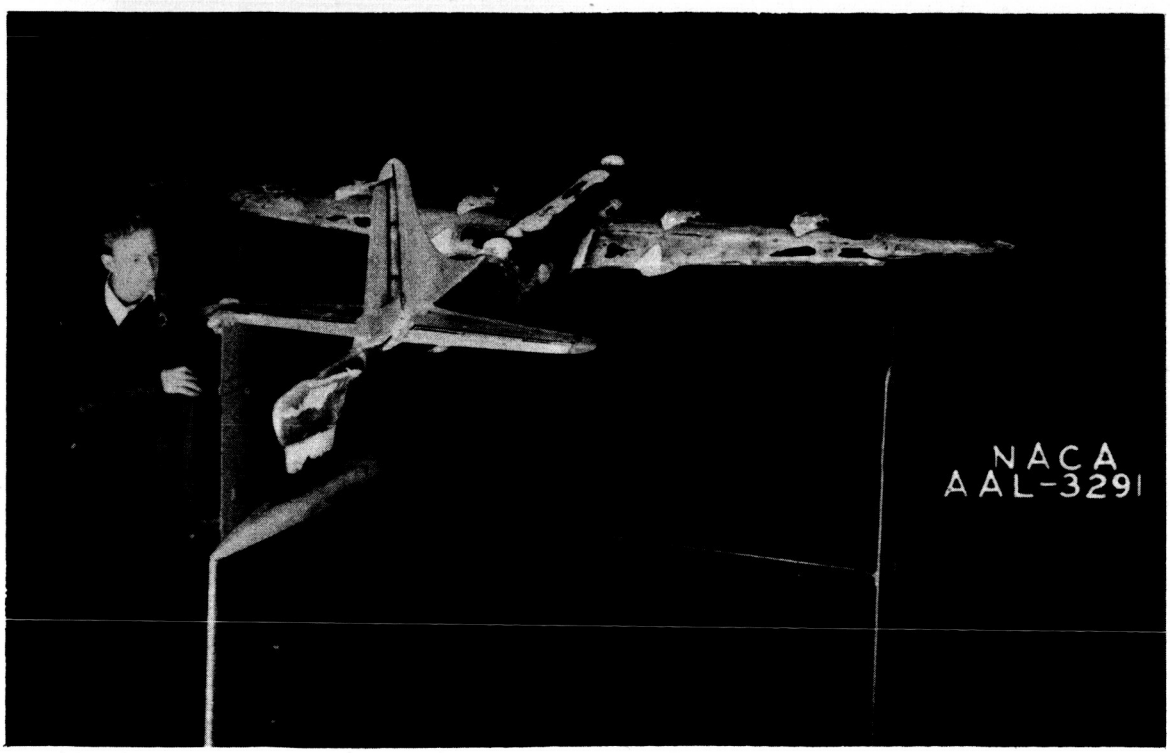

Figure 11.- The model mounted in the 16-foot high-speed wind tunnel.

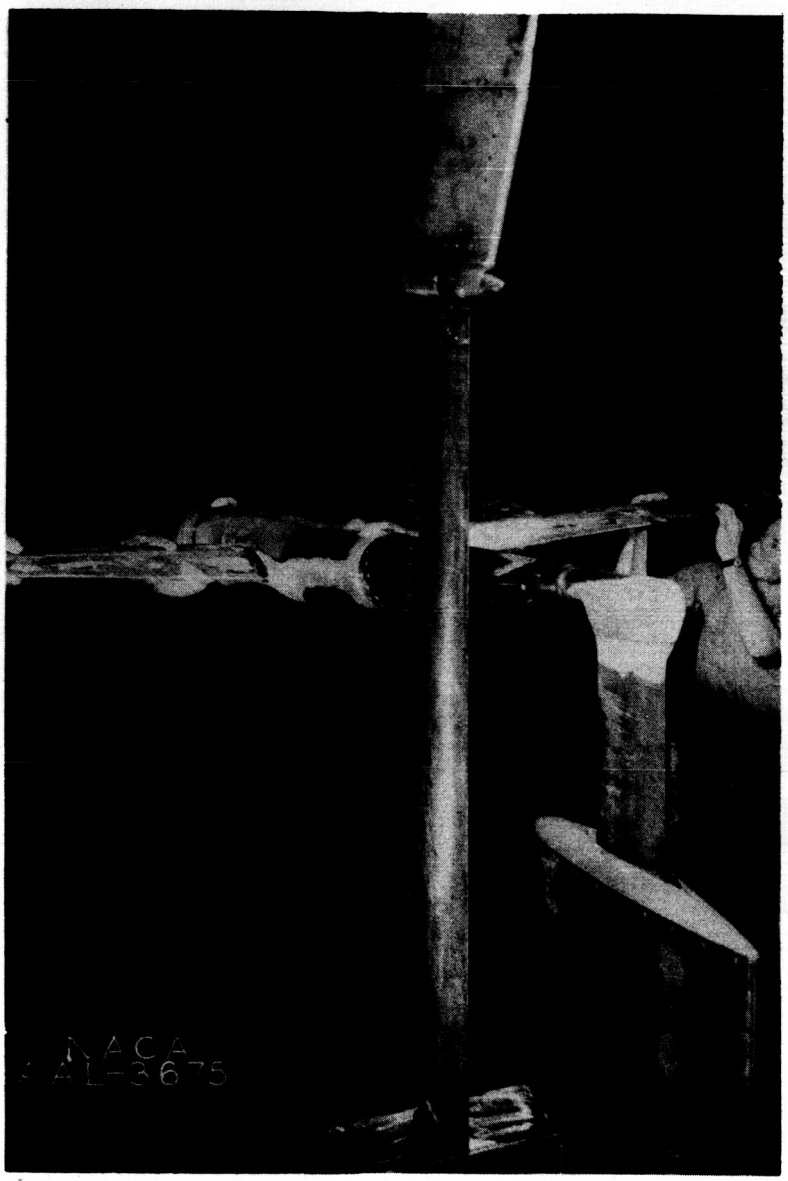

Figure 12.- Wake-survey rake.

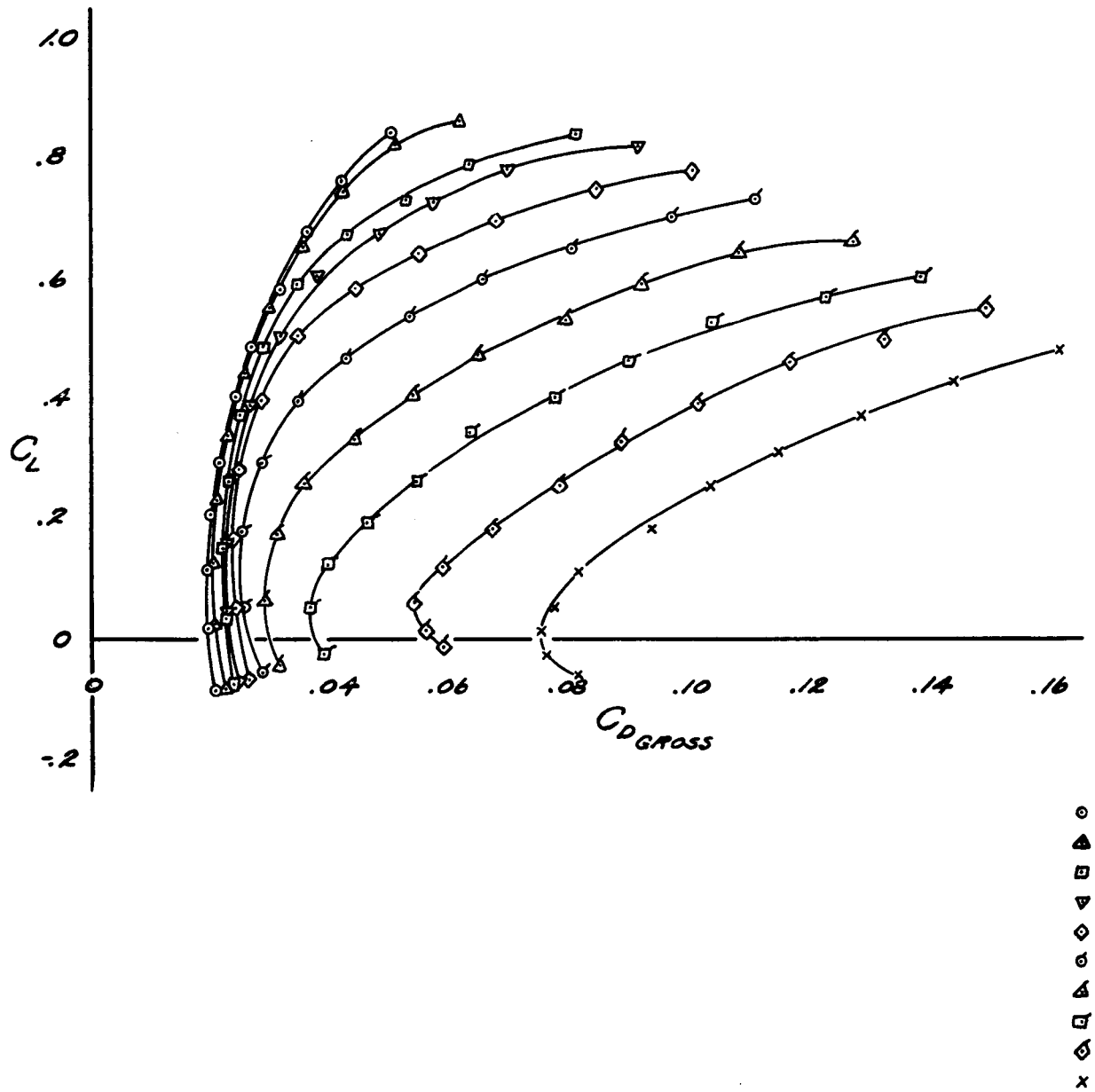

FIGURE 13A

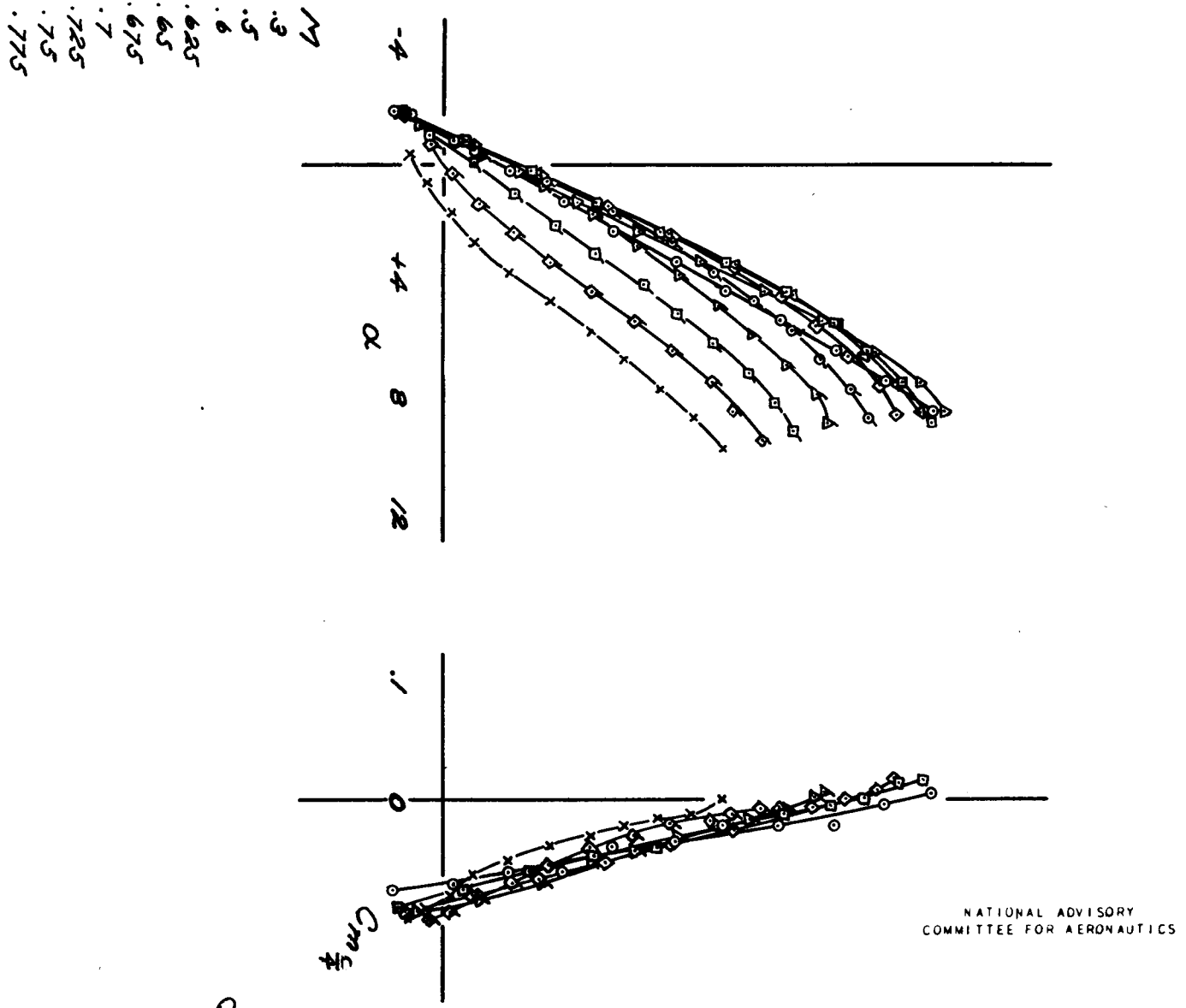

FIGURE 13.- VARIATION OF DRAG COEFFICIENT, ANGLE OF ATTACK, AND PITCHING-MOMENT COEFFICIENT WITH LIFT COEFFICIENT FOR VARIOUS MACH NUMBERS. WING, NACELLES, AND FUSELAGE.

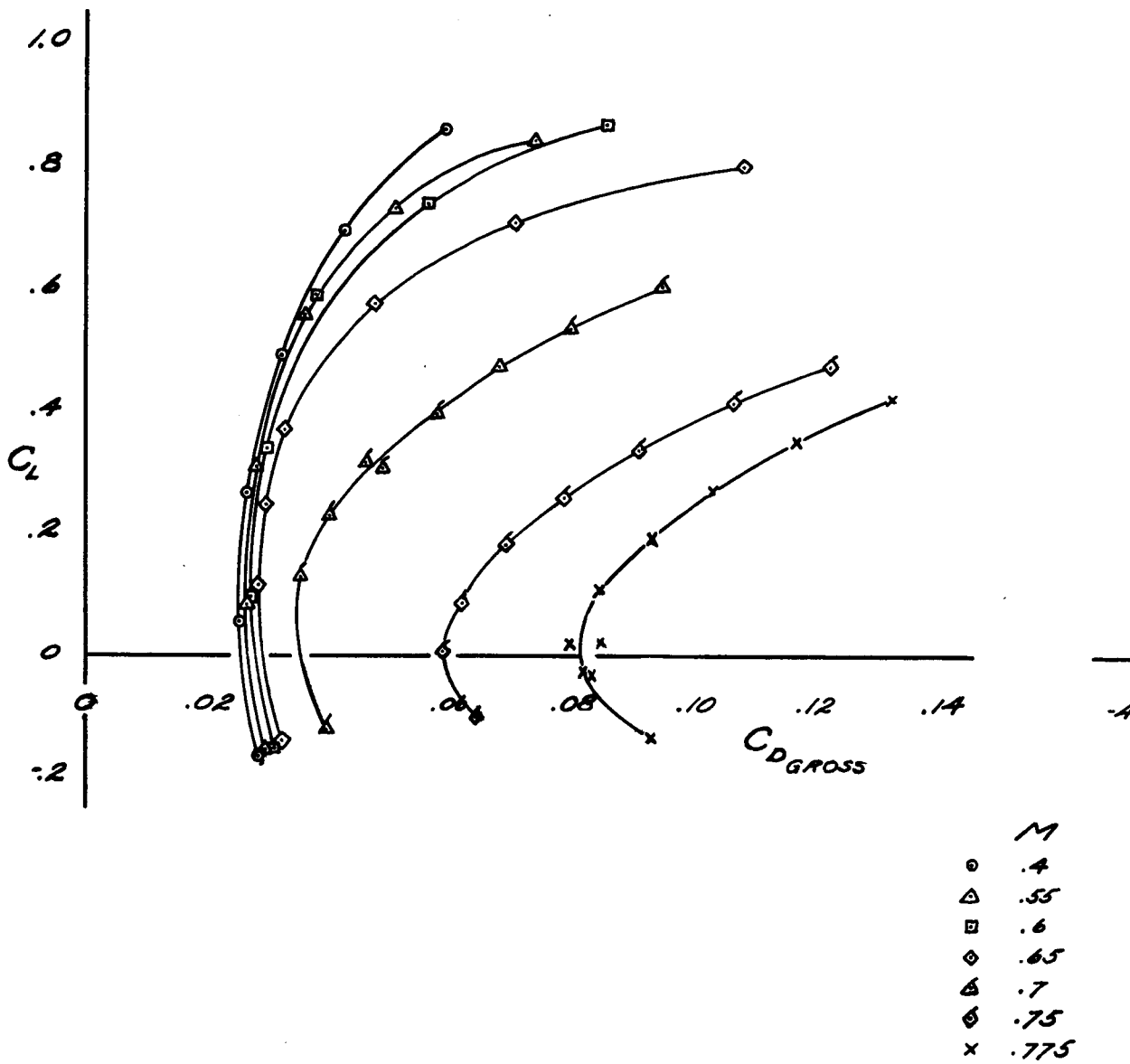

FIGURE 14A

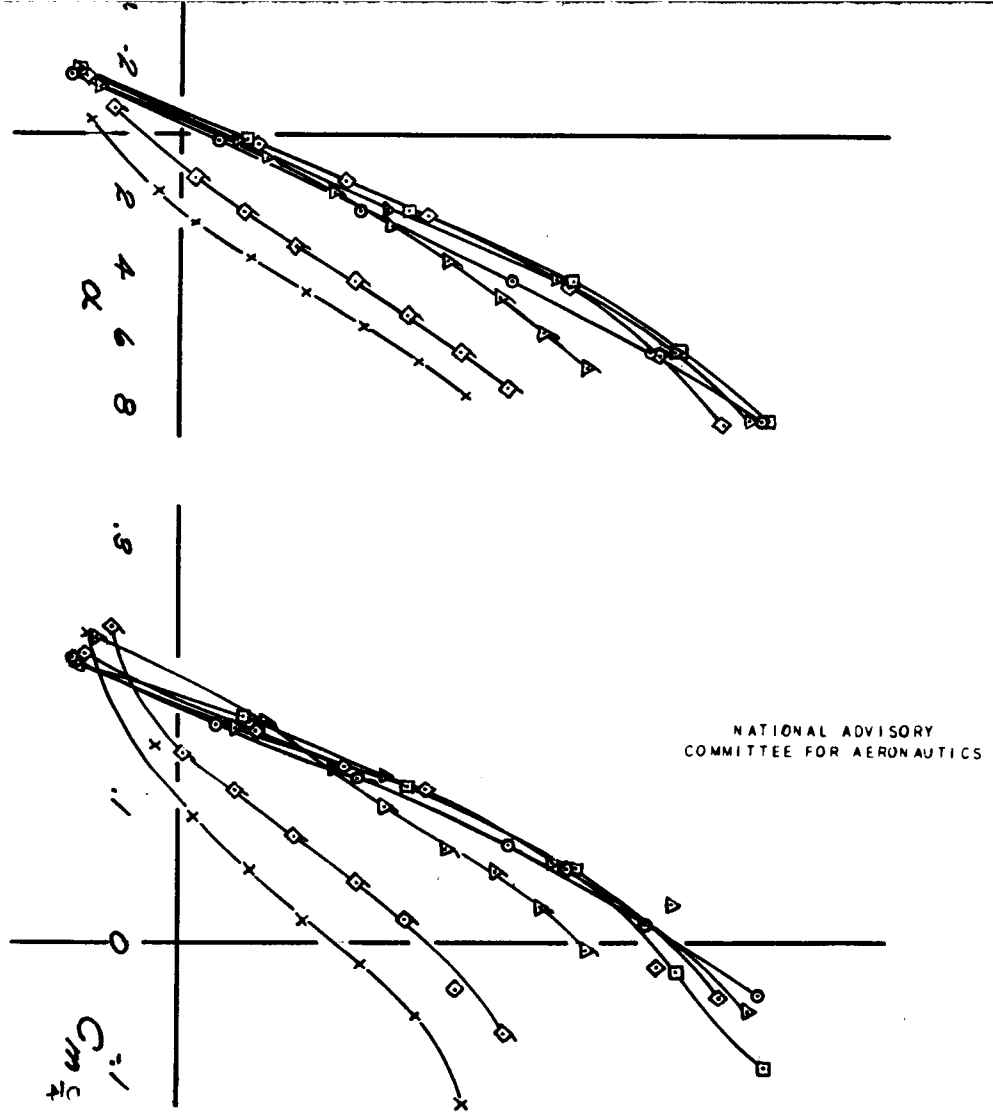

FIGURE 14.B - VARIATION OF DRAG COEFFICIENT, ANGLE OF ATTACK, AND PITCHING-MOMENT COEFFICIENT WITH LIFT COEFFICIENT FOR VARIOUS MACH NUMBERS. WING, NACELLES, FUSELAGE AND TAIL.

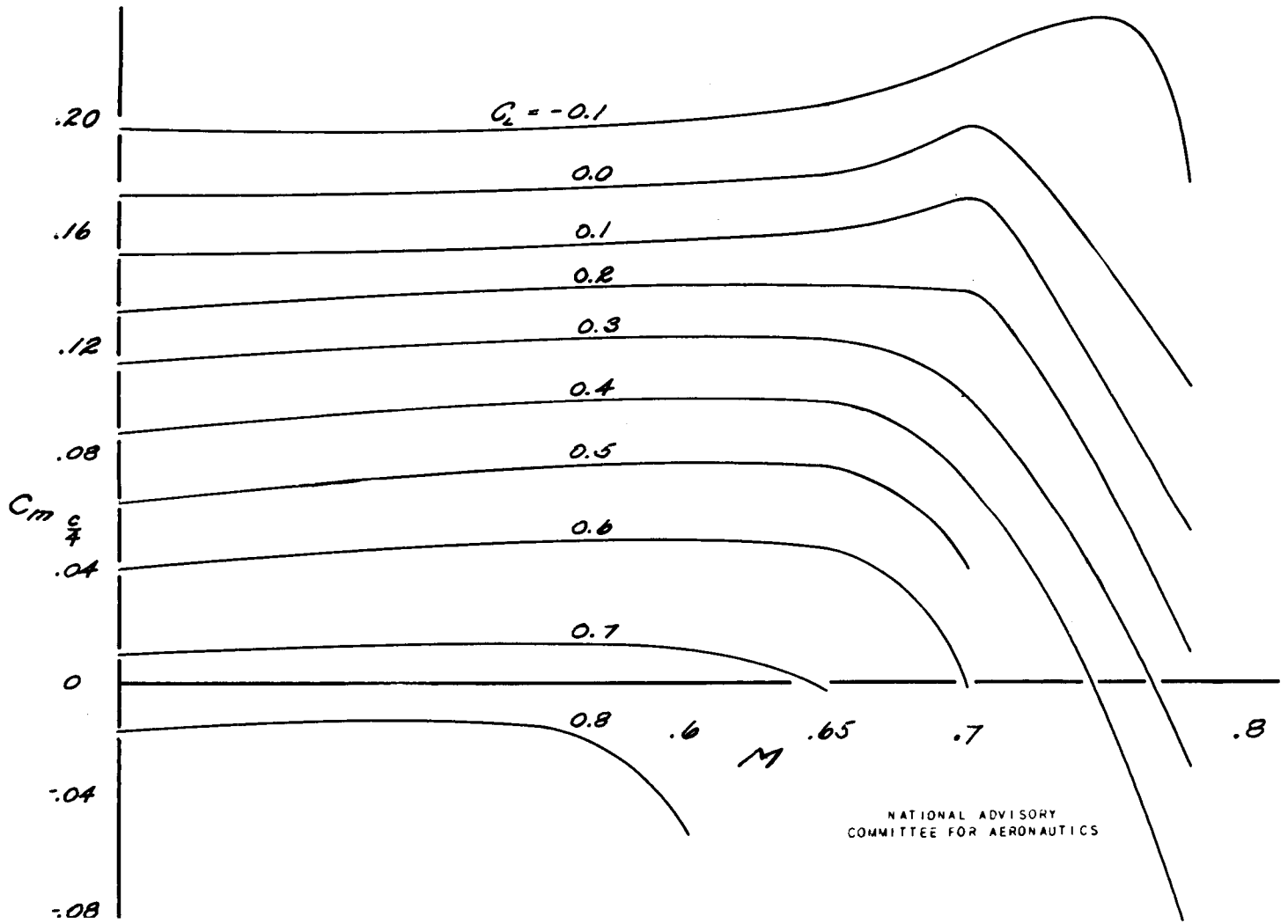

FIGURE 15.- VARIATION OF PITCHING-MOMENT COEFFICIENT WITH MACH NUMBER FOR CONSTANT VALUES OF THE LIFT COEFFICIENT. WING, NACELLES, FUSELAGE, AND TAIL.

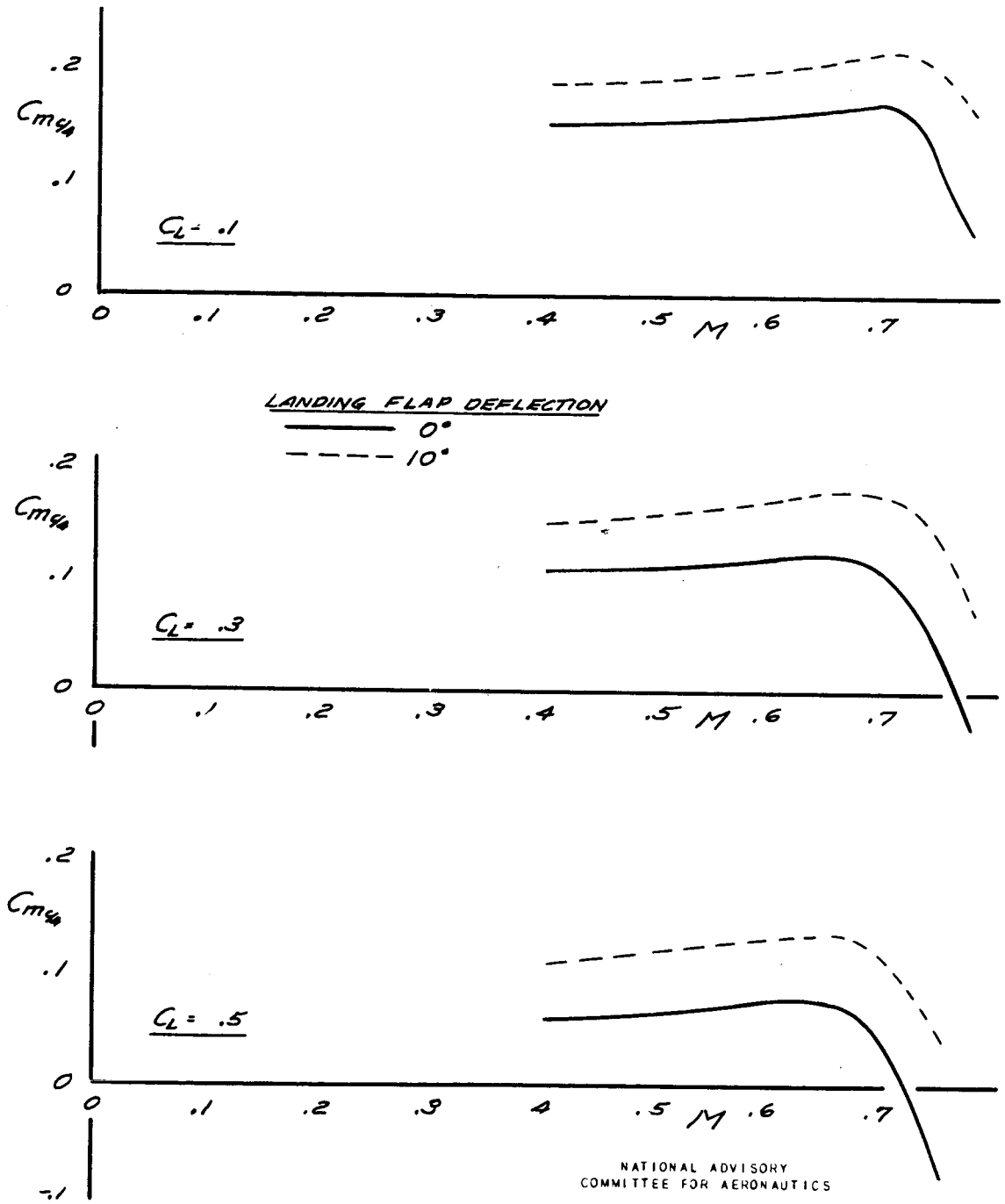

FIGURE 16.- EFFECT OF 10° LANDING FLAP DEFLECTION ON PITCHING-MOMENT COEFFICIENT FOR CONSTANT VALUES OF THE LIFT COEFFICIENT.

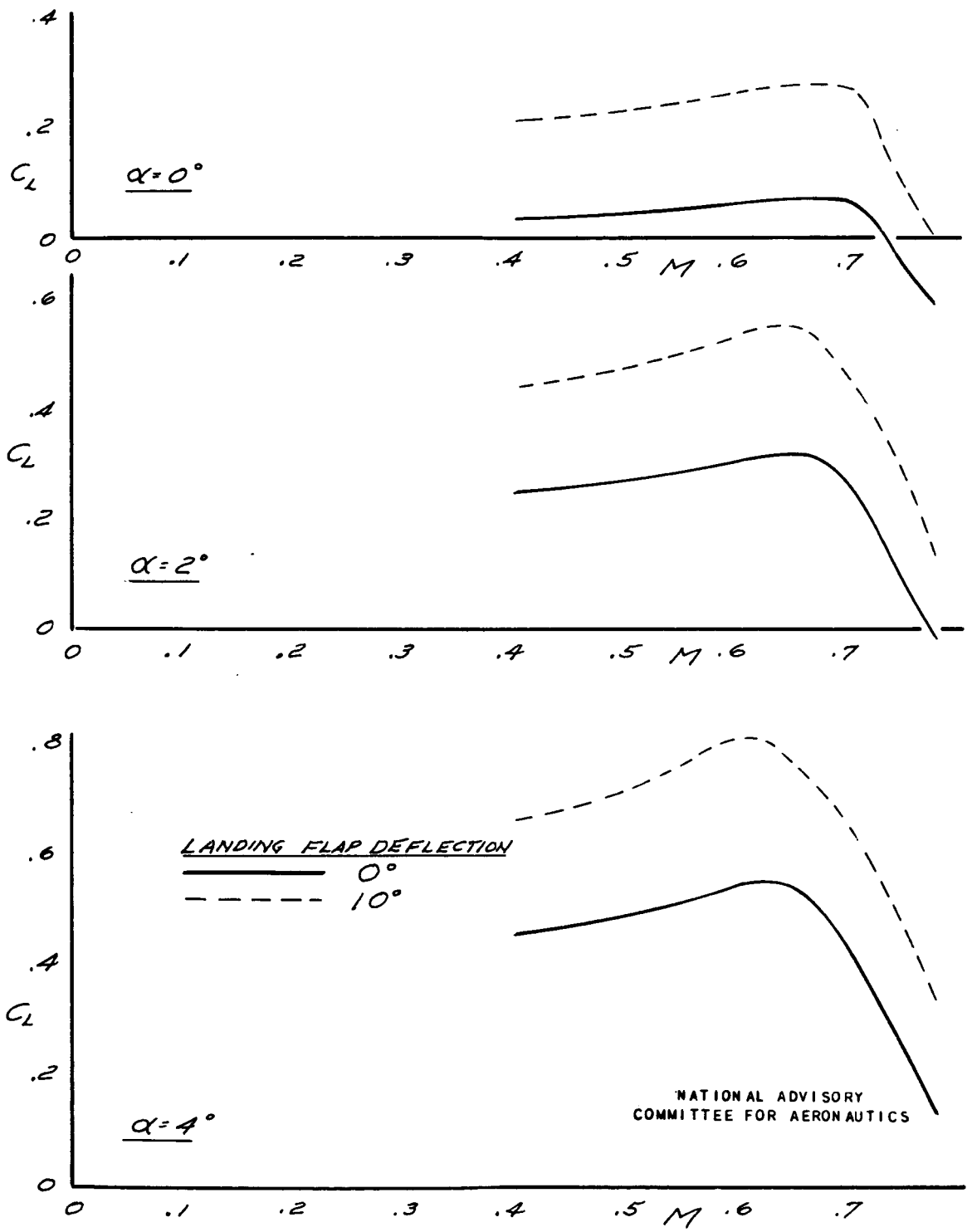

FIGURE 17.- EFFECT OF 10° LANDING FLAP DEFLECTION ON LIFT COEFFICIENT FOR CONSTANT ANGLE OF ATTACK.

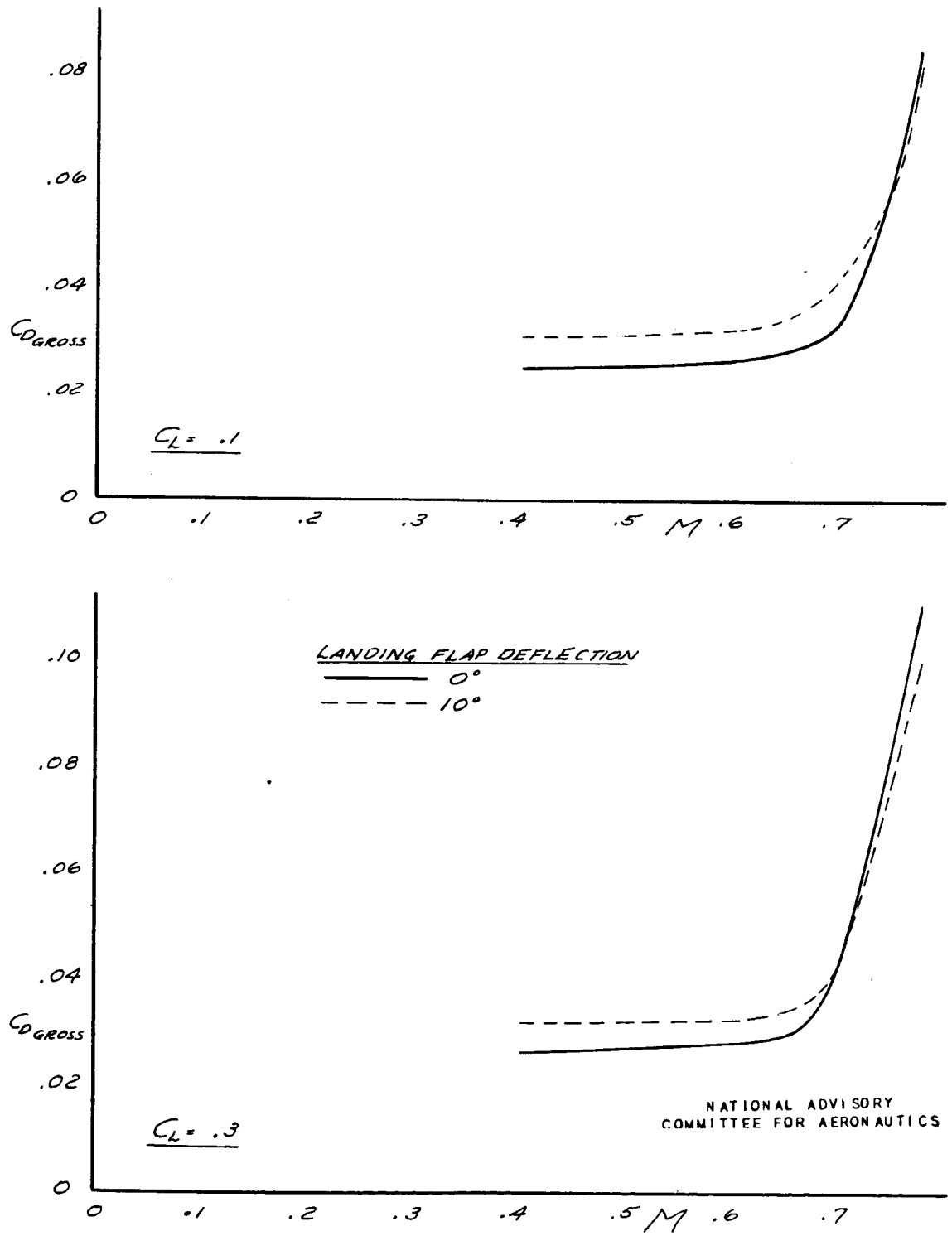

FIGURE 18 (a). - EFFECT OF 10° LANDING FLAP DEFLECTION ON DRAG COEFFICIENT FOR CONSTANT LIFT COEFFICIENT. LIFT COEFFICIENT = 0.1 AND 0.3

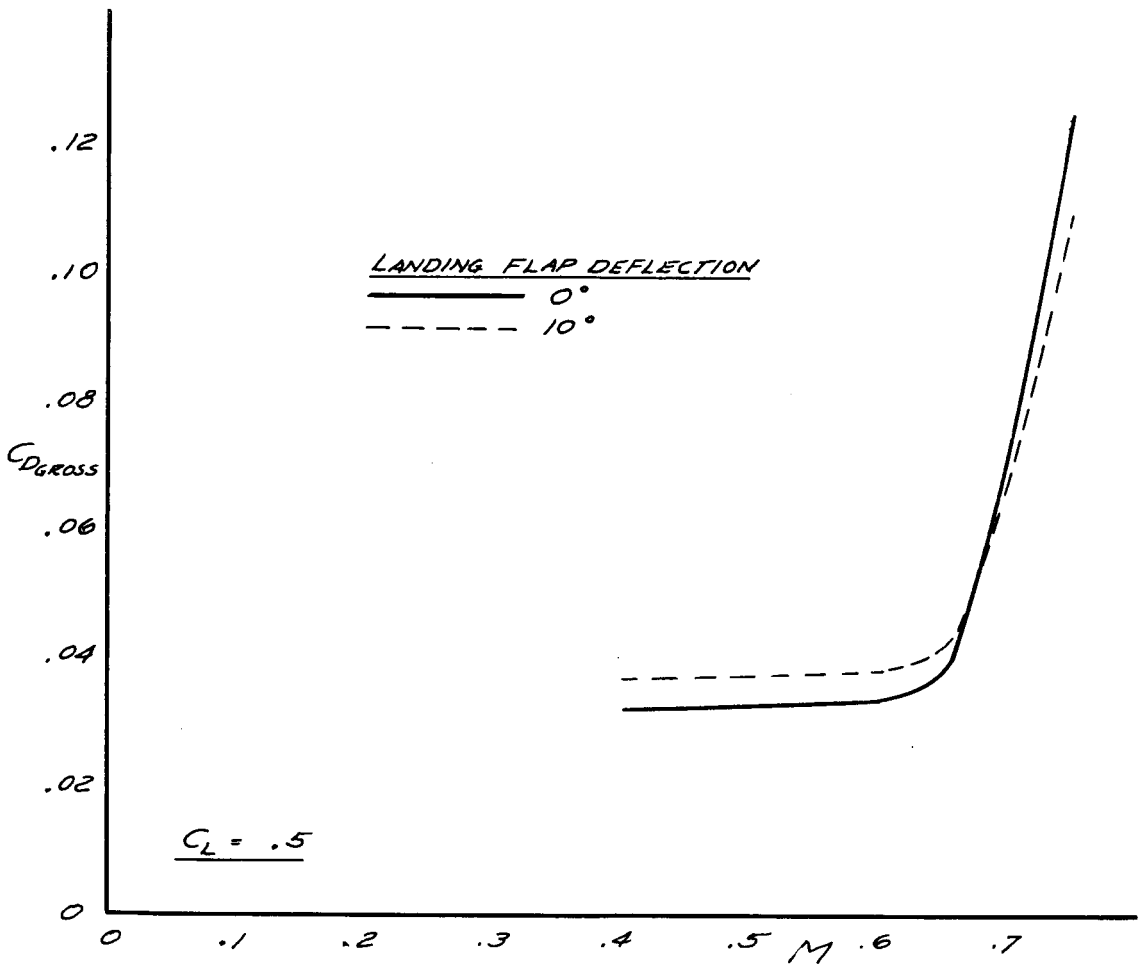

NATIONAL ADVISORY
COMMITTEE FOR AERONAUTICS

FIGURE 18 (b). - EFFECT OF 10° LANDING FLAP DEFLECTION ON DRAG COEFFICIENT FOR CONSTANT LIFT COEFFICIENT. LIFT COEFFICIENT = 0.5.

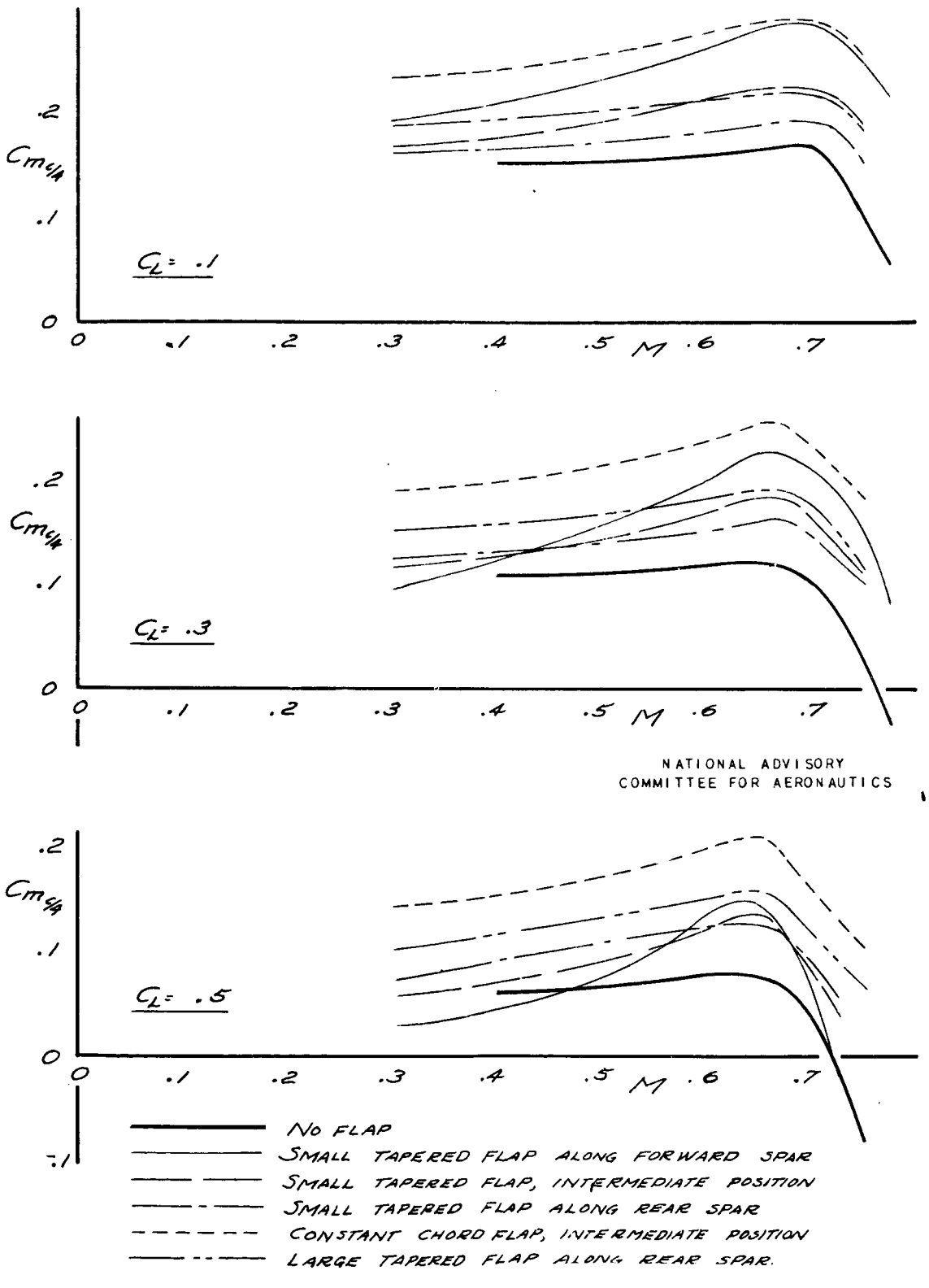

FIGURE 19.- EFFECT OF 0.16 SPAN 45° AUXILIARY FLAPS ON PITCHING-MOMENT COEFFICIENT.

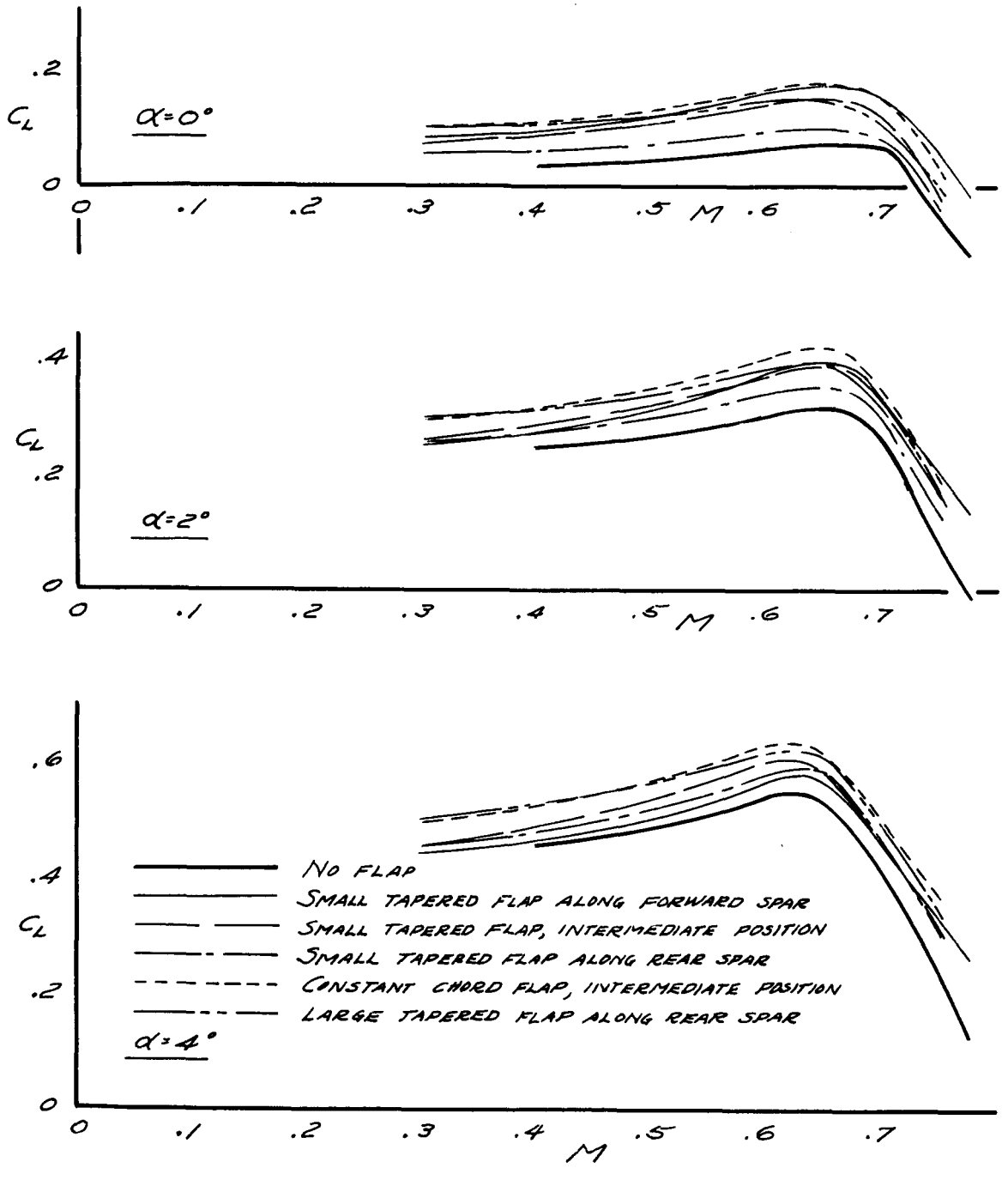

NATIONAL ADVISORY
COMMITTEE FOR AERONAUTICS

FIGURE 20. - EFFECT OF 0.16 SPAN 45° AUXILIARY FLAPS ON LIFT COEFFICIENT.

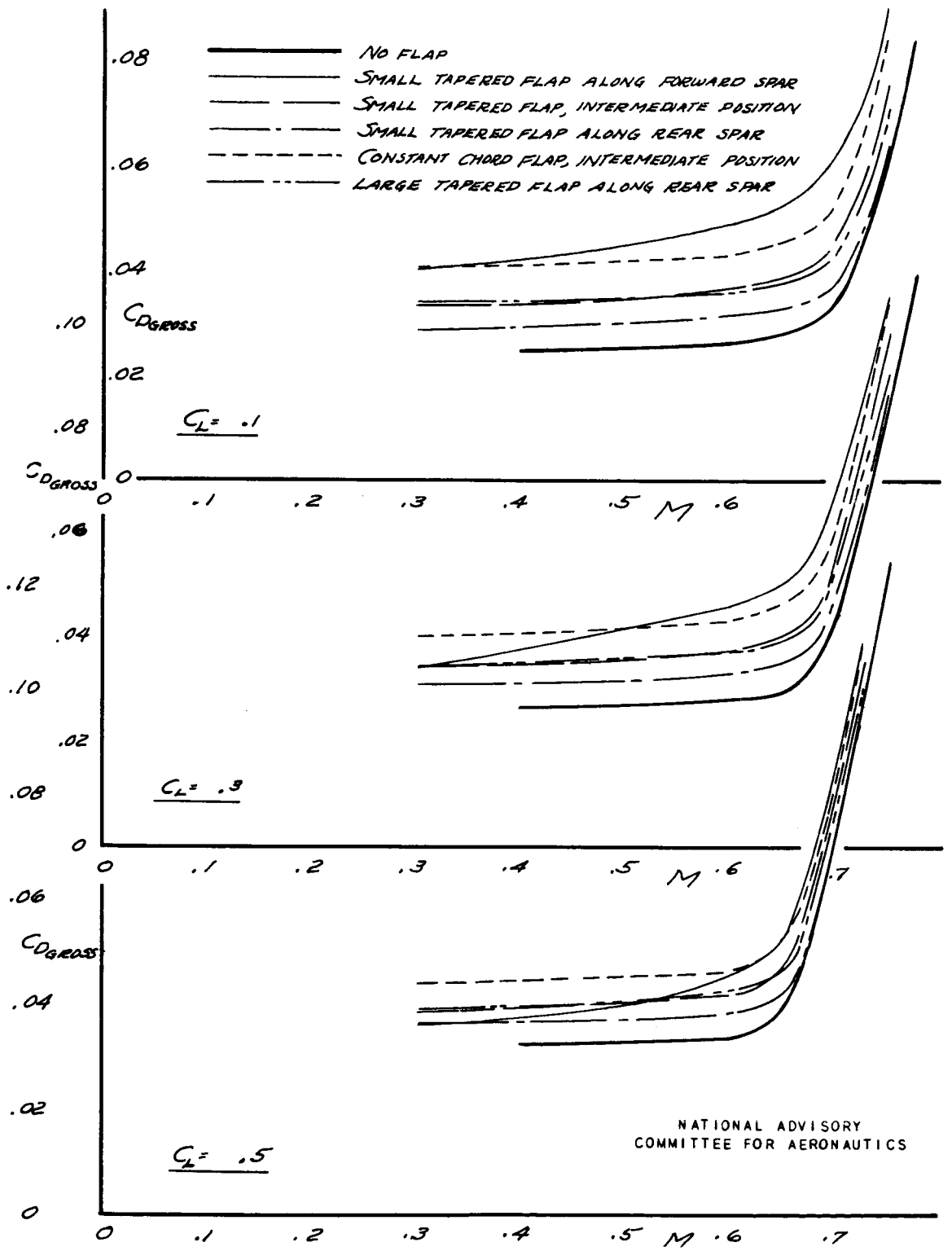

FIGURE 21.- EFFECT OF 0.16 SPAN 45° AUXILIARY FLAPS ON DRAG COEFFICIENT.

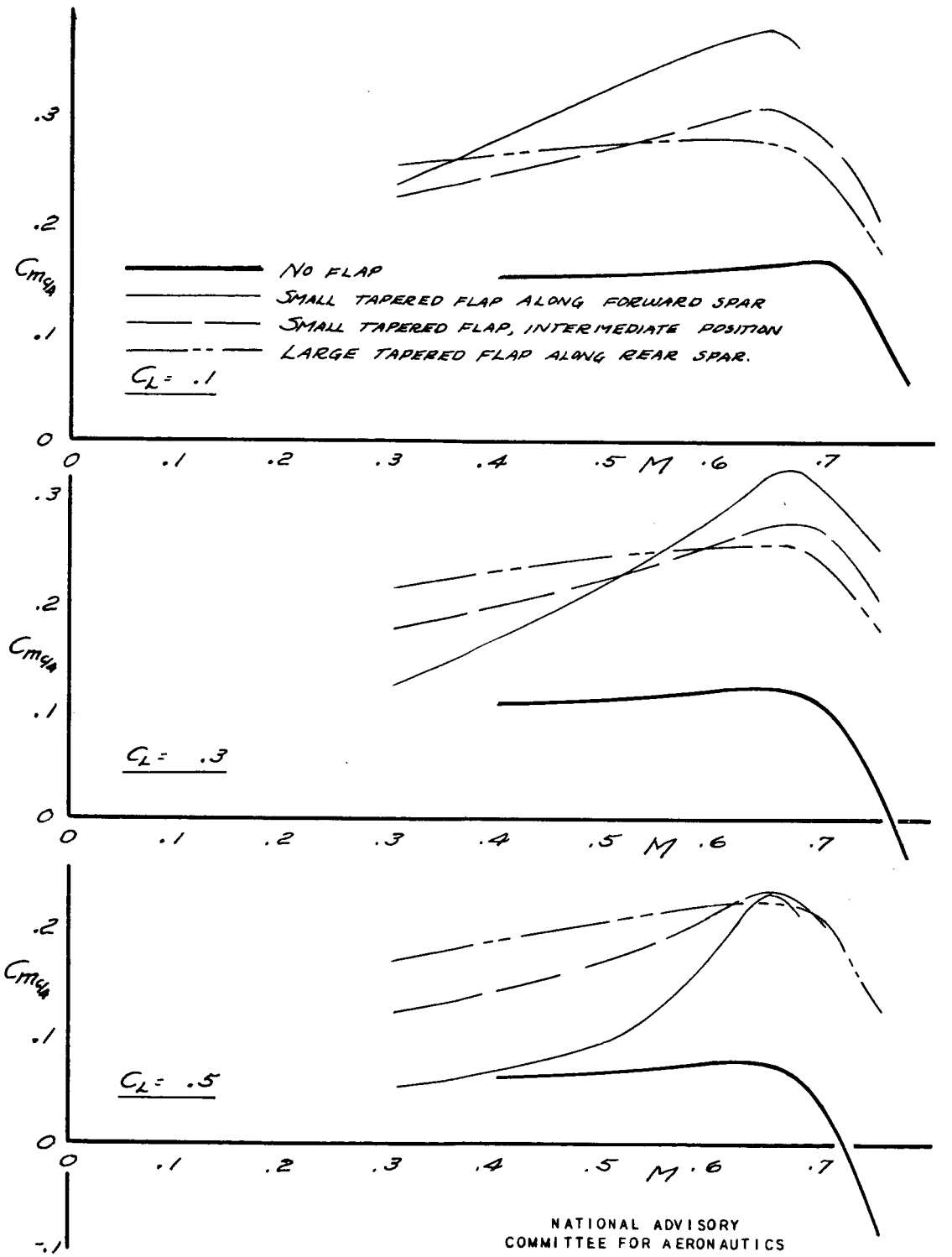

FIGURE 22.- EFFECT OF 0.60 SPAN 45° AUXILIARY FLAPS ON PITCHING-MOMENT COEFFICIENT.

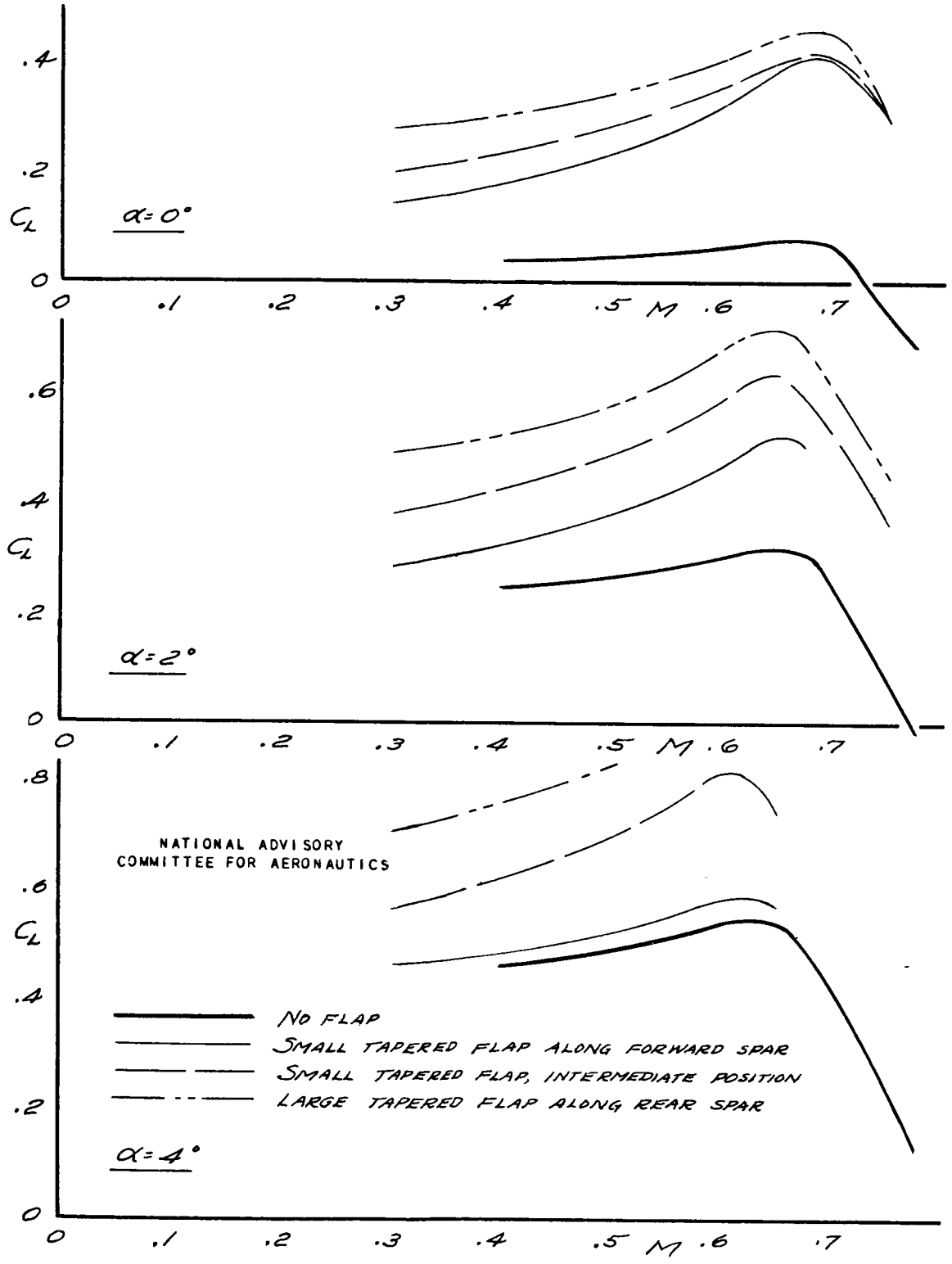

FIGURE 23.- EFFECT OF 0.60 SPAN 45° AUXILIARY FLAPS ON LIFT COEFFICIENT.

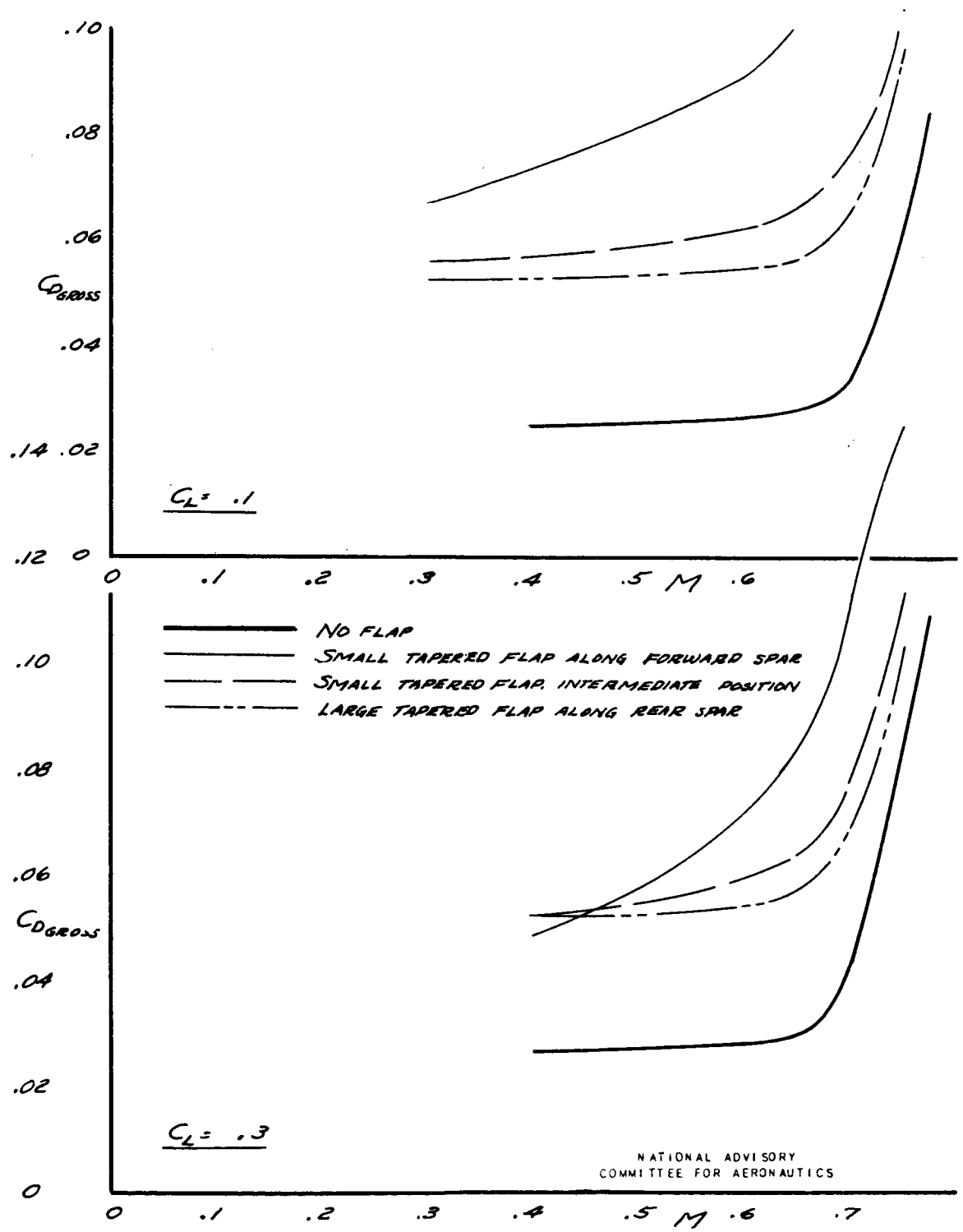

FIGURE 24(a). - EFFECT OF 0.60 SPAN 45° AUXILIARY FLAPS ON DRAG COEFFICIENT. LIFT COEFFICIENT = 0.1 AND 0.3.

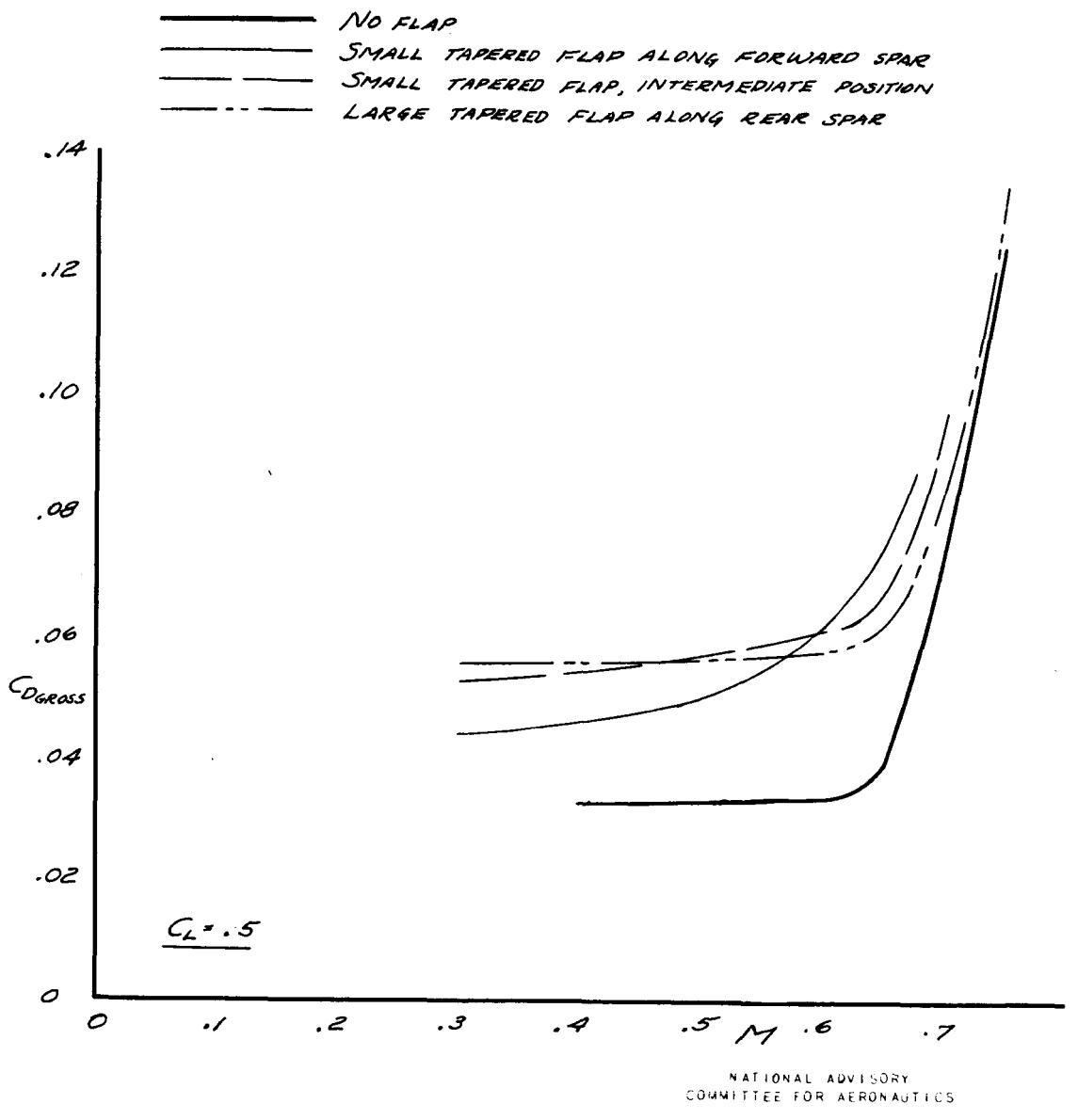

FIGURE 24(b). - EFFECT OF 0.60 SPAN 45° AUXILIARY FLAPS ON DRAG COEFFICIENT. LIFT COEFFICIENT = 0.5

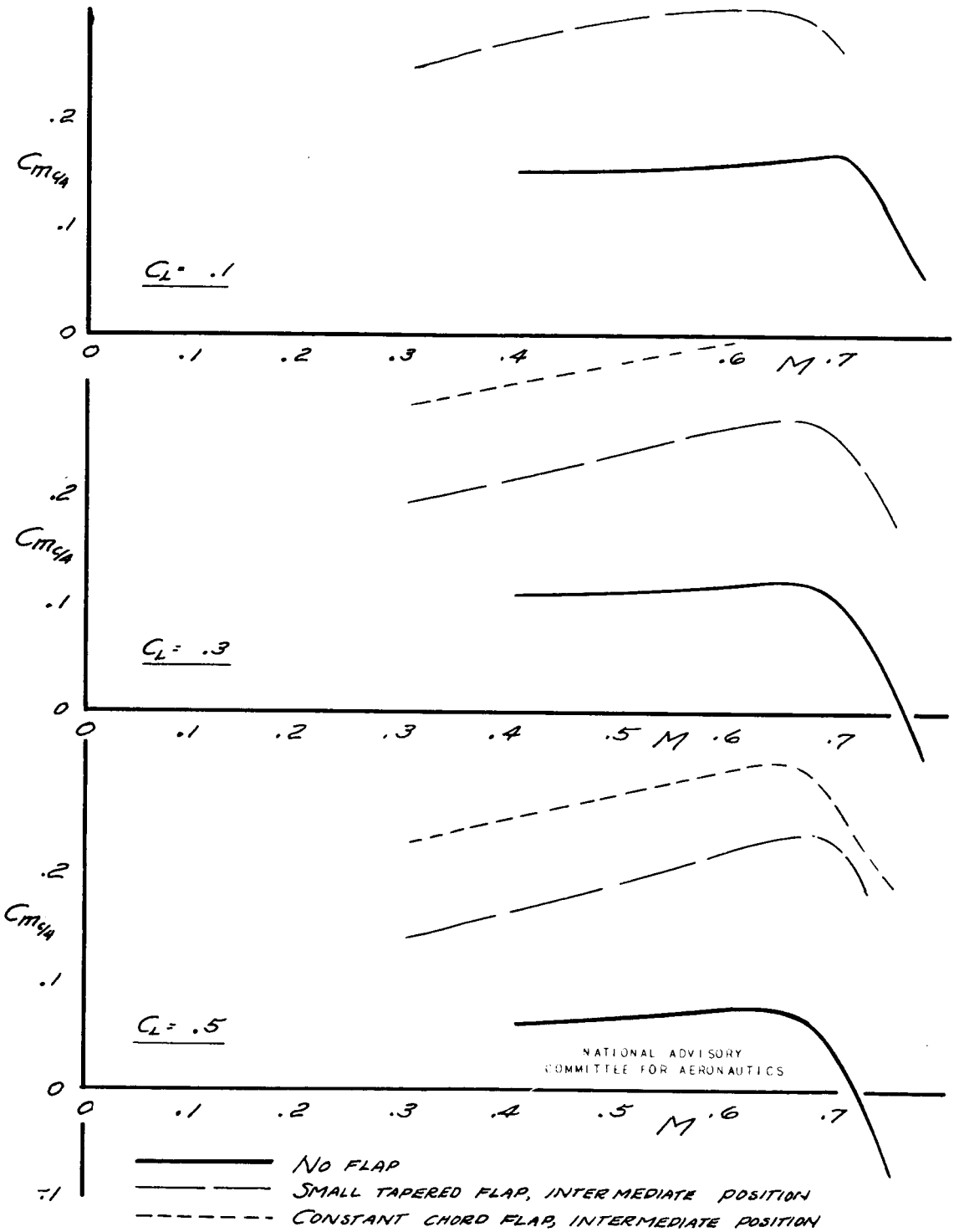

FIGURE 25. - EFFECT OF 0.97 SPAN 45° AUXILIARY FLAPS ON PITCHING-MOMENT COEFFICIENT.

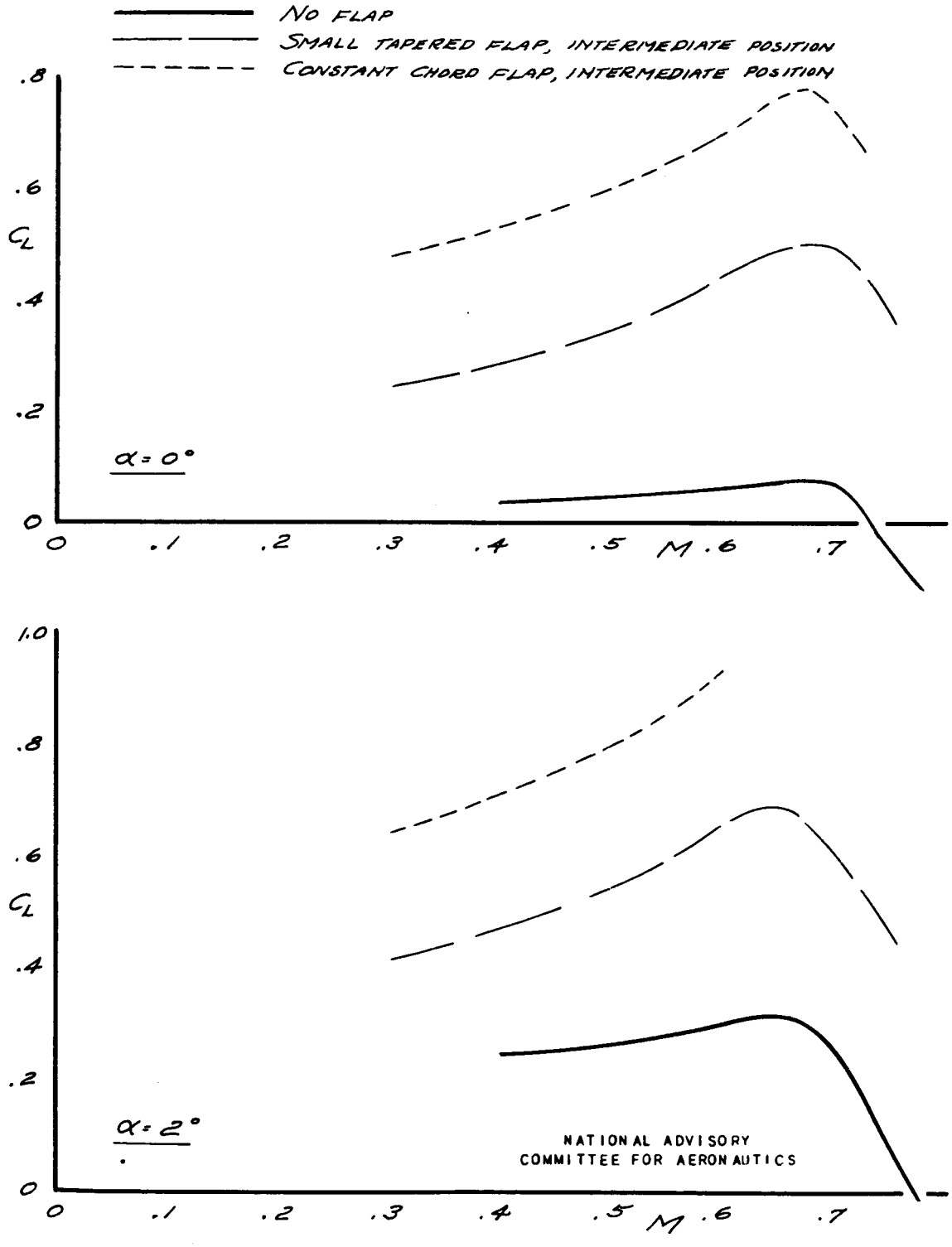

FIGURE 26 (a). - EFFECT OF 0.97 SPAN 45° AUXILIARY FLAPS ON LIFT COEFFICIENT. ANGLE OF ATTACK = 0° AND 2°.

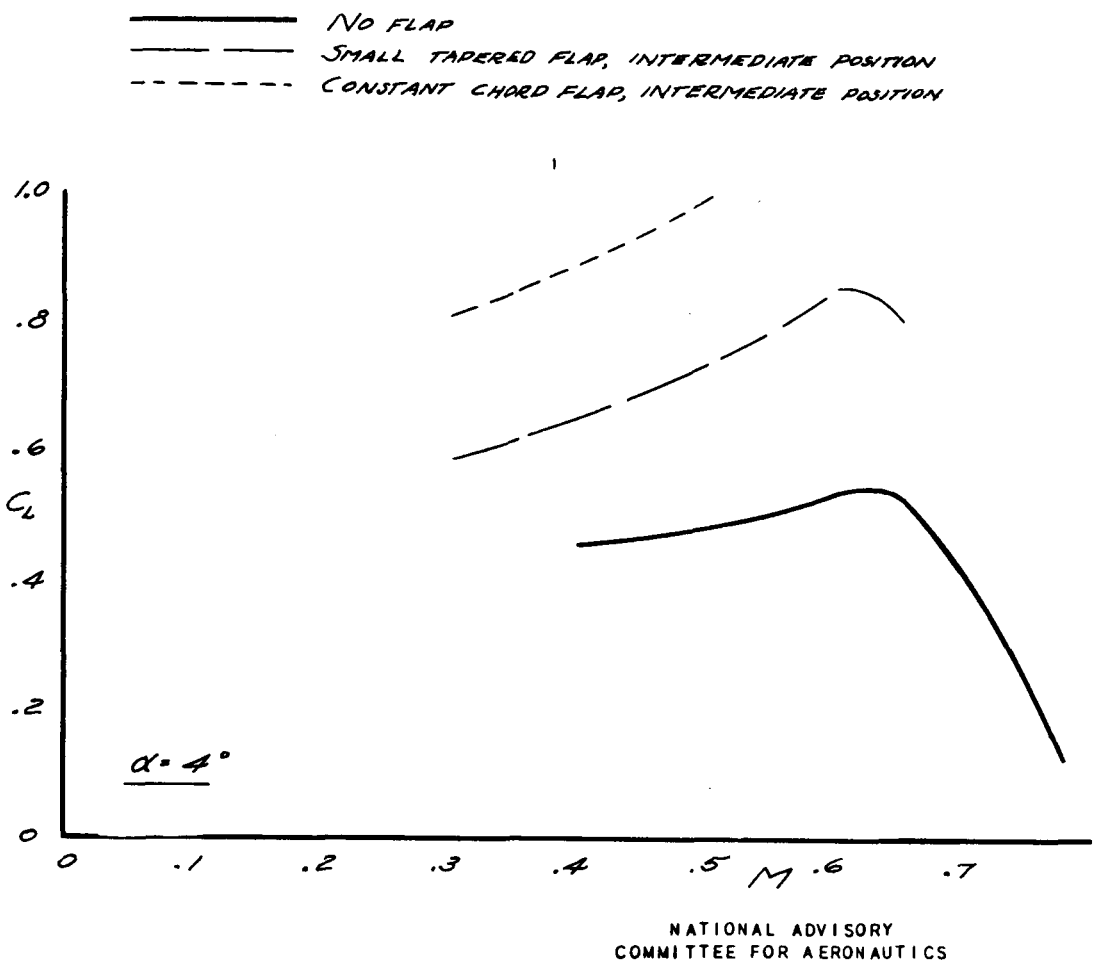

FIGURE 26 (b). - EFFECT OF 0.97 SPAN 45° AUXILIARY FLAPS ON LIFT COEFFICIENT. ANGLE OF ATTACK = 4°.

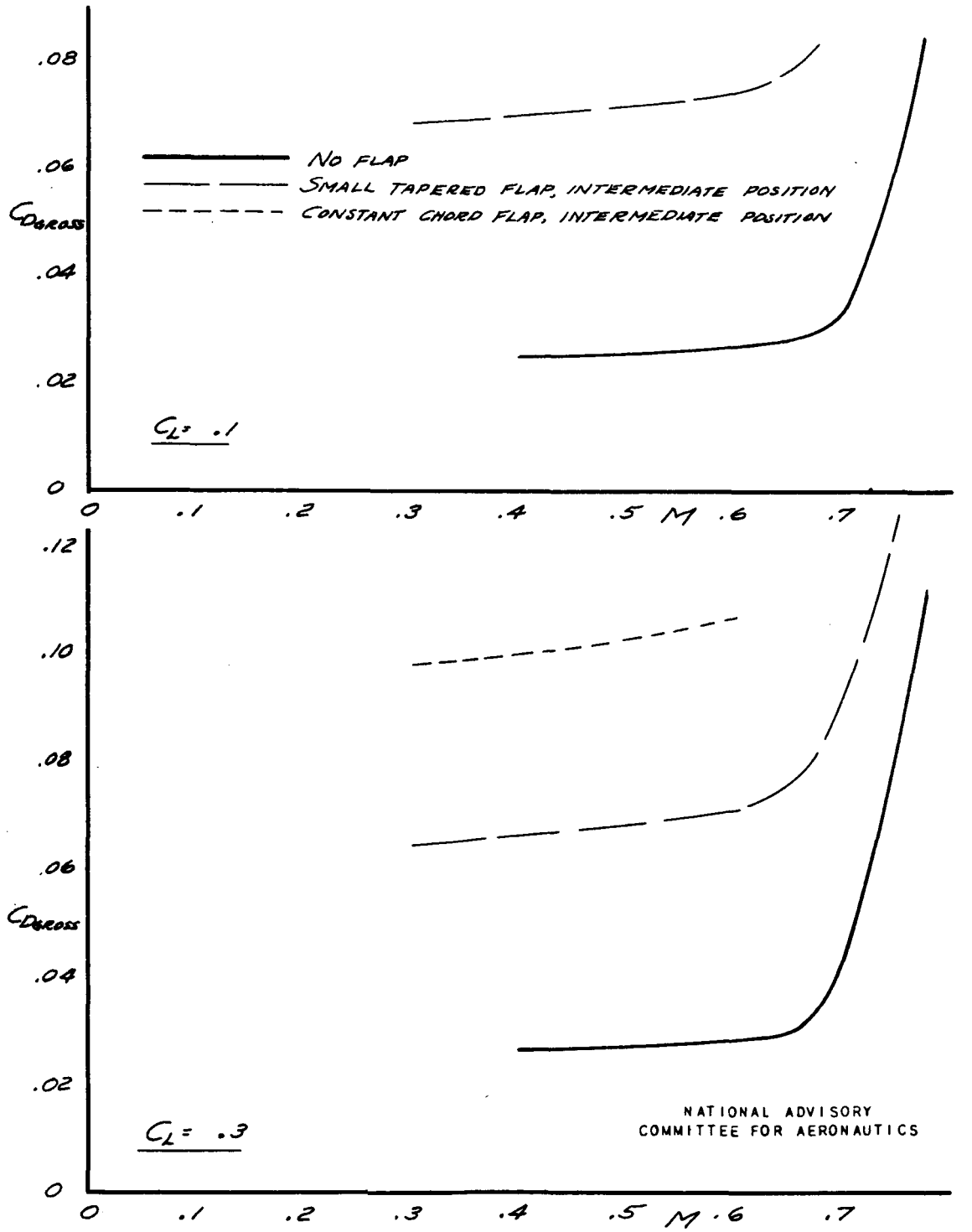

FIGURE 27(a). - EFFECT OF 0.97 SPAN 45° AUXILIARY FLAPS ON DRAG COEFFICIENT. LIFT COEFFICIENT = 0.1 AND 0.3.

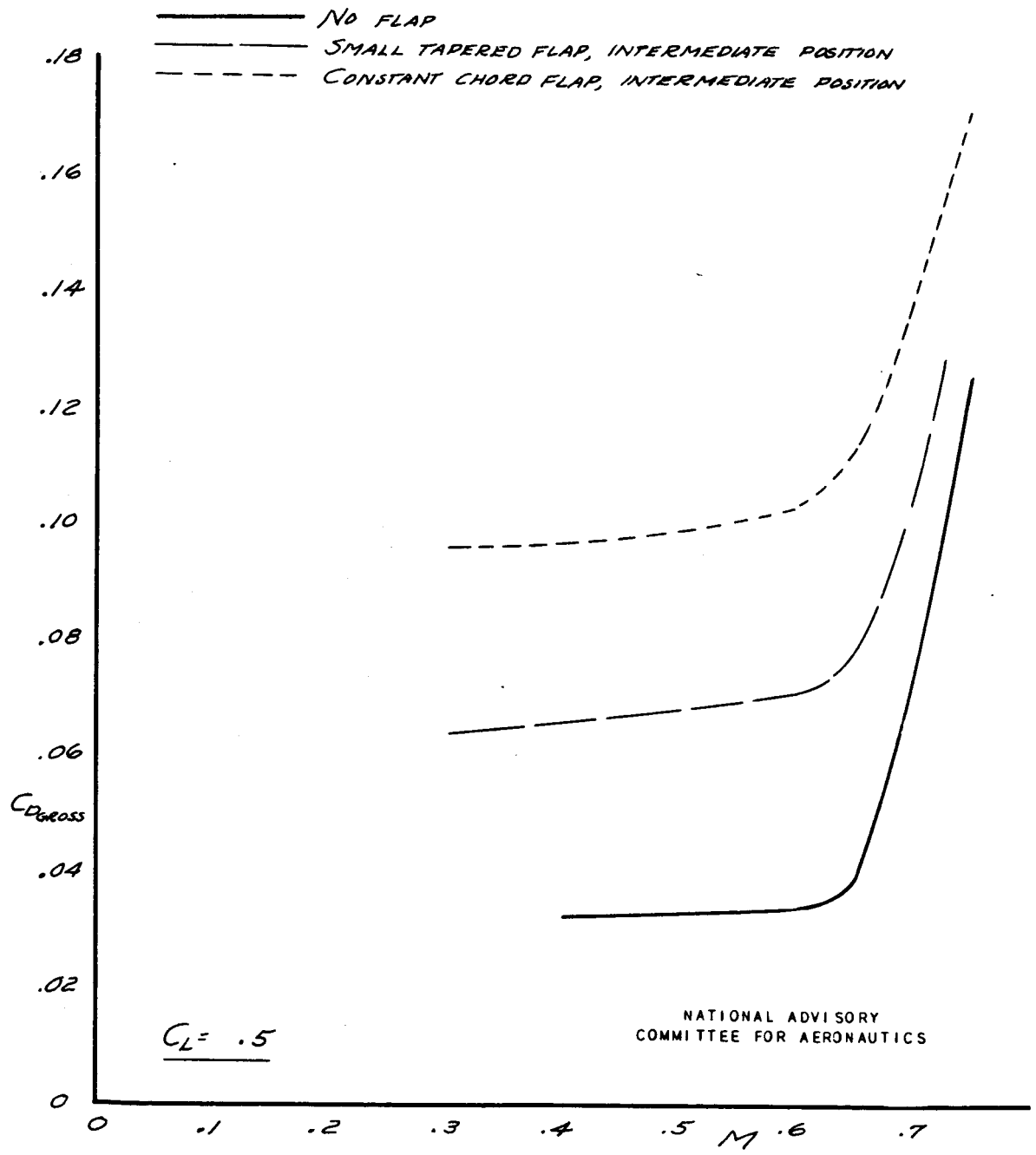

FIGURE 27(b). - EFFECT OF 0.97 SPAN 45° AUXILIARY FLAPS ON DRAG COEFFICIENT. LIFT COEFFICIENT = 0.5.

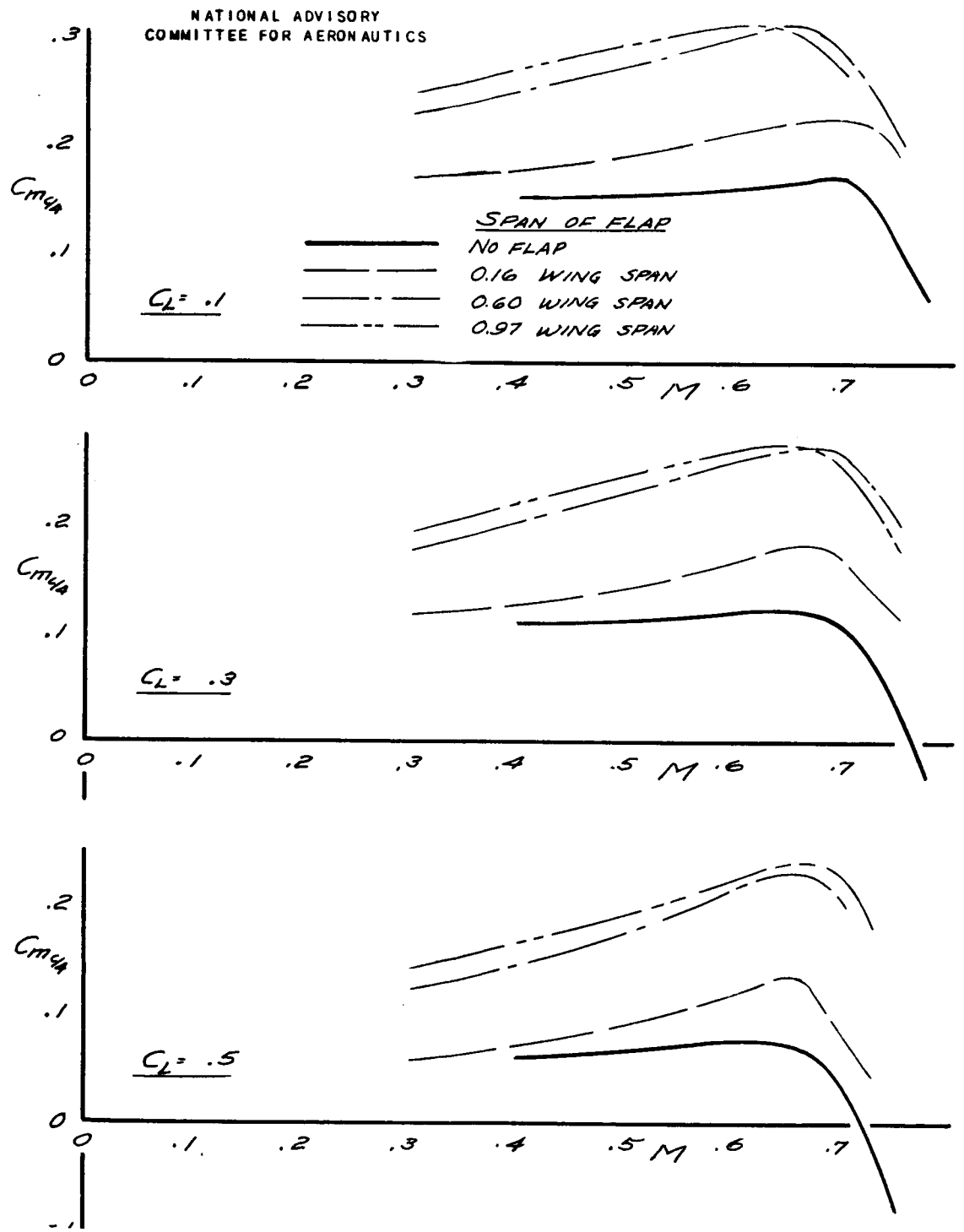

FIGURE 28. - EFFECT OF AUXILIARY FLAP SPAN ON PITCHING-MOMENT COEFFICIENT. SMALL TAPERED FLAPS, 45°, INTERMEDIATE POSITION.

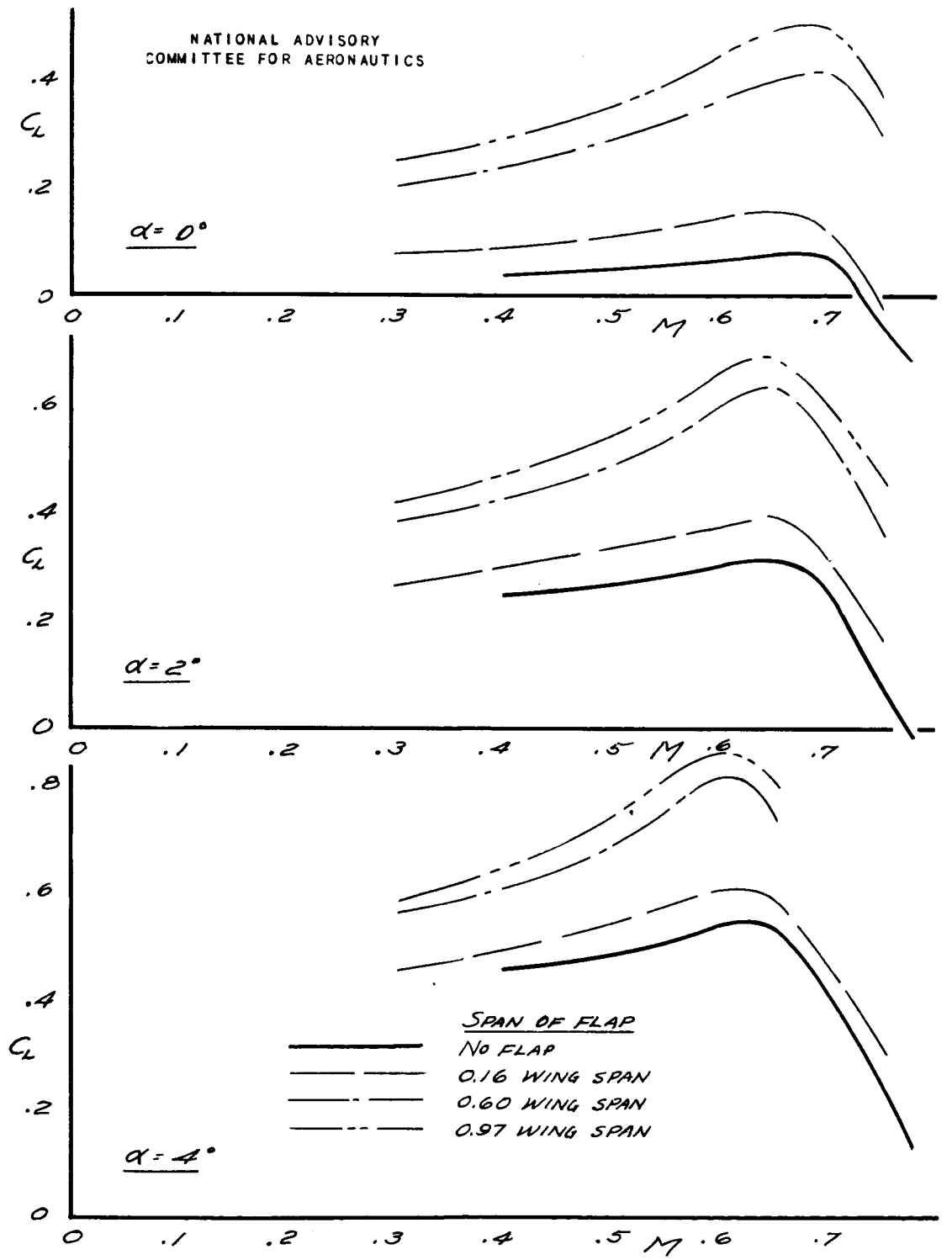

FIGURE 29. - EFFECT OF AUXILIARY FLAP SPAN ON LIFT COEFFICIENT. SMALL TAPERED FLAPS, 45°, INTERMEDIATE POSITION.

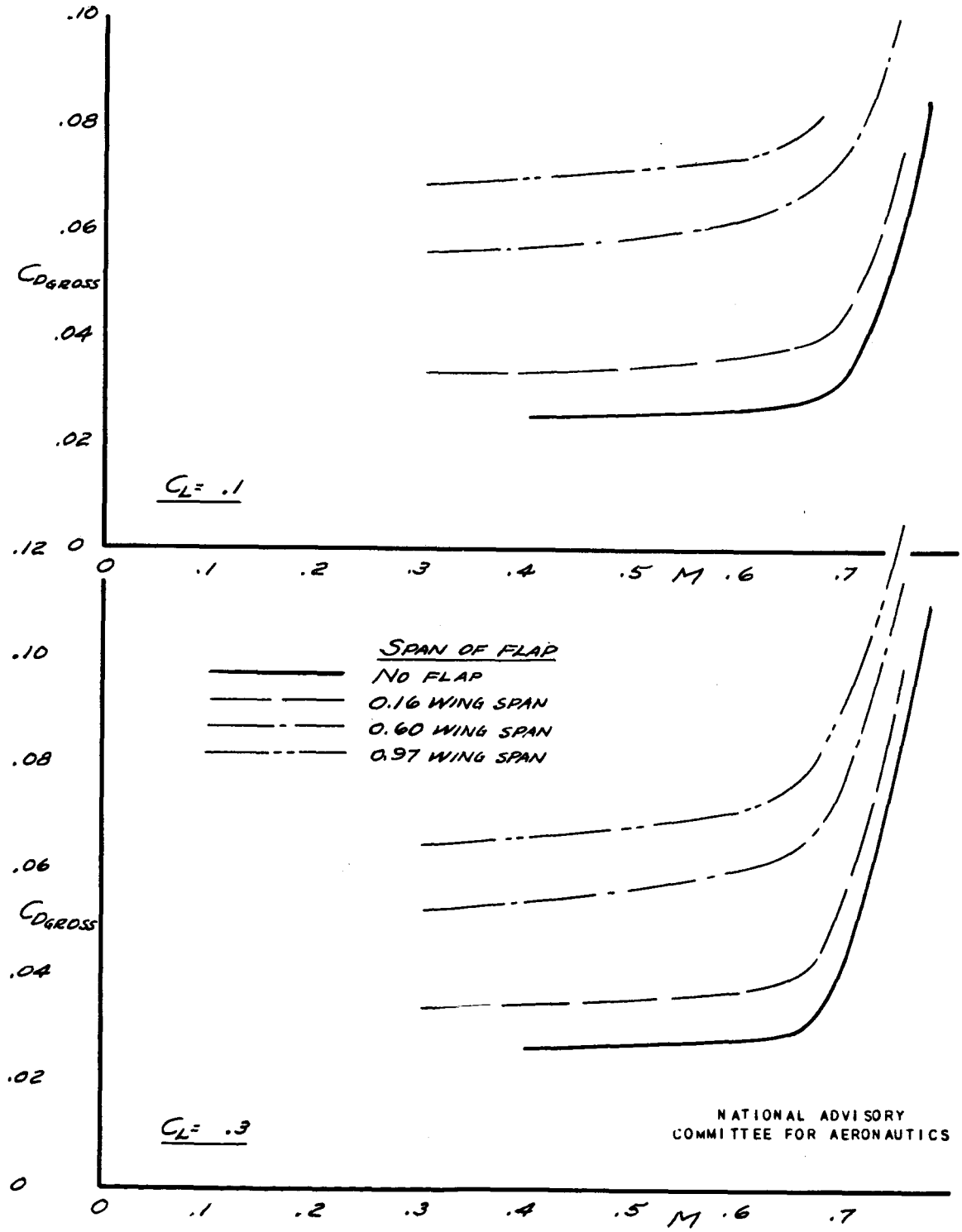

FIGURE 30(a). - EFFECT OF AUXILIARY FLAP SPAN ON DRAG COEFFICIENT. SMALL TAPERED FLAPS, 45°, INTERMEDIATE POSITION. LIFT COEFFICIENT = 0.1 AND 0.3.

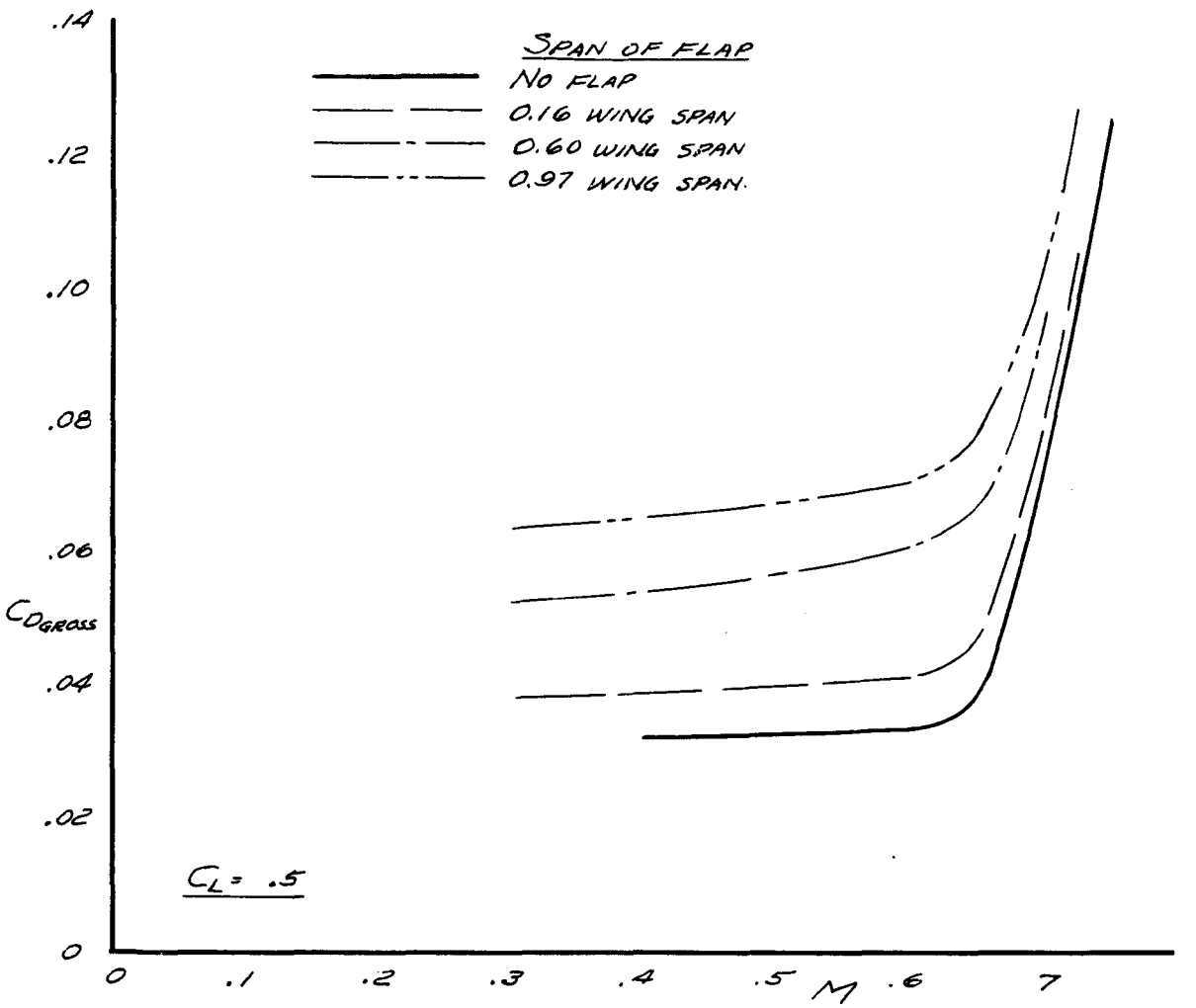

NATIONAL ADVISORY
COMMITTEE FOR AERONAUTICS

FIGURE 30(b). - EFFECT OF AUXILIARY FLAP SPAN ON DRAG COEFFICIENT. SMALL TAPERED FLAPS, 45°, INTERMEDIATE POSITION. LIFT COEFFICIENT = 0.5.

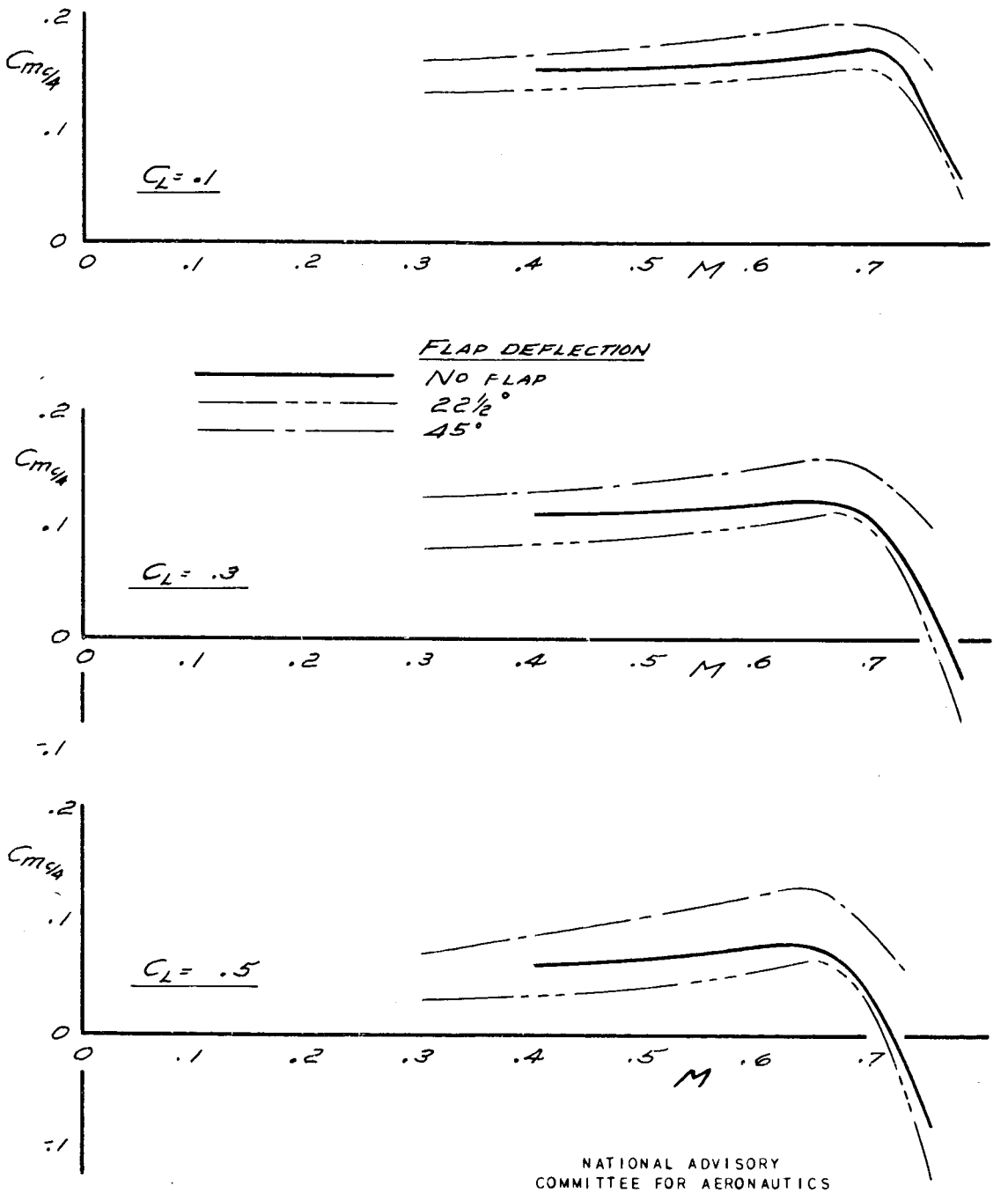

FIGURE 31. - EFFECT OF AUXILIARY FLAP DEFLECTION ON PITCHING-MOMENT COEFFICIENT. SMALL TAPERED FLAP ALONG REAR SPAR; FLAP SPAN, 0.16 WING SPAN.

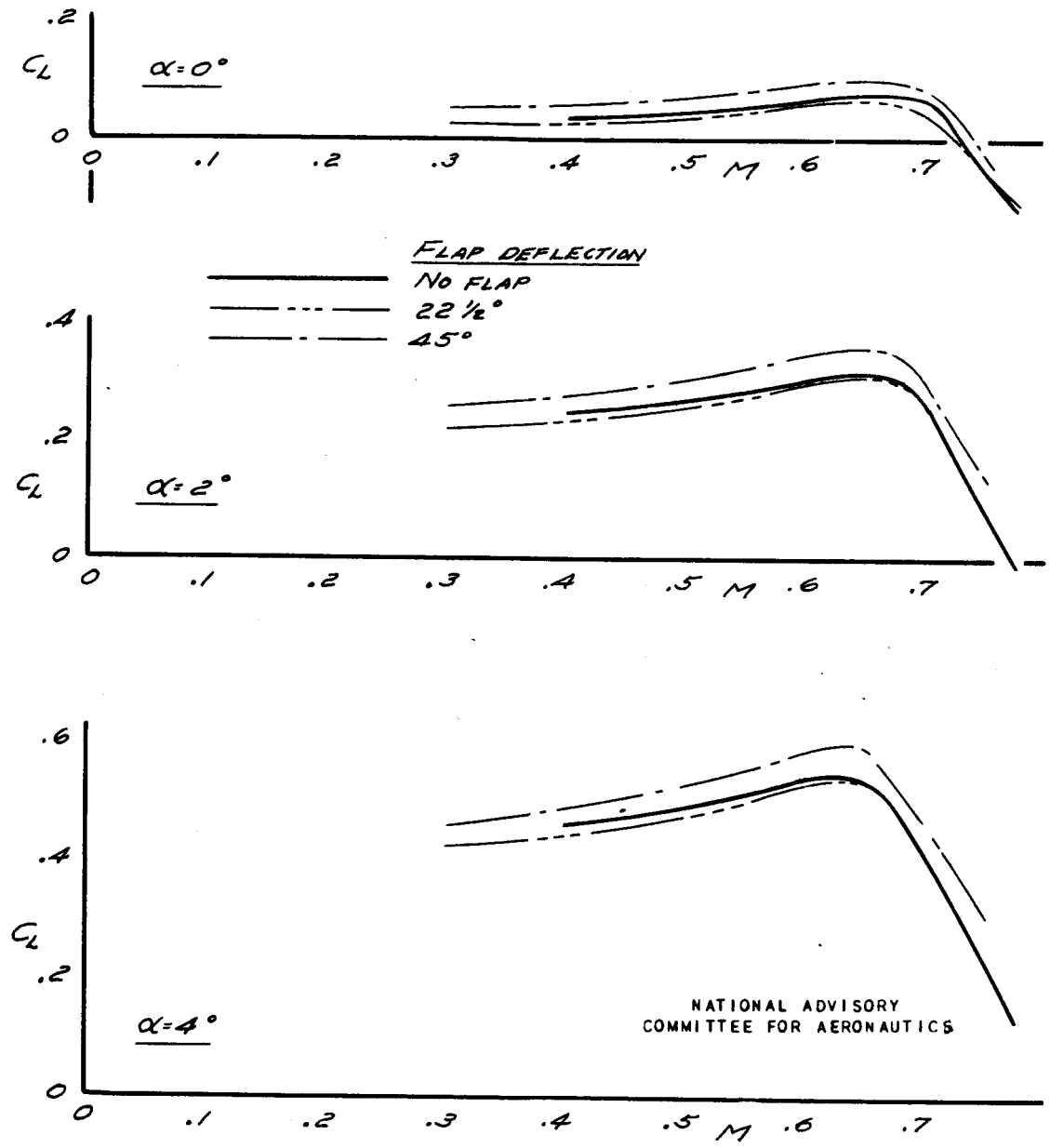

FIGURE 32. - EFFECT OF AUXILIARY FLAP DEFLECTION ON LIFT COEFFICIENT. SMALL TAPERED FLAP ALONG REAR SPAR; FLAP SPAN, 0.16 WING SPAN.

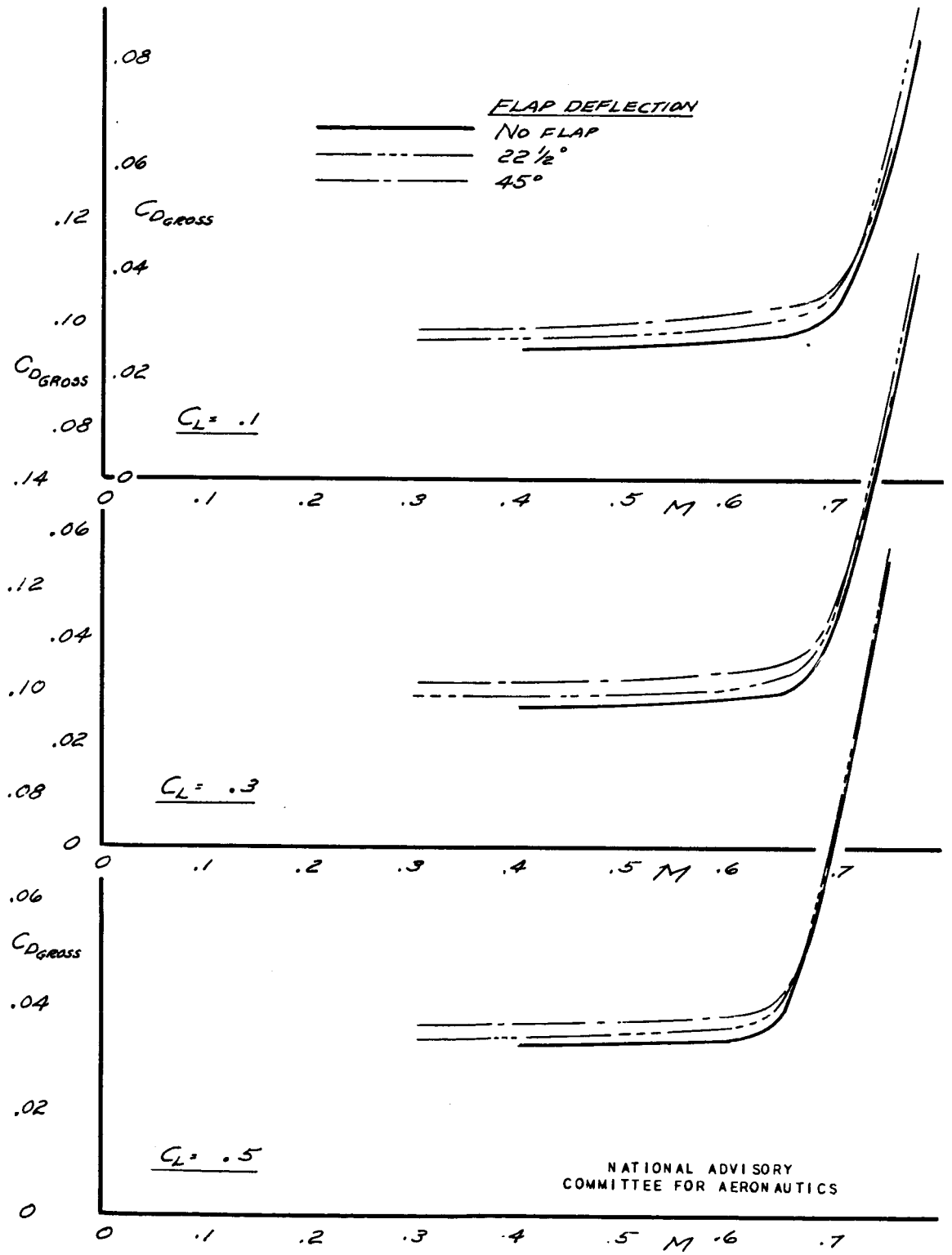

FIGURE 33. - EFFECT OF AUXILIARY FLAP DEFLECTION ON DRAG COEFFICIENT. SMALL TAPERED FLAP ALONG REAR SPAR; FLAP SPAN, 0.16 WING SPAN.

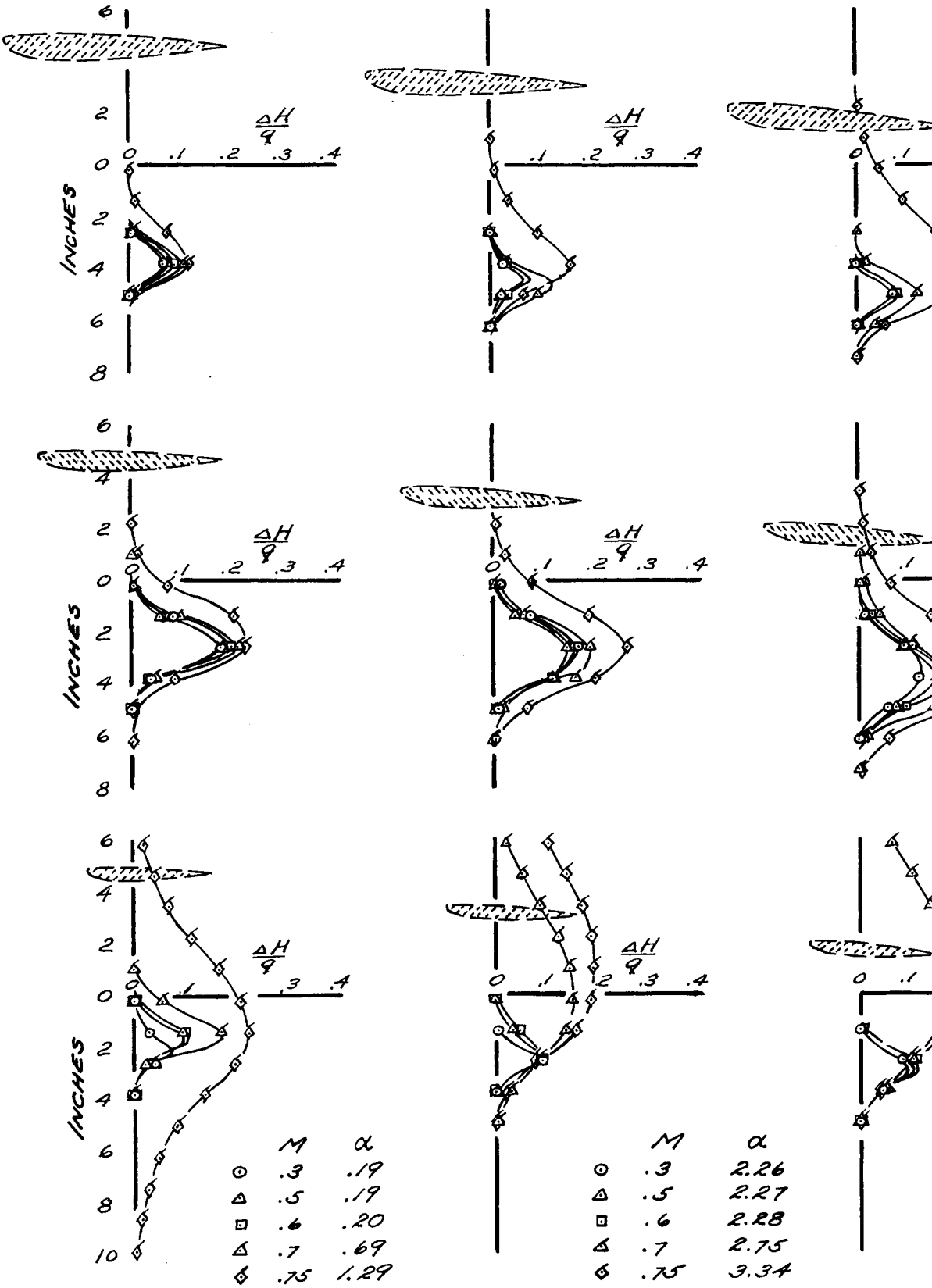
INCHES
ΔH/q
0 .1 .2 .3 .4
M α
.3 .19
.5 .19
.6 .20
.7 .69
.75 1.29
M α
.3 2.26
.5 2.27
.6 2.28
.7 2.75
.75 3.34

FIGURE 34A

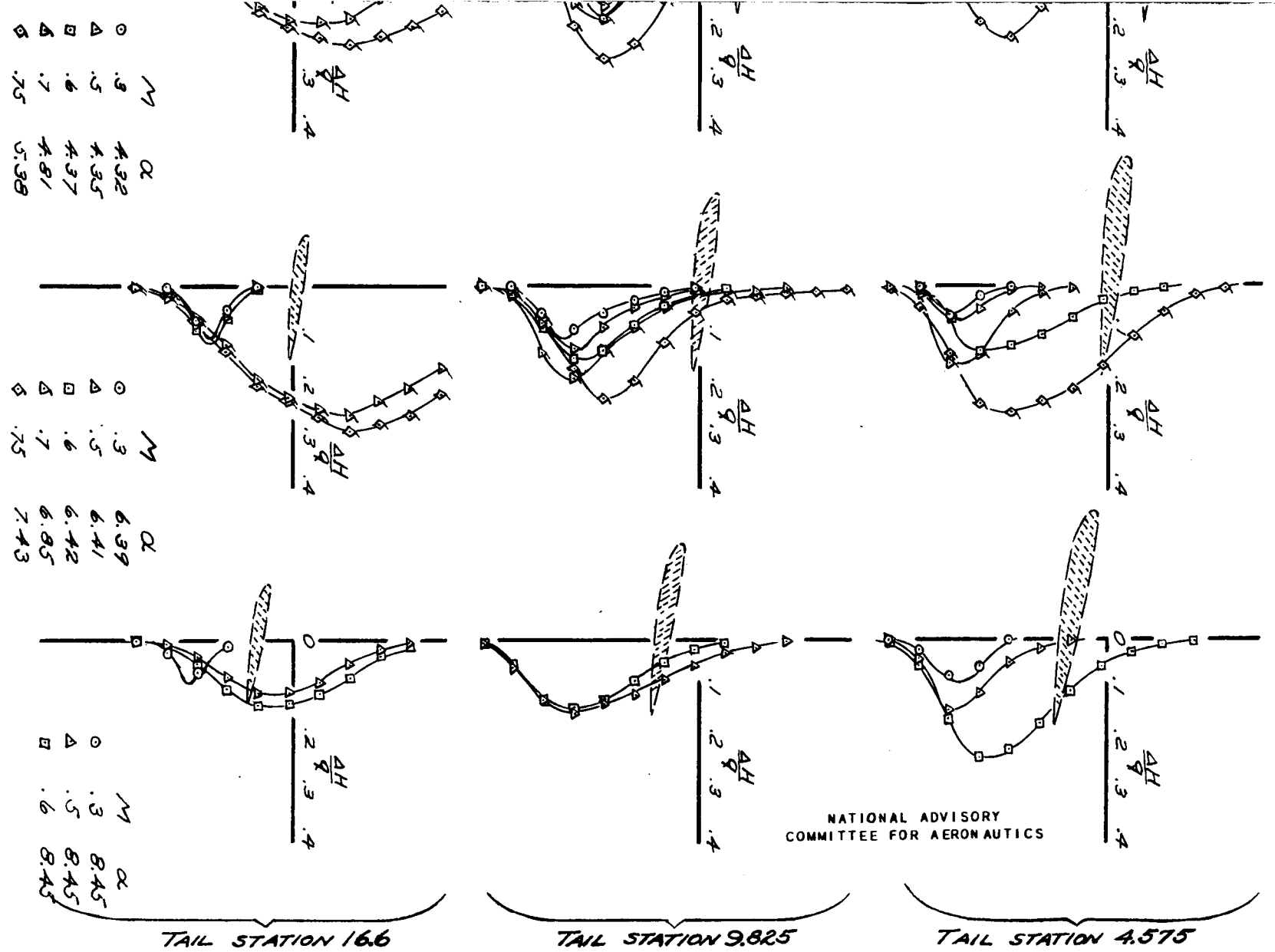

FIGURE 34.B POSITION OF WING WAKE RELATIVE TO THE TAIL AT VARIOUS MACH NUMBERS AND ANGLES OF ATTACK. WING, NACELLES, FUSELAGE, AND TURRETS AND SIGHTING DOMES.

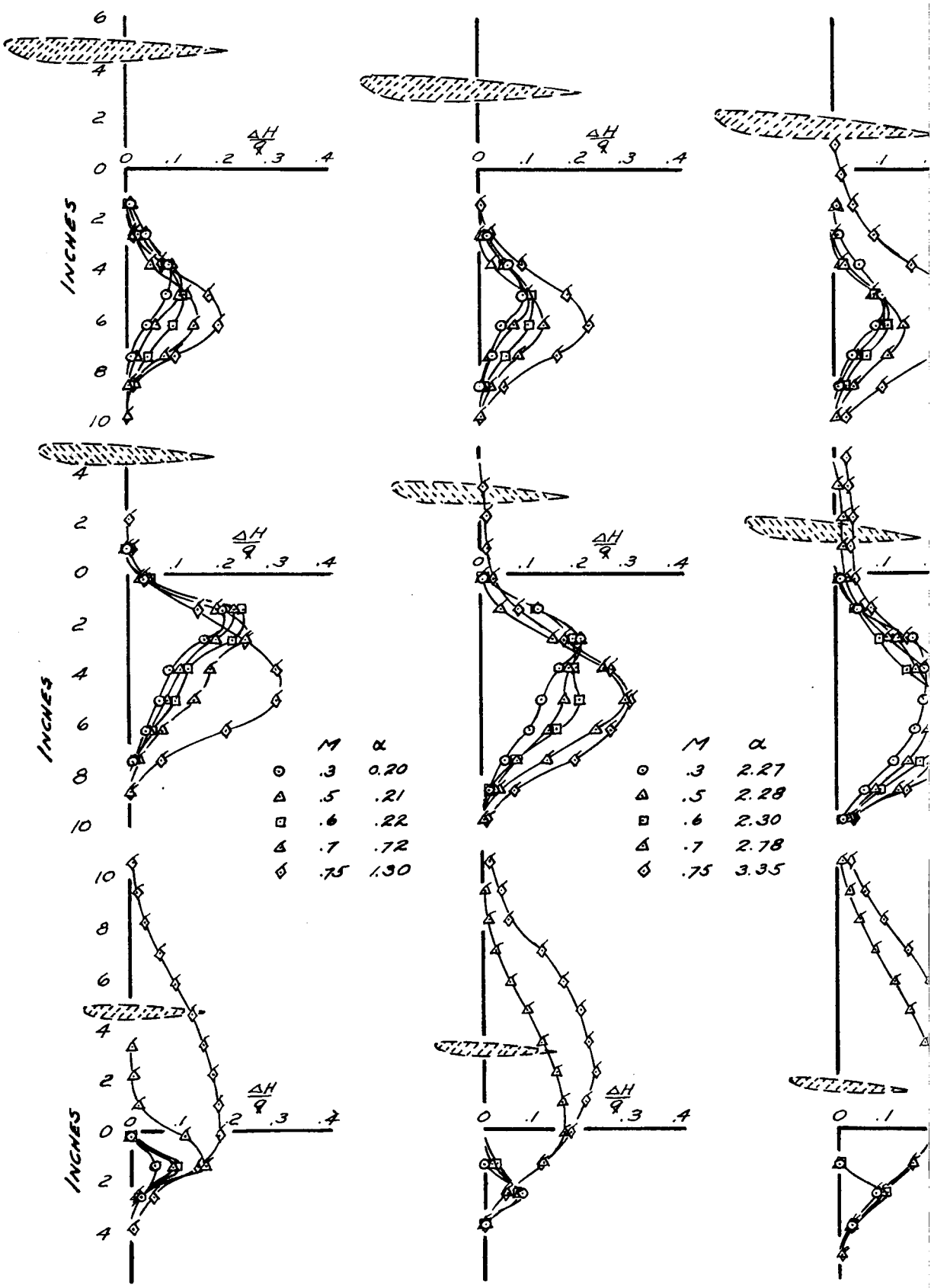
INCHES
ΔH/q
M α
.3 0.20
.5 .21
.6 .22
.7 .72
.75 1.30
M α
.3 2.27
.5 2.28
.6 2.30
.7 2.78
.75 3.35

FIGURE 35A

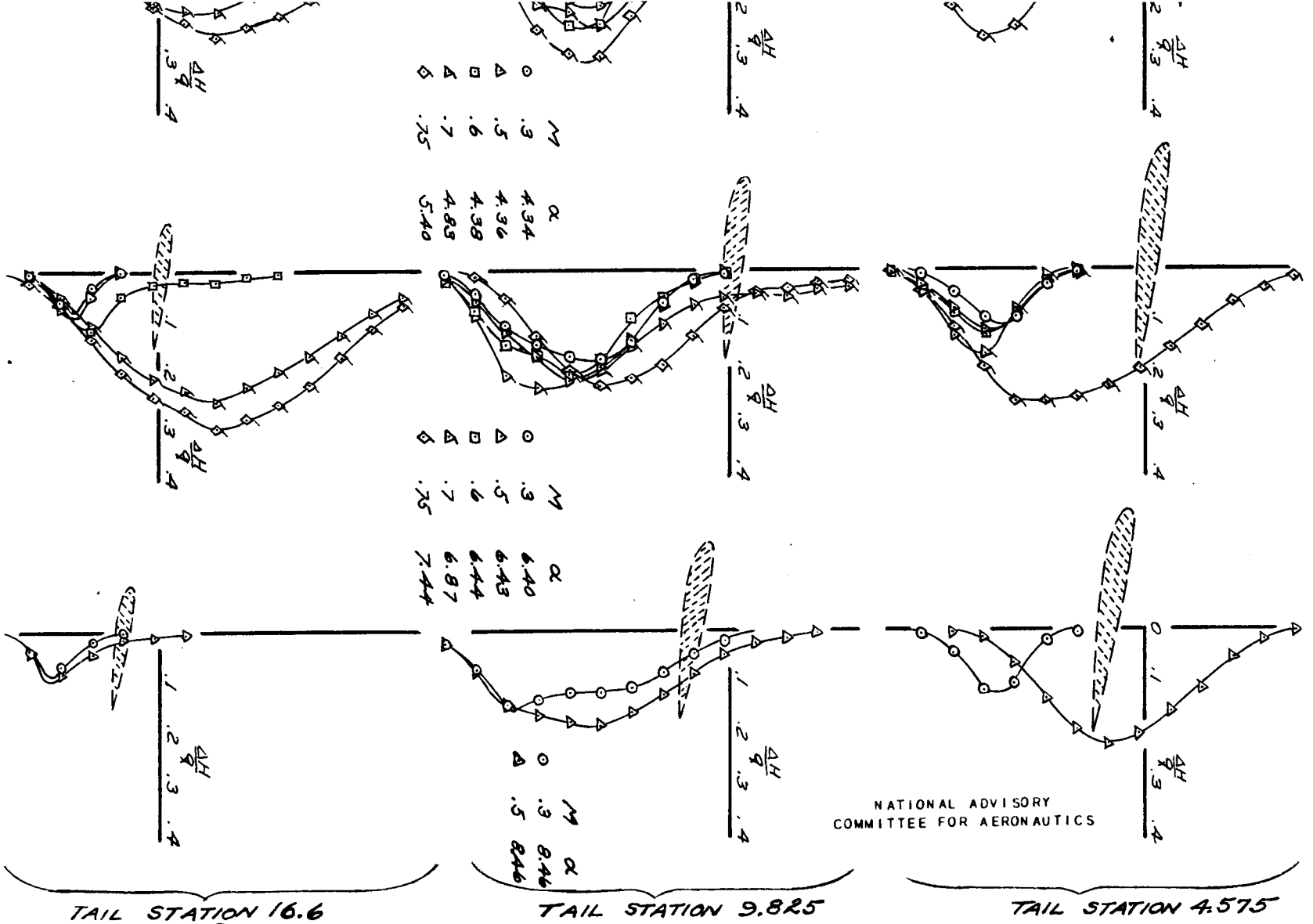

FIGURE 35.B POSITION OF WING WAKE RELATIVE TO THE TAIL AT VARIOUS MACH NUMBERS AND ANGLES OF ATTACK. WING, NACELLES, FUSELAGE, TURRETS AND SIGHTING DOMES, AND SMALL 45° TAPERED FLAPS ALONG REAR SPAR BETWEEN FUSELAGE AND INBOARD NACELLES.

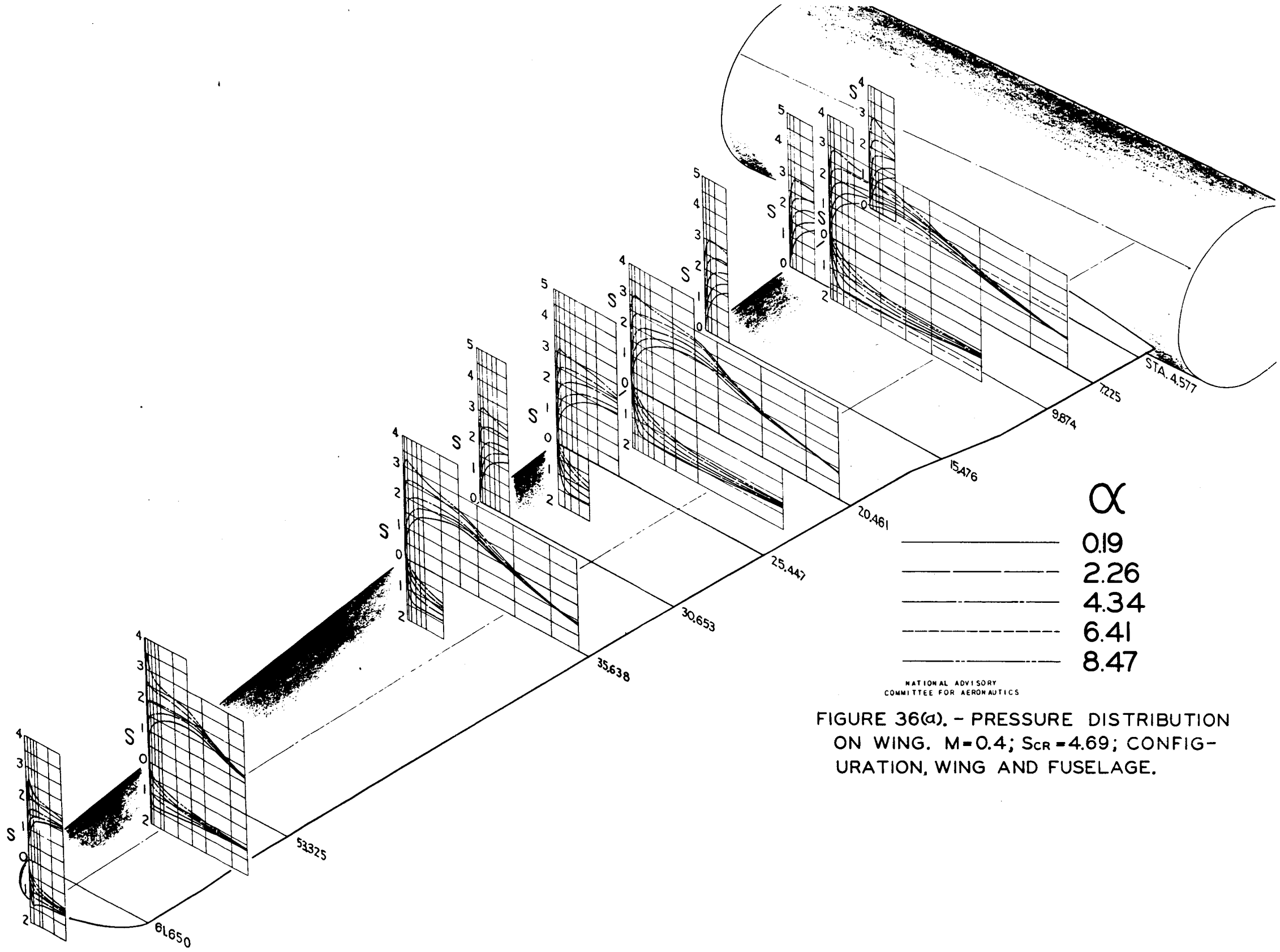

α
0.19
2.26
4.34
6.41
8.47

NATIONAL ADVISORY
COMMITTEE FOR AERONAUTICS

FIGURE 36(a). - PRESSURE DISTRIBUTION ON WING. M=0.4; S_{CR}=4.69; CONFIGURATION, WING AND FUSELAGE.

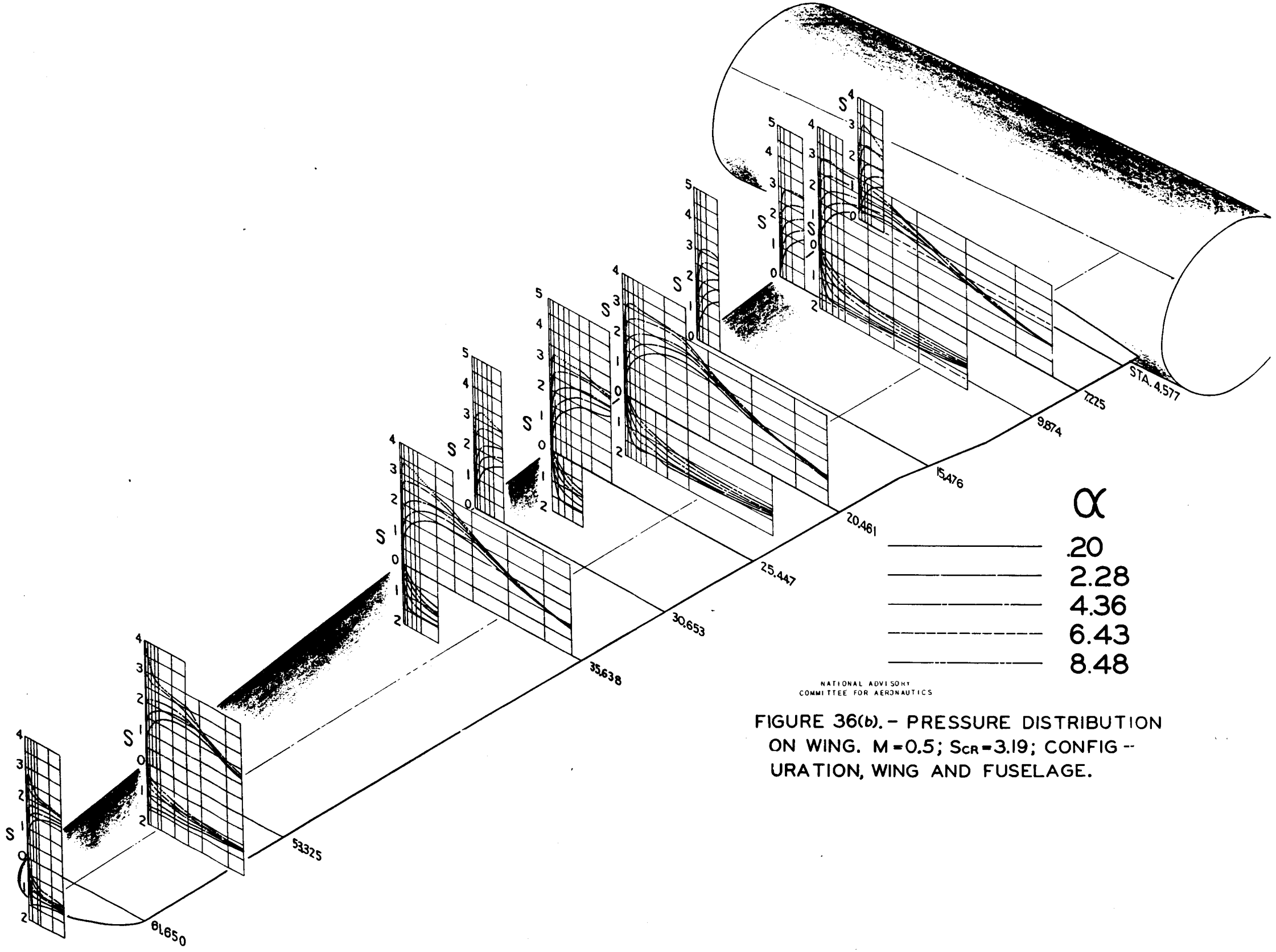

FIGURE 36(b). – PRESSURE DISTRIBUTION ON WING. M = 0.5; S_{CR} = 3.19; CONFIG-URATION, WING AND FUSELAGE.

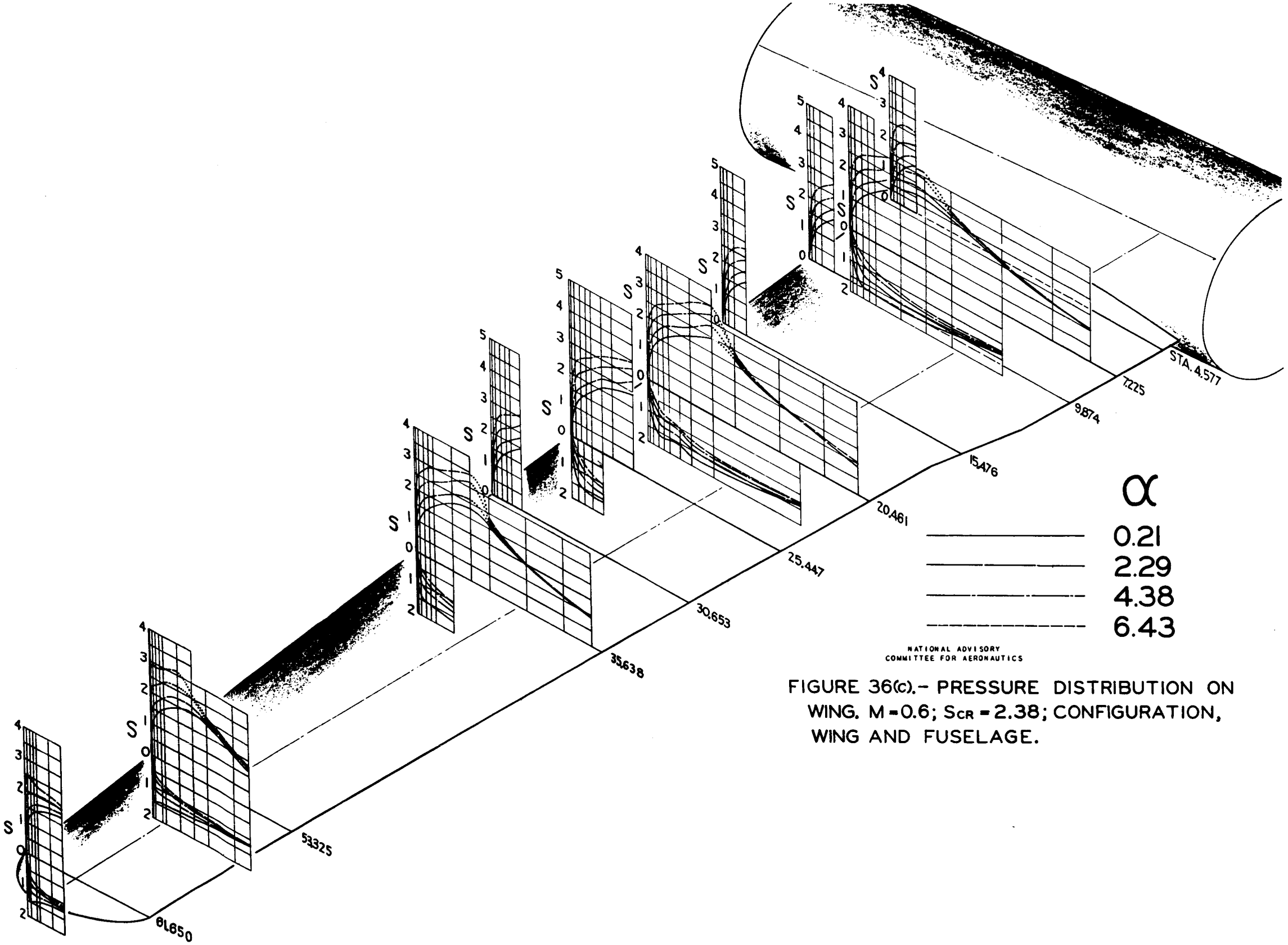

FIGURE 36(c).- PRESSURE DISTRIBUTION ON WING. M = 0.6; S_{CR} = 2.38; CONFIGURATION, WING AND FUSELAGE.

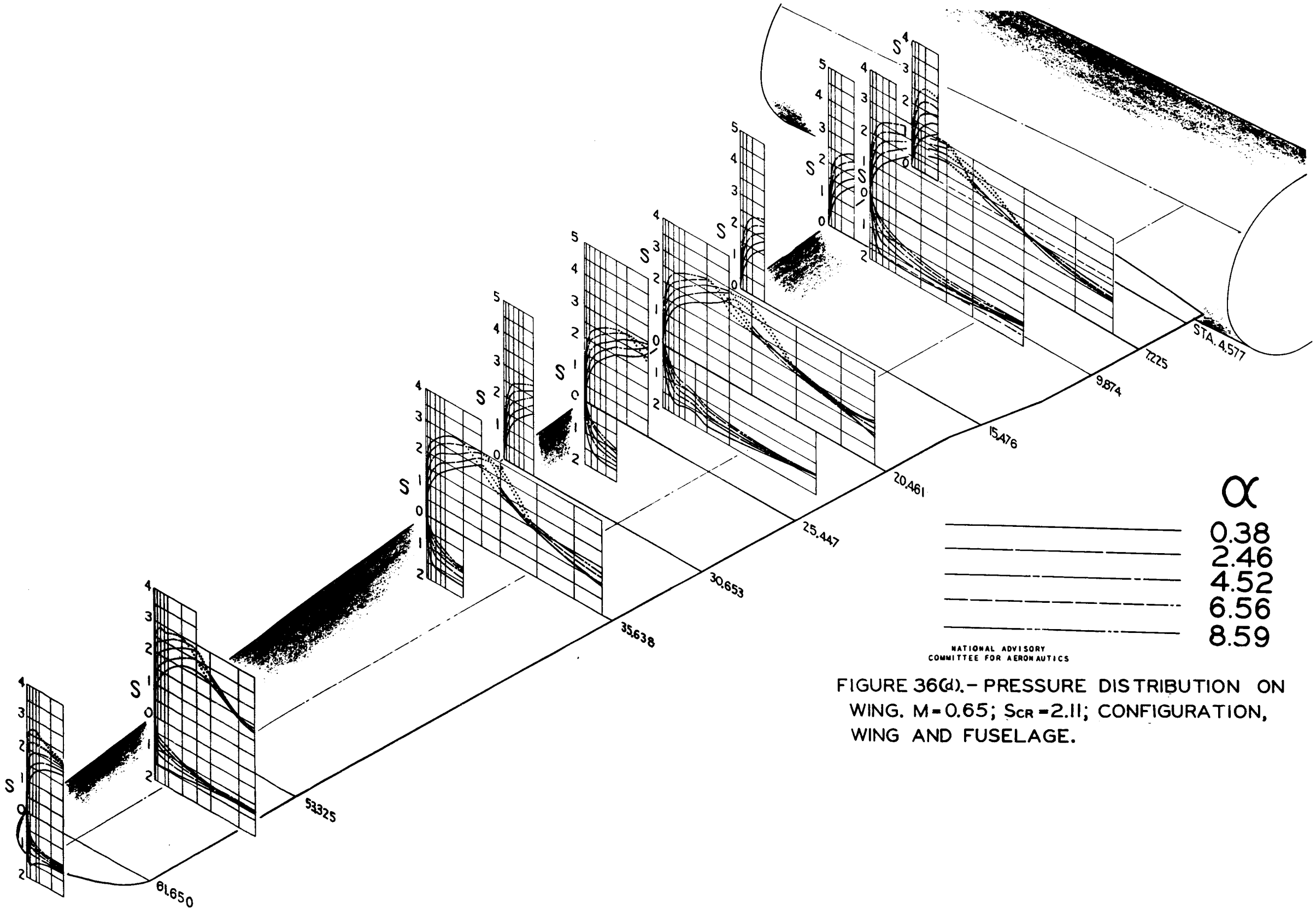

FIGURE 36(d).- PRESSURE DISTRIBUTION ON WING. M = 0.65; S_{CR} = 2.11; CONFIGURATION, WING AND FUSELAGE.

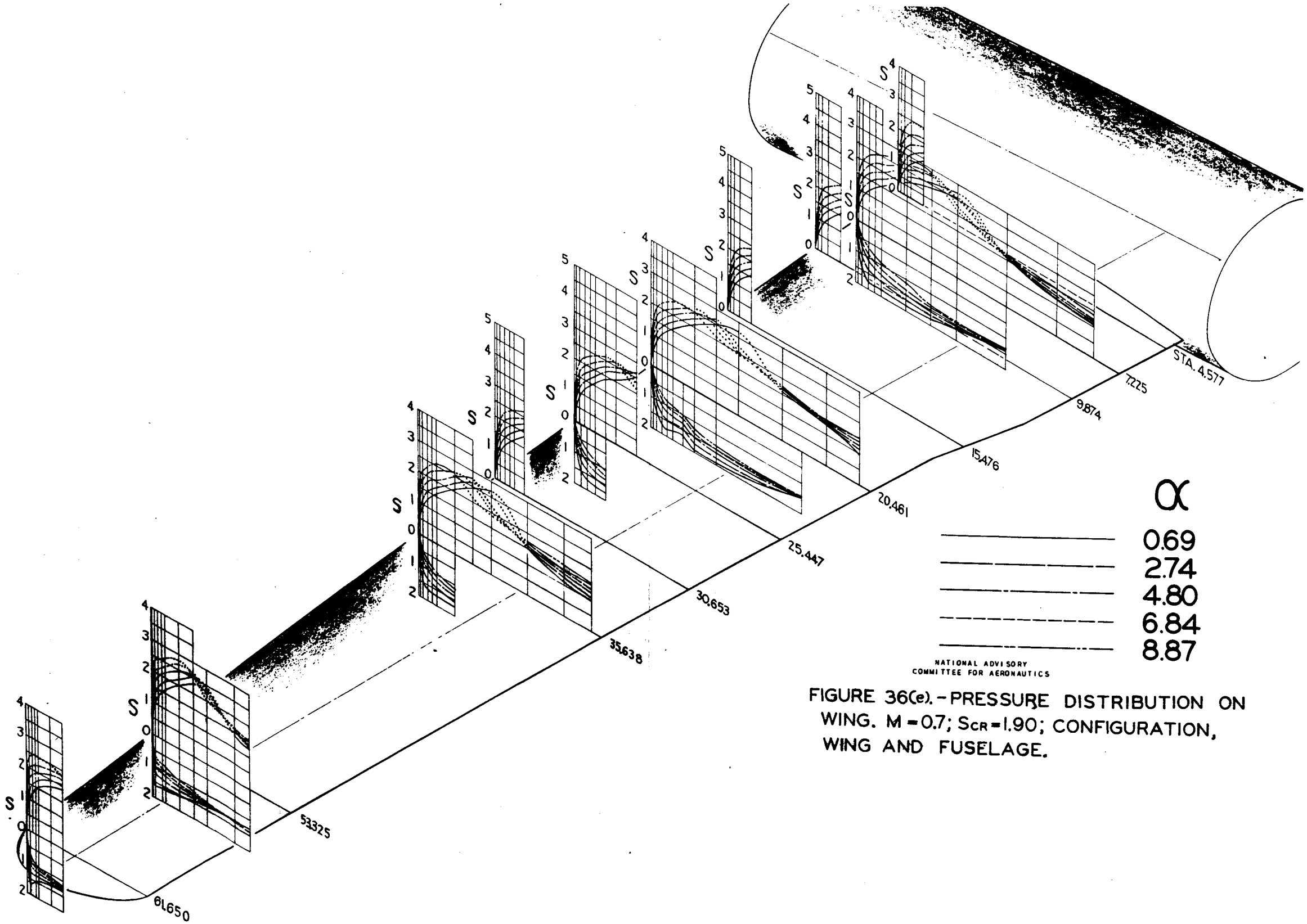

FIGURE 36(e). - PRESSURE DISTRIBUTION ON WING. M = 0.7; S_{CR} = 1.90; CONFIGURATION, WING AND FUSELAGE.

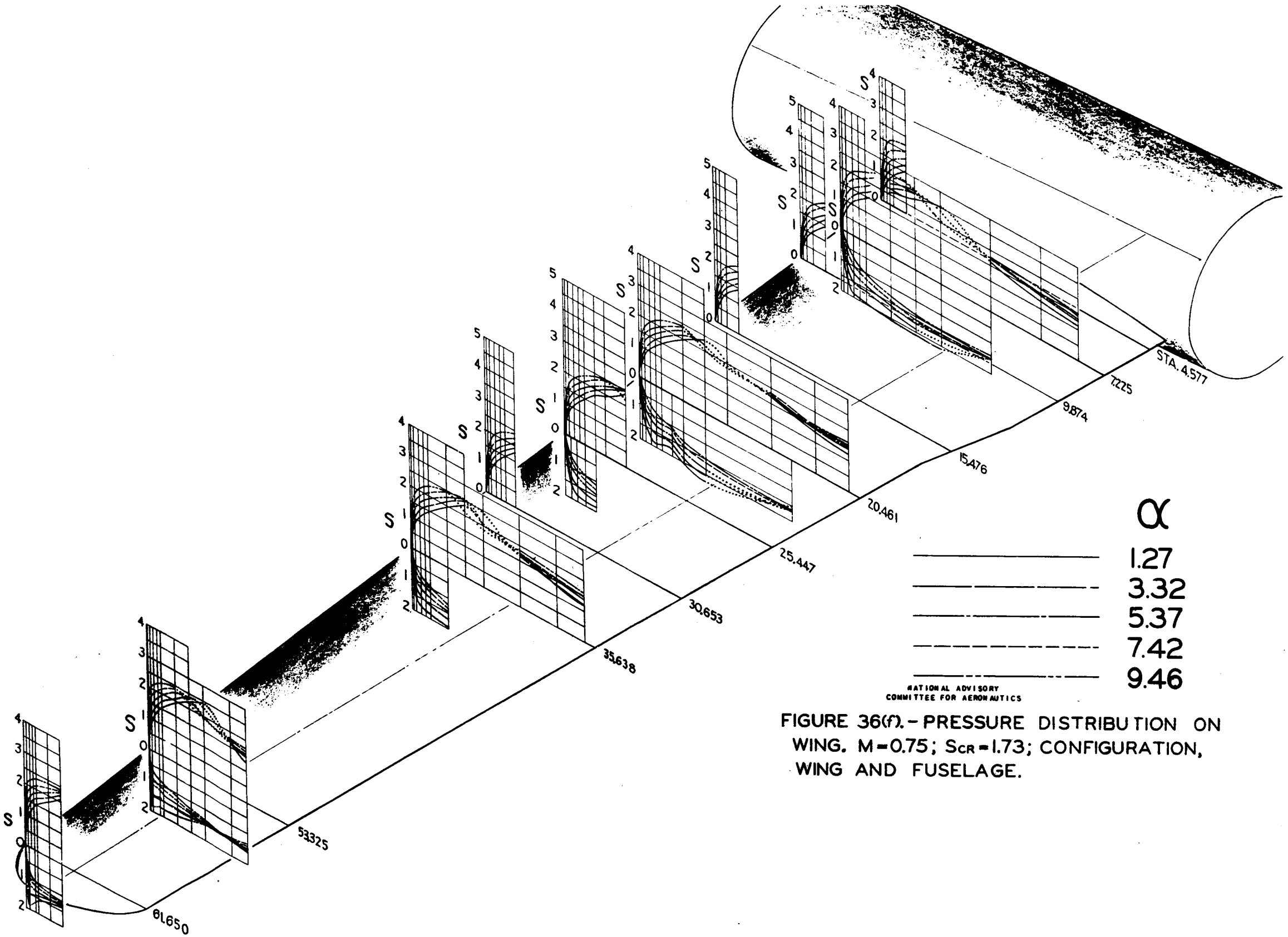

FIGURE 36(f). – PRESSURE DISTRIBUTION ON WING. M=0.75; S_{CR}=1.73; CONFIGURATION, WING AND FUSELAGE.

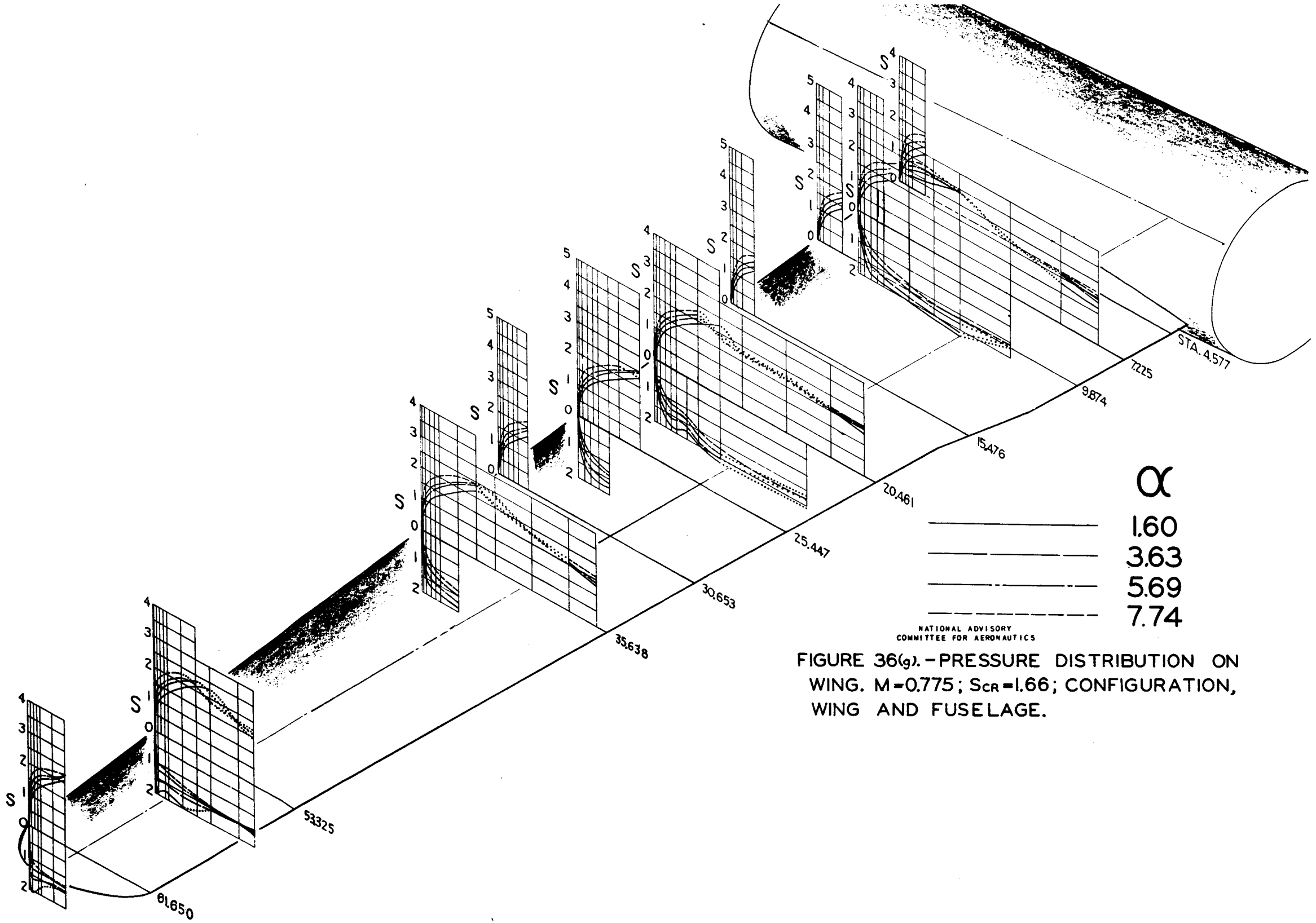

FIGURE 36(g). – PRESSURE DISTRIBUTION ON WING. M=0.775; S_{CR}=1.66; CONFIGURATION, WING AND FUSELAGE.

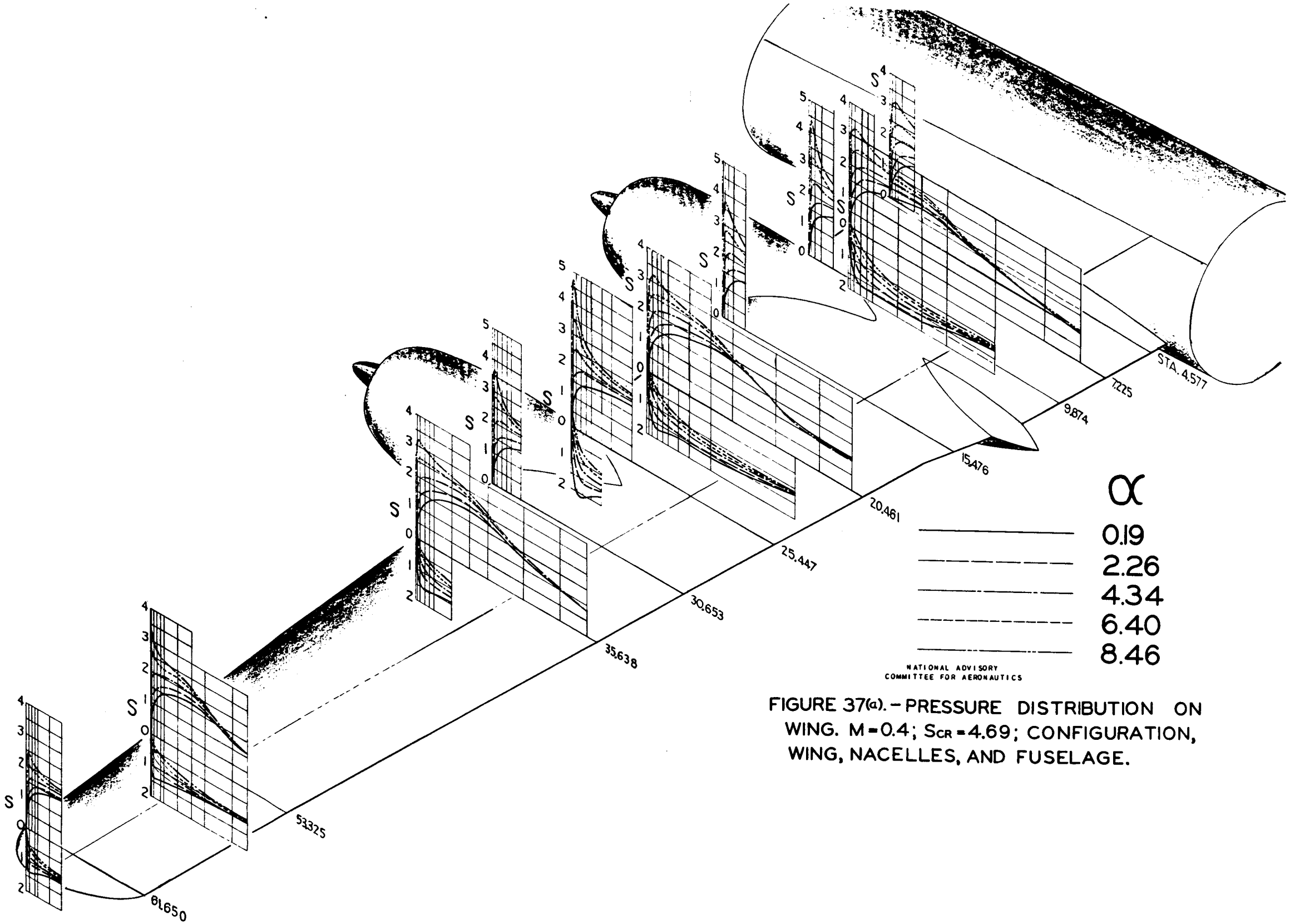

FIGURE 37(a). – PRESSURE DISTRIBUTION ON WING. M = 0.4; S_{CR} = 4.69; CONFIGURATION, WING, NACELLES, AND FUSELAGE.

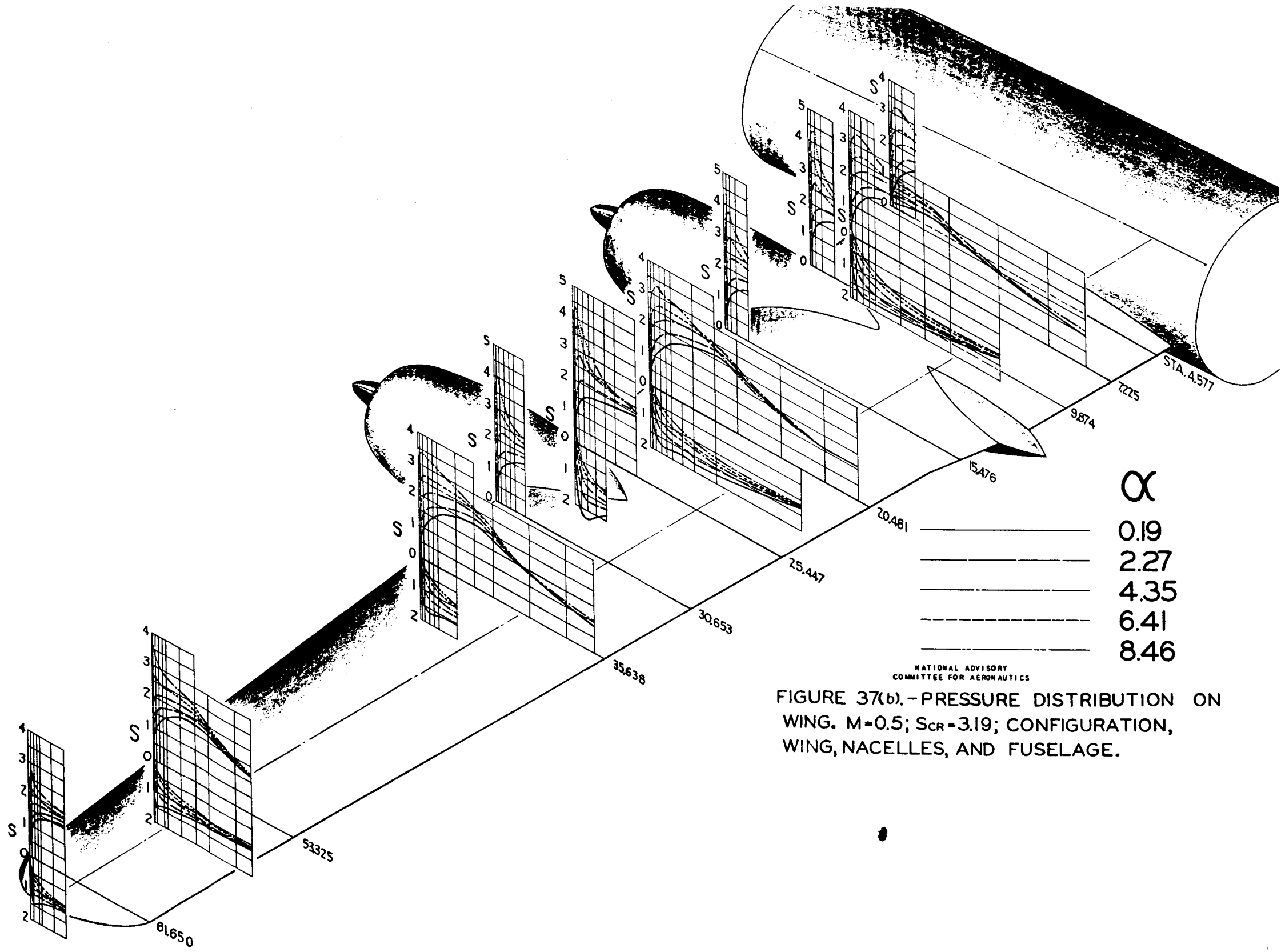

FIGURE 37(b).- PRESSURE DISTRIBUTION ON WING. M=0.5; S_{CR}=3.19; CONFIGURATION, WING, NACELLES, AND FUSELAGE.

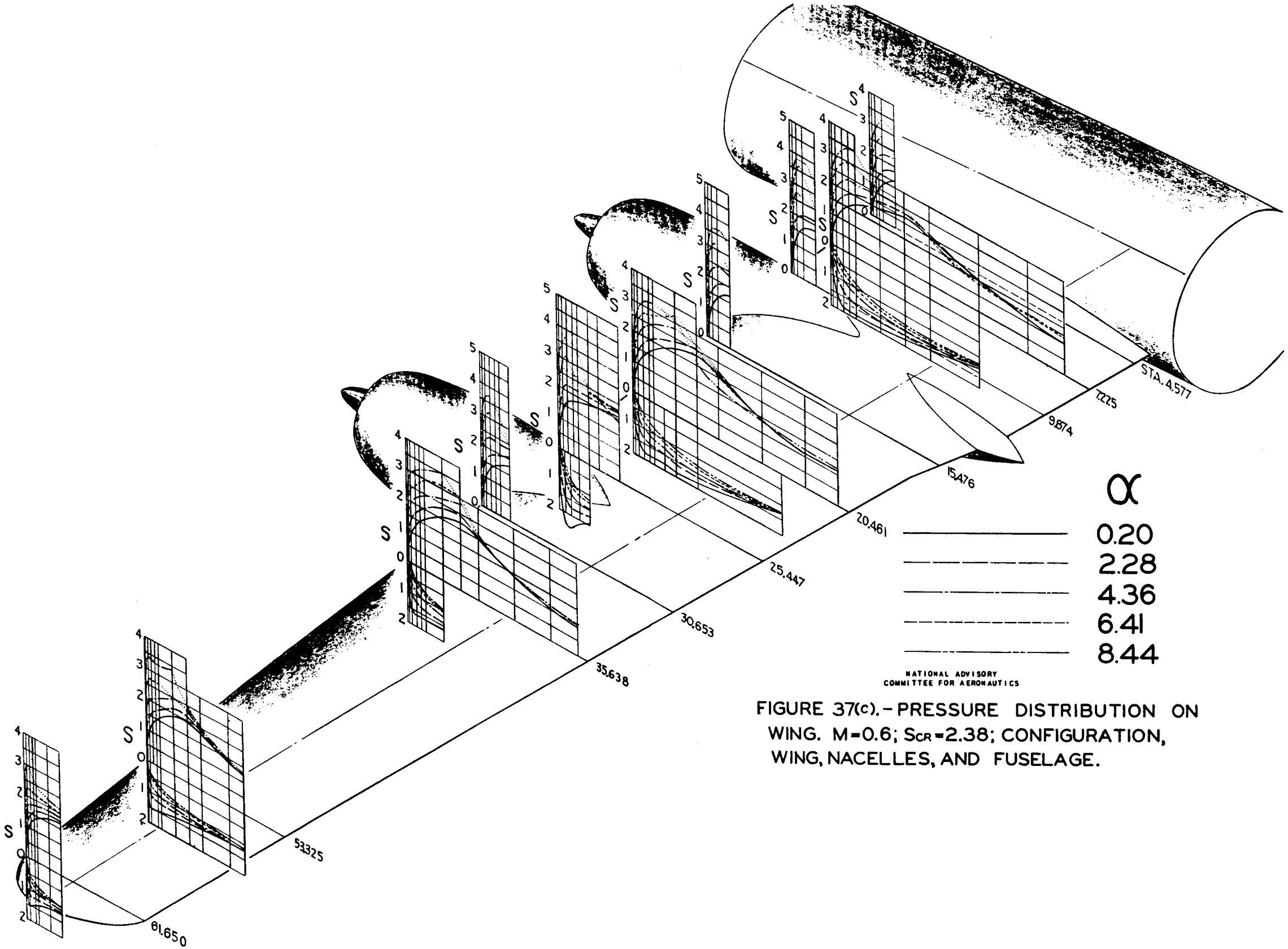

FIGURE 37(c).- PRESSURE DISTRIBUTION ON WING. M=0.6; S_{CR}=2.38; CONFIGURATION, WING, NACELLES, AND FUSELAGE.

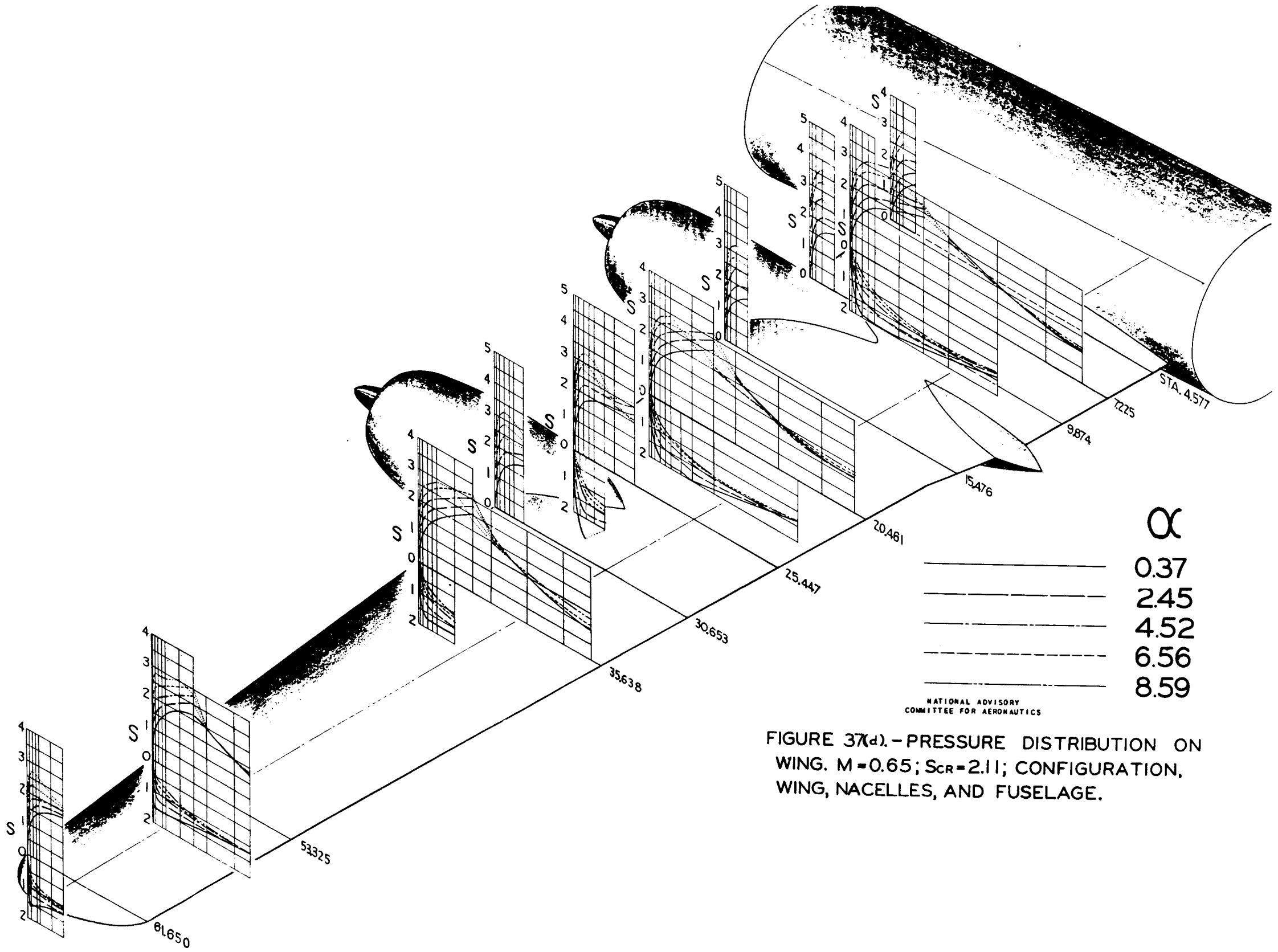

FIGURE 37(d). – PRESSURE DISTRIBUTION ON WING. M = 0.65; S_{CR} = 2.11; CONFIGURATION, WING, NACELLES, AND FUSELAGE.

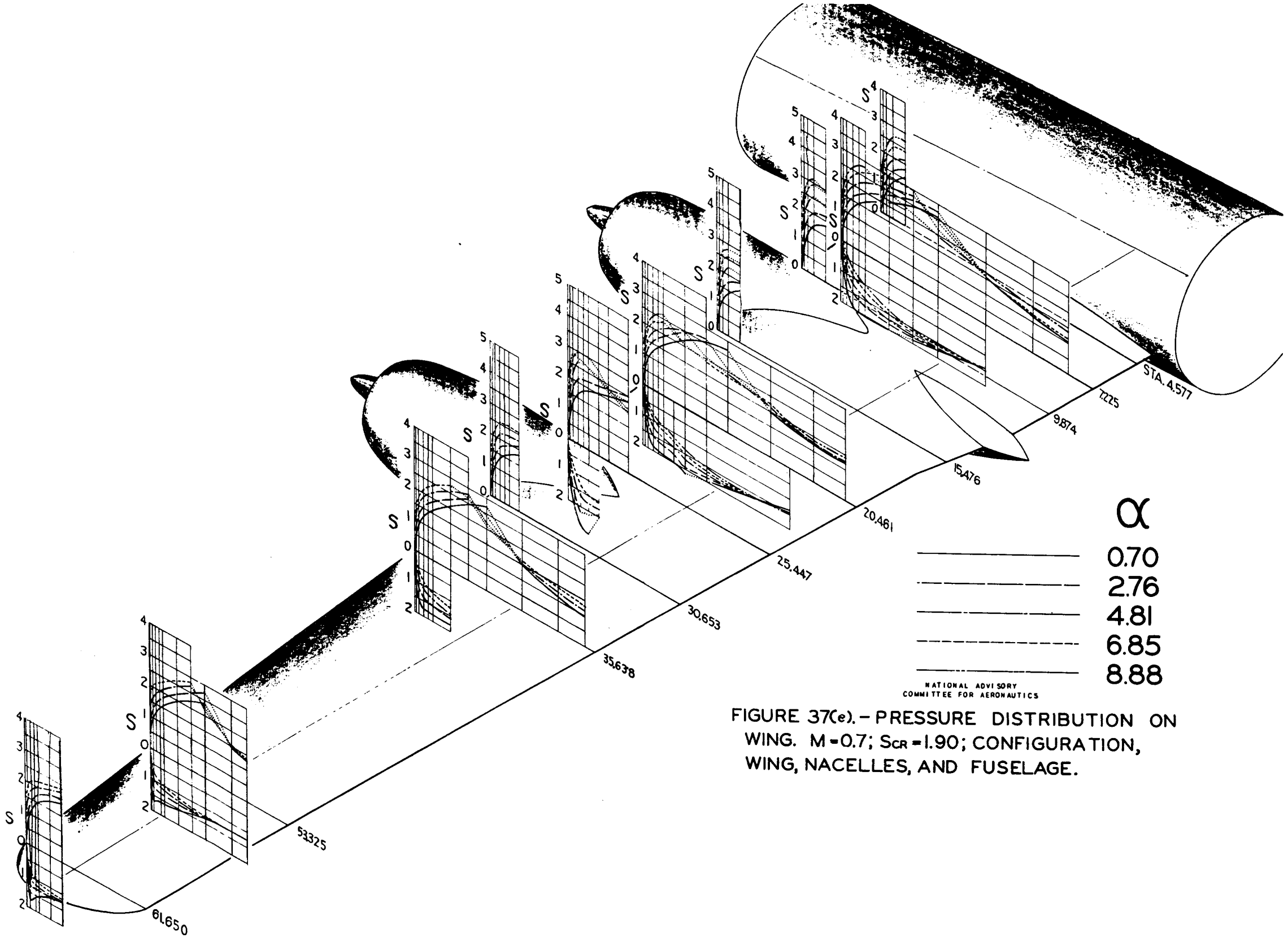

FIGURE 37(e). – PRESSURE DISTRIBUTION ON WING. M = 0.7; S_{CR} = 1.90; CONFIGURATION, WING, NACELLES, AND FUSELAGE.

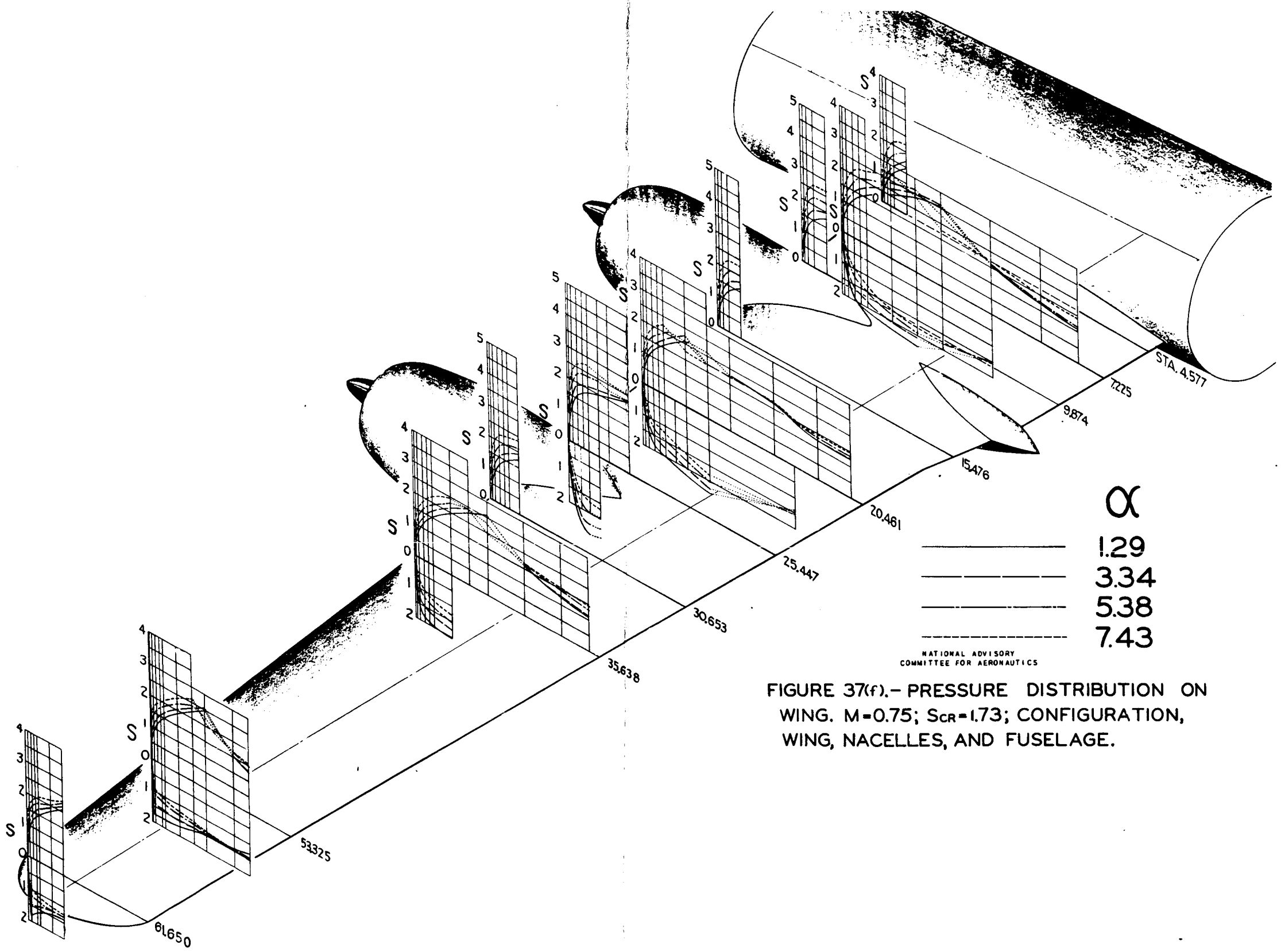

FIGURE 37(f).– PRESSURE DISTRIBUTION ON WING. M=0.75; S_{CR}=1.73; CONFIGURATION, WING, NACELLES, AND FUSELAGE.

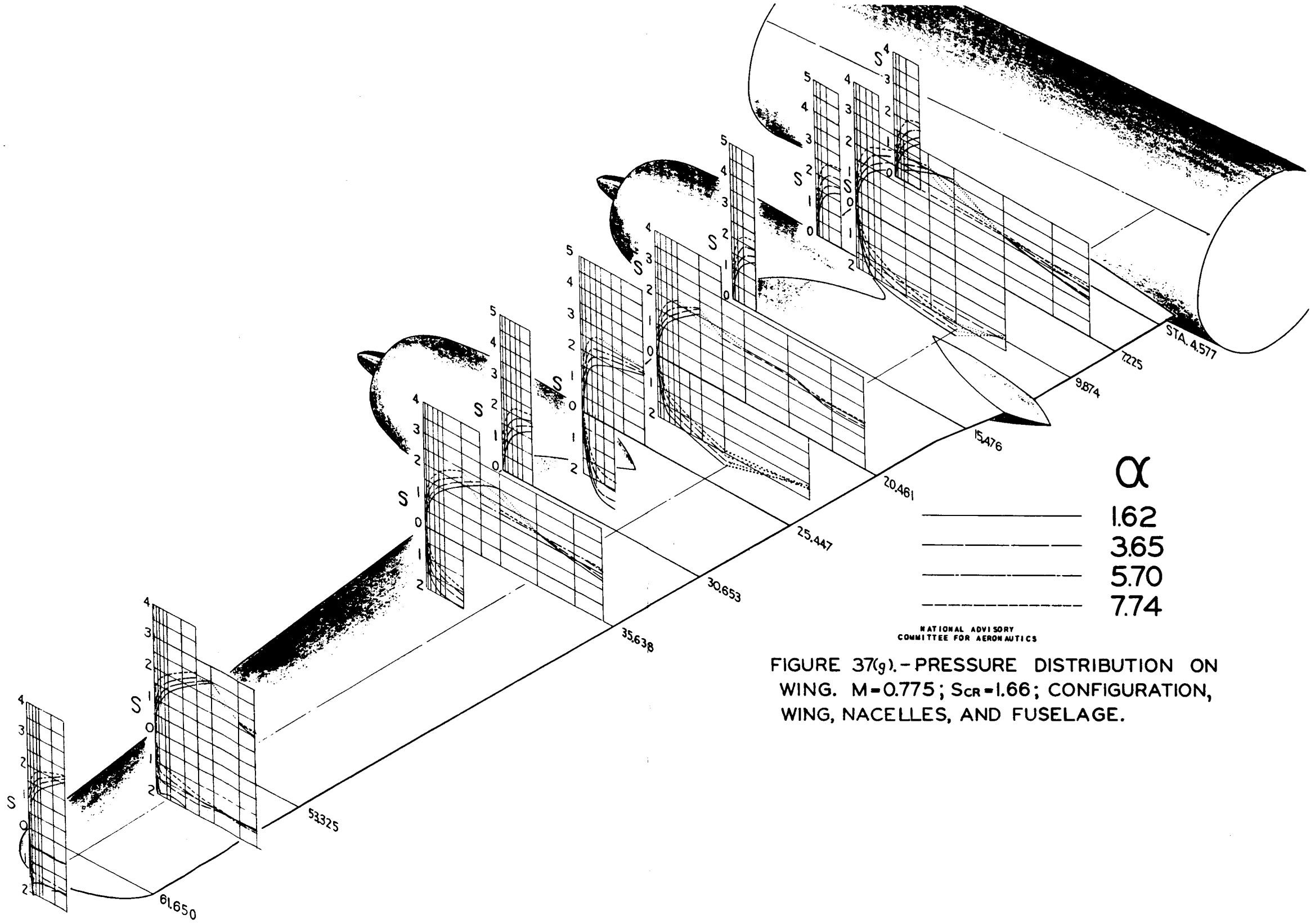

FIGURE 37(g).- PRESSURE DISTRIBUTION ON WING. M=0.775; S_{CR}=1.66; CONFIGURATION, WING, NACELLES, AND FUSELAGE.

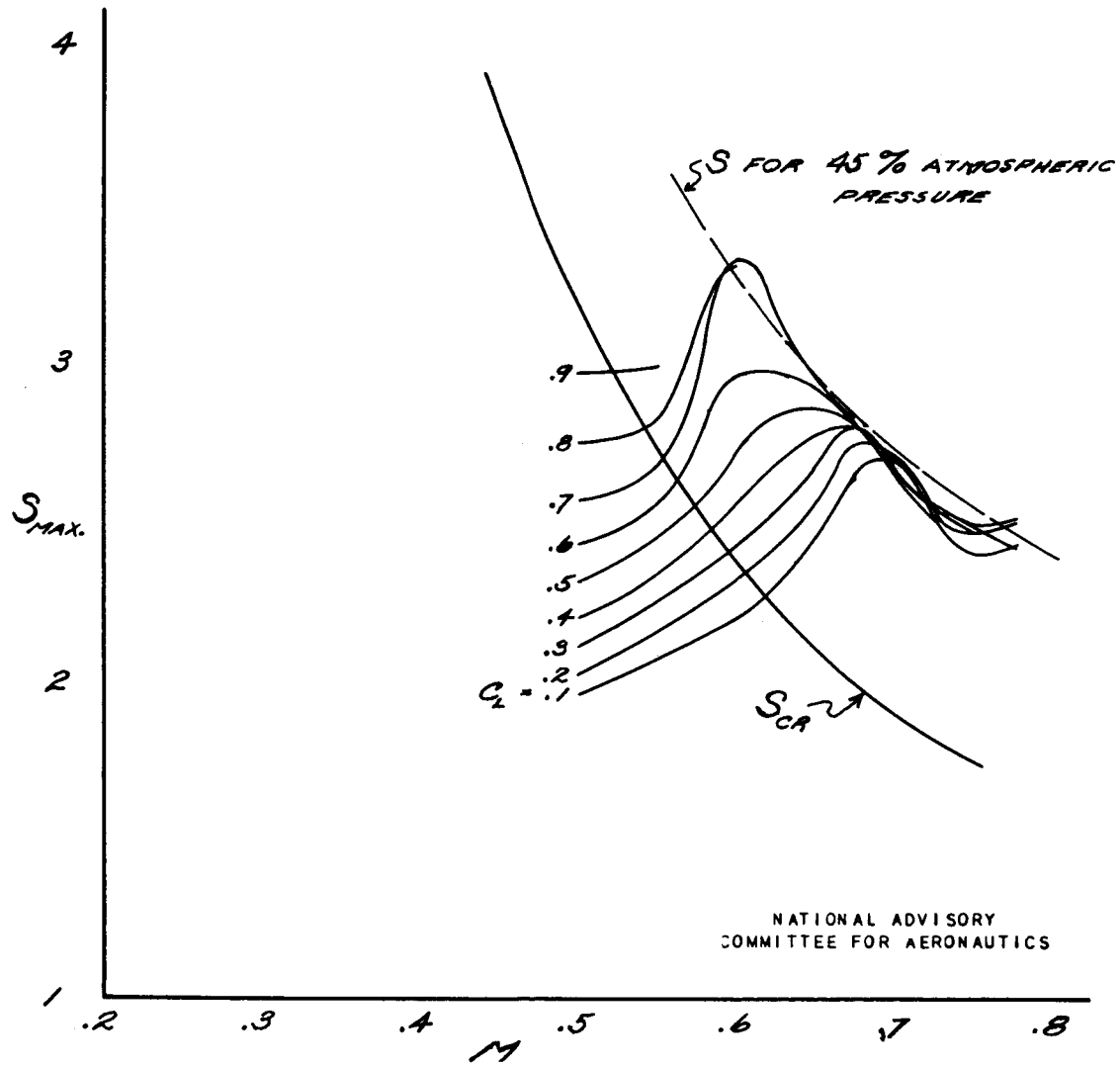

FIGURE 38. - VARIATION OF THE MAXIMUM PRESSURE COEFFICIENT WITH MACH NUMBER FOR CONSTANT LIFT COEFFICIENT AT WING STATION 35.64. WING, FUSELAGE, AND TAIL.

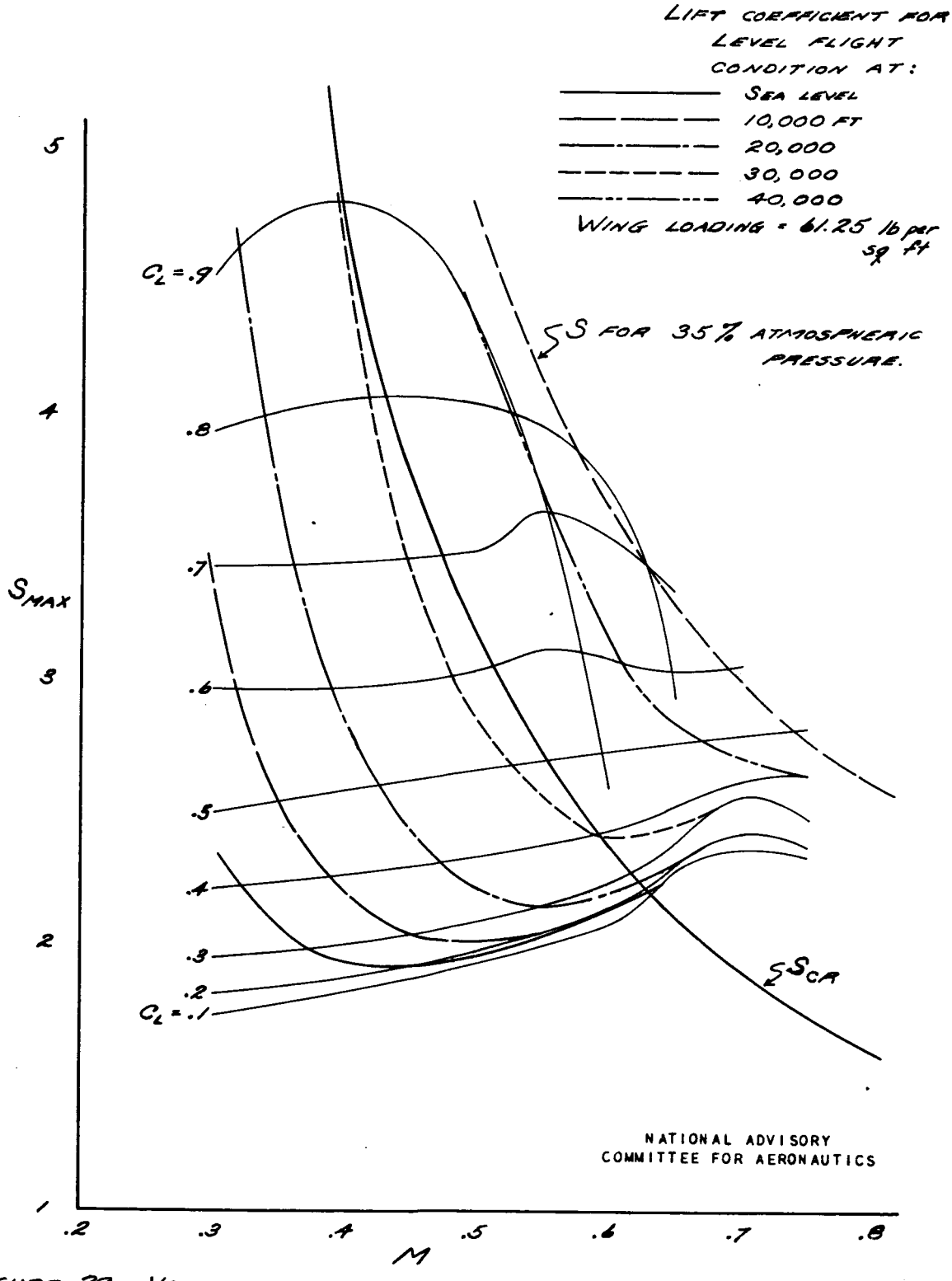

FIGURE 39. - VARIATION OF THE MAXIMUM PRESSURE COEFFICIENT WITH MACH NUMBER FOR CONSTANT LIFT COEFFICIENT AT WING STATION 25.45. WING, NACELLES, FUSELAGE, AND TAIL.

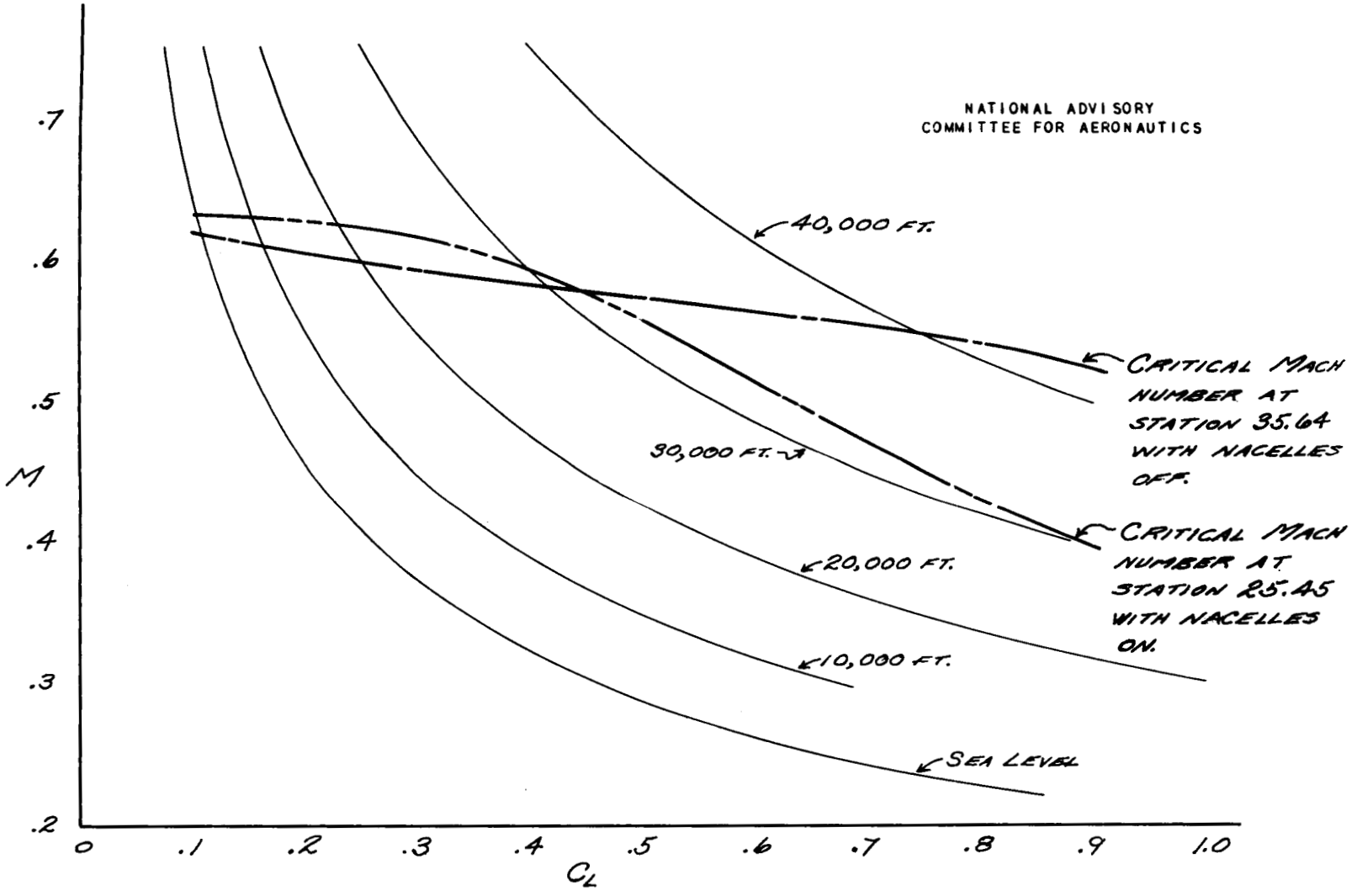

FIGURE 40. - CRITICAL MACH NUMBER OF WING ALONE AND WITH NACELLES. LEVEL FLIGHT CONDITIONS AT A WING LOADING OF 61.25 POUNDS PER SQUARE FOOT.

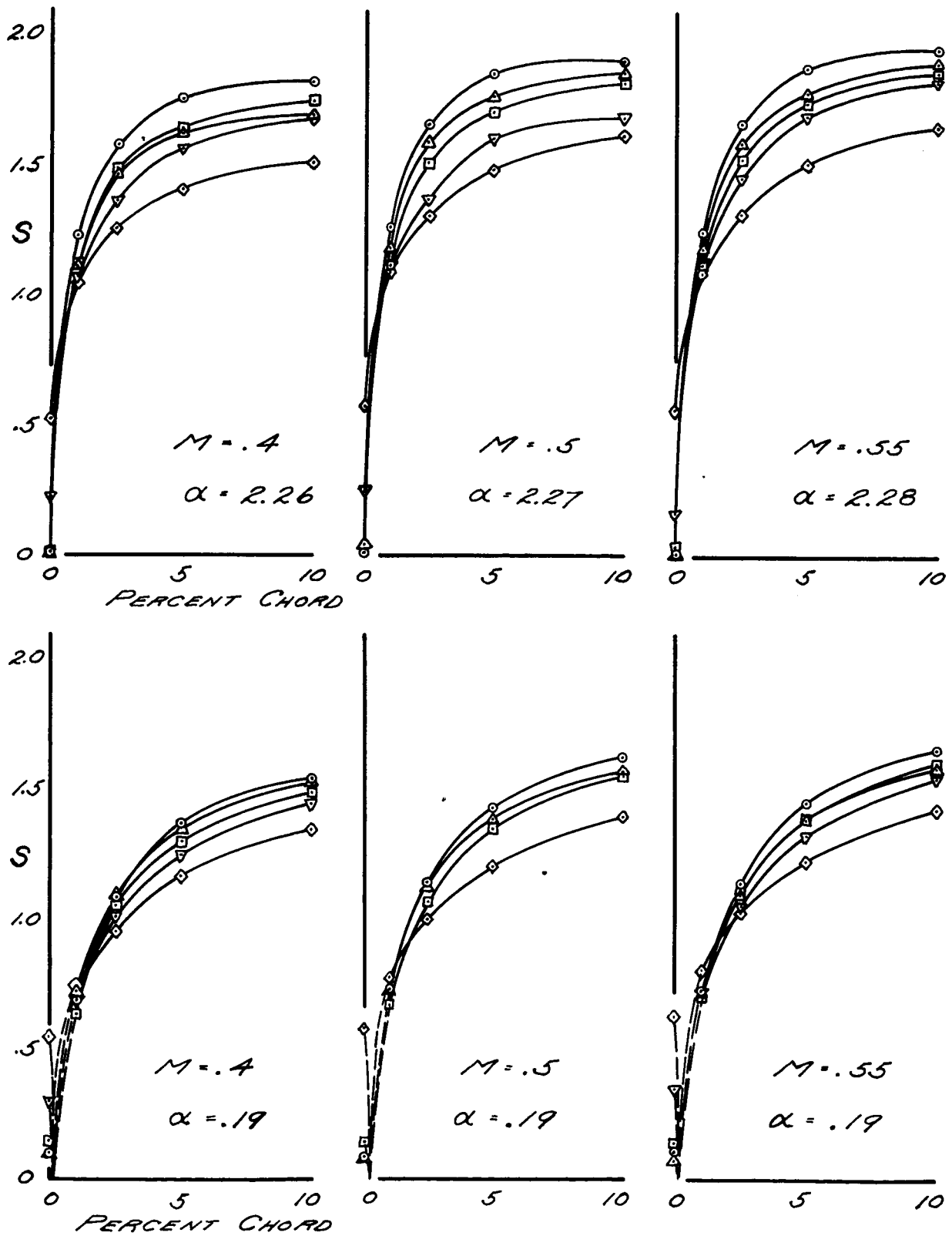
2.0
1.5
S
1.0
.5
0
M = .4
α = 2.26
M = .5
α = 2.27
M = .55
α = 2.28
0
5
10
PERCENT CHORD
M = .4
α = .19
M = .5
α = .19
M = .55
α = .19

FIGURE 41

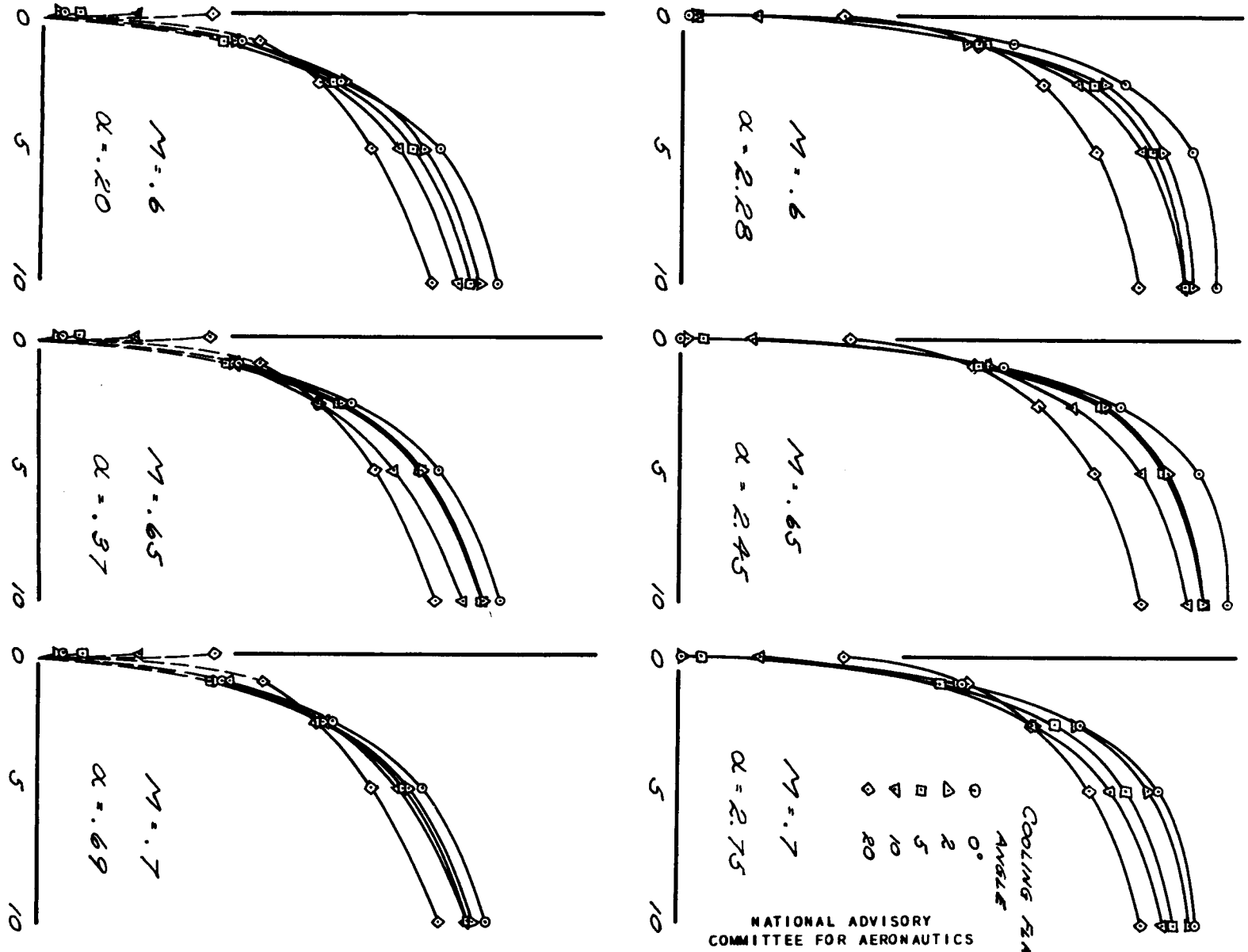

FIGURE 41(a).- PRESSURE DISTRIBUTION ON UPPER SURFACE OF WING AT DIFFERENT COOLING FLAP DEFLECTIONS. WING STATION 15.476; UNCORRECTED ANGLE OF ATTACK = 0° AND 2°.

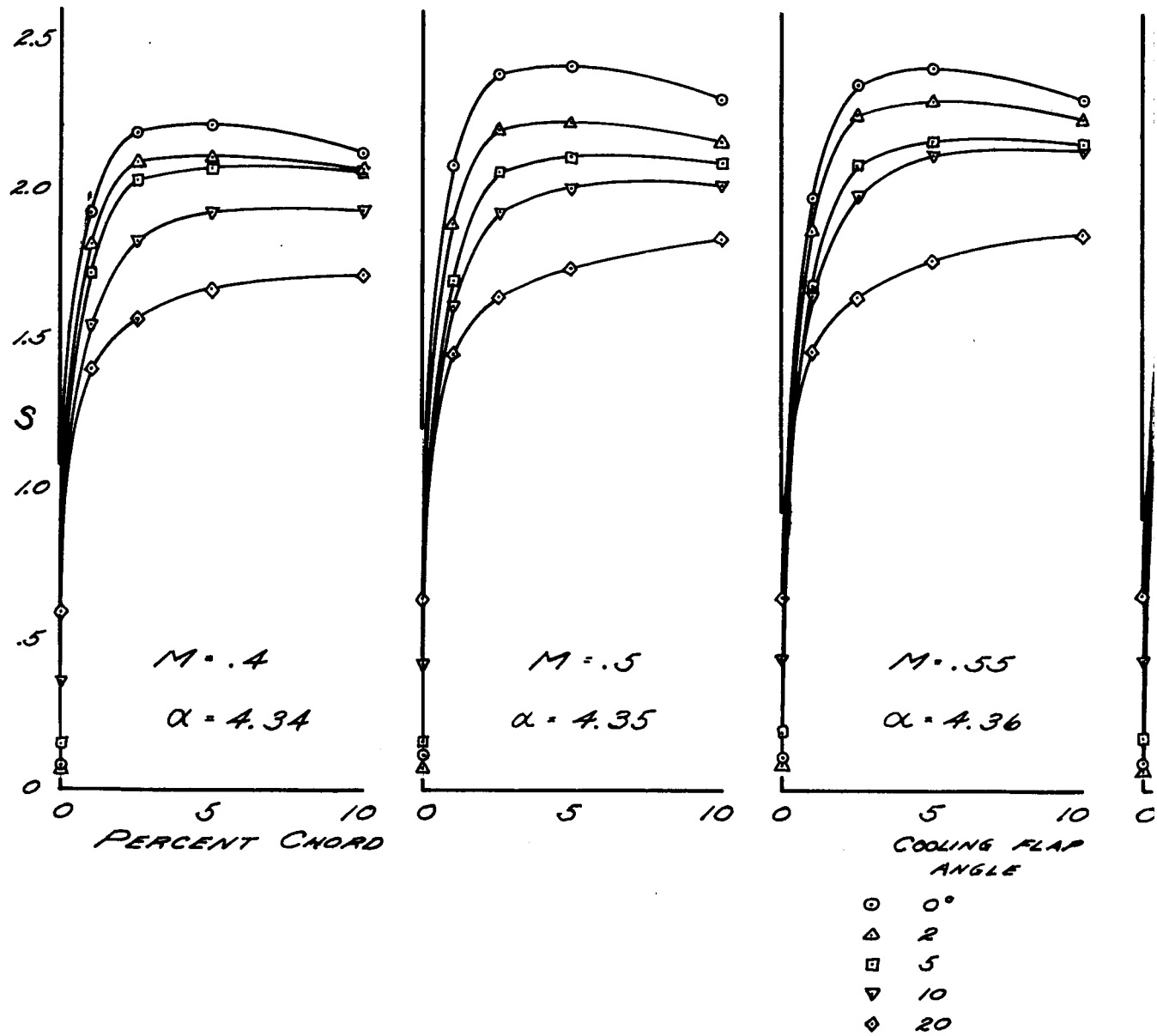
2.5
2.0
1.5
S
1.0
.5
0
M = .4
α = 4.34
M = .5
α = 4.35
M = .55
α = 4.36
0
5
10
PERCENT CHORD
COOLING FLAP ANGLE
0°
2
5
10
20

FIGURE B41B

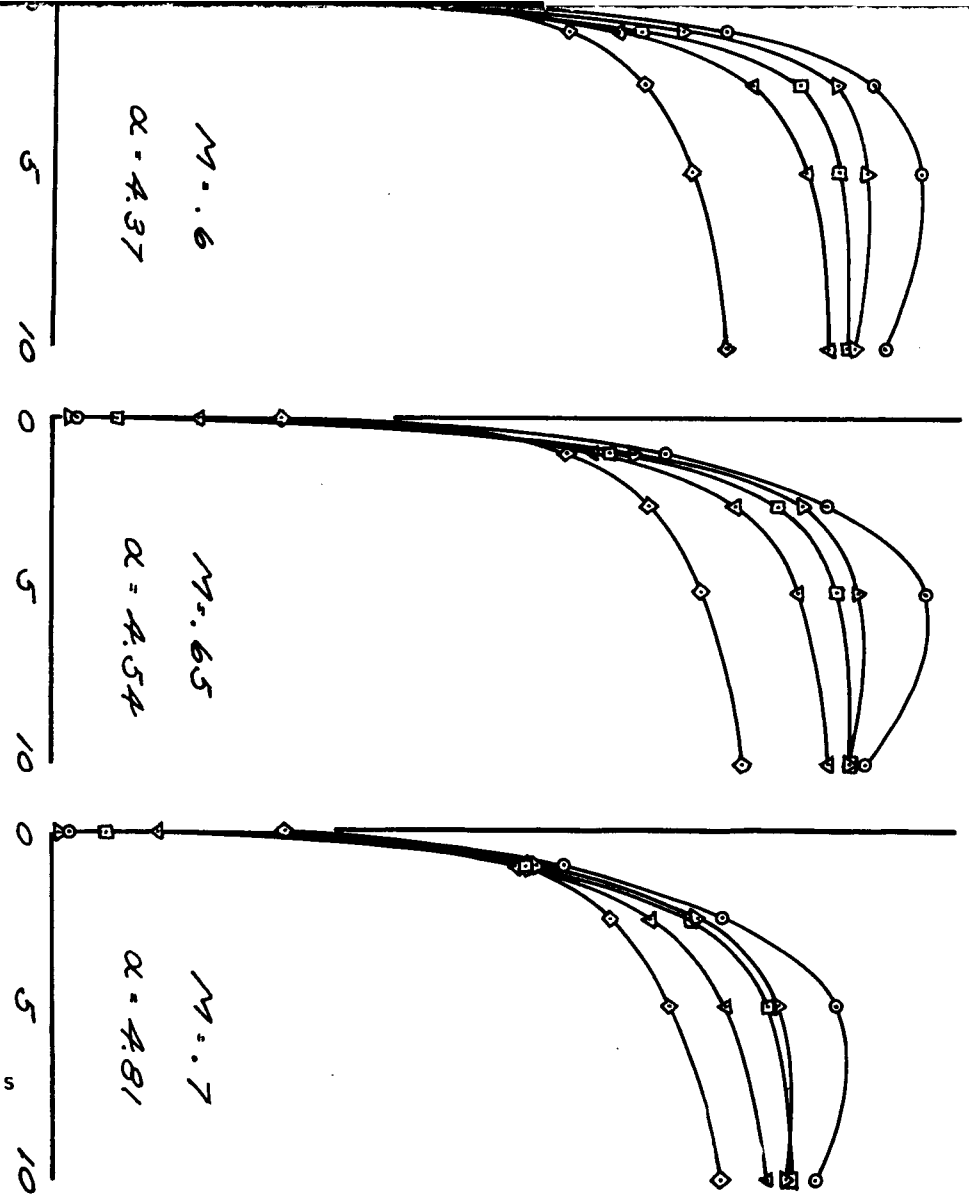

NATIONAL ADVISORY
COMMITTEE FOR AERONAUTICS

FIGURE 41(b).- PRESSURE DISTRIBUTION ON UPPER SURFACE OF WING AT DIFFERENT COOLING FLAP DEFLECTIONS. WING STATION 15.476; UNCORRECTED ANGLE OF ATTACK = 4°.

AB 2

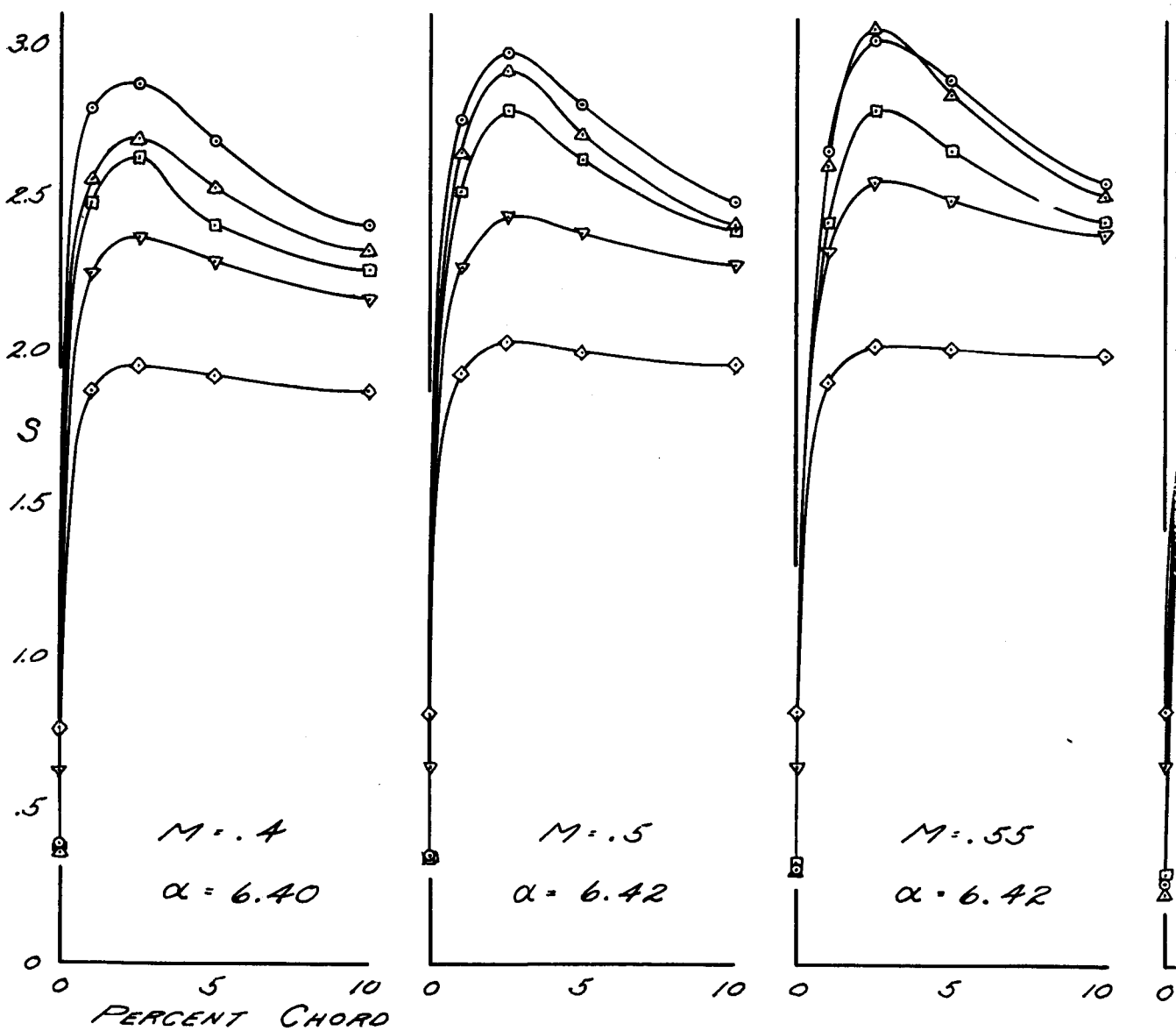

FIGURE 41 D

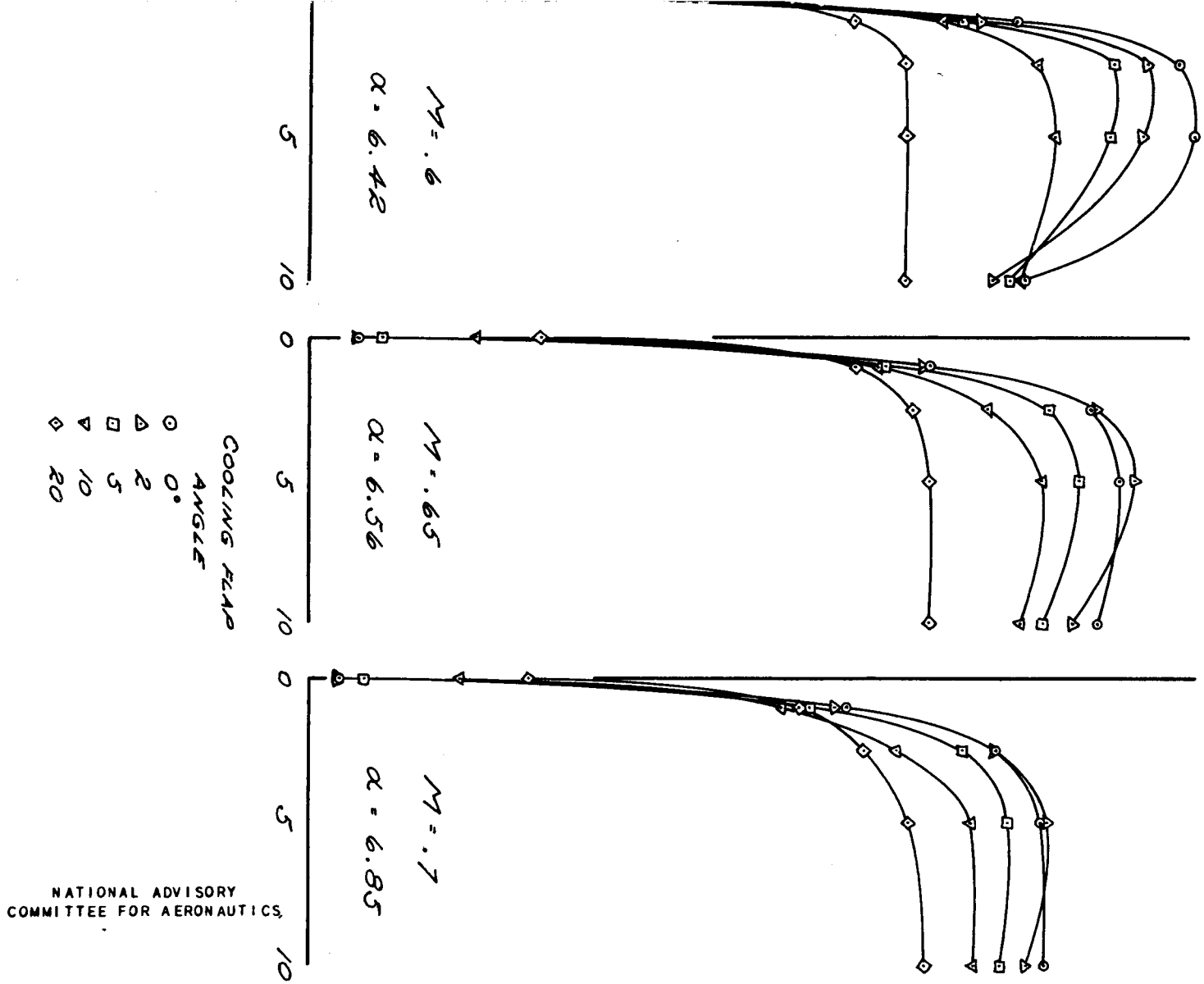

FIGURE 41 (E). - PRESSURE DISTRIBUTION ON UPPER SURFACE OF WING AT DIFFERENT COOLING FLAP DEFLECTIONS. WING STATION 15.476; UNCORRECTED ANGLE OF ATTACK = 6°

A82

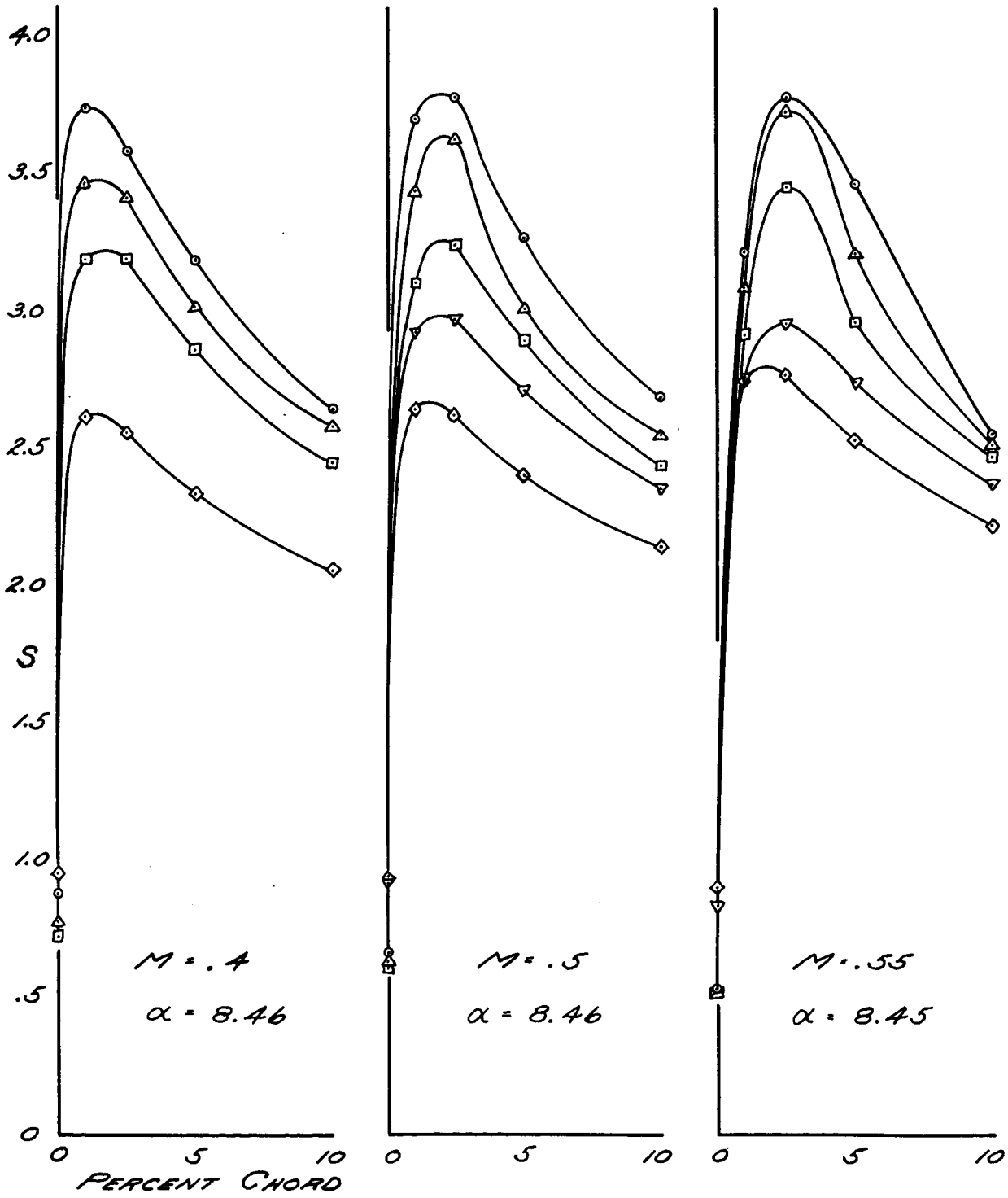

FIGURE 41 F

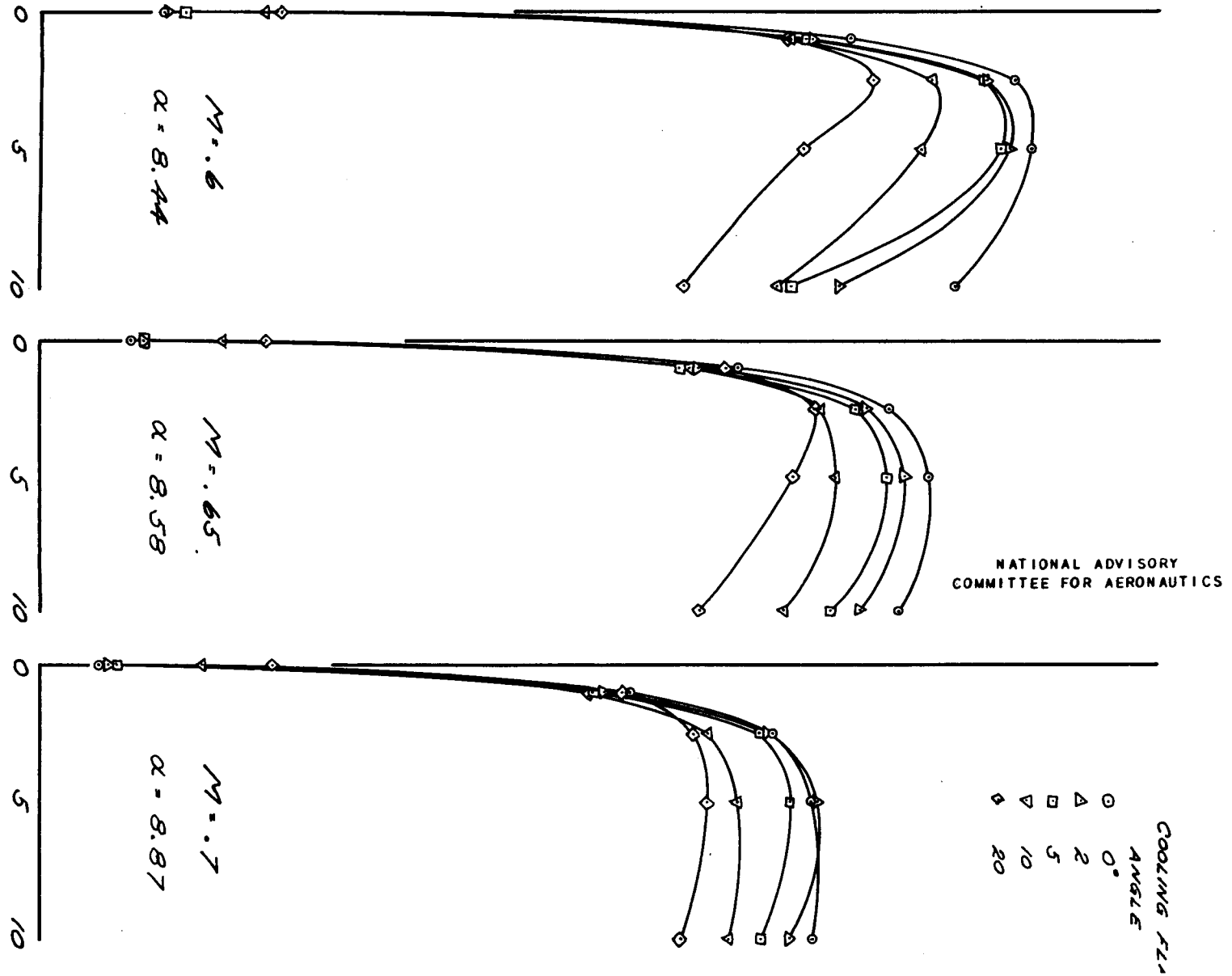

FIGURE 41(G.- PRESSURE DISTRIBUTION ON UPPER SURFACE OF WING AT DIFFERENT COOLING FLAP DEFLECTIONS. WING STATION 15.476; UNCORRECTED ANGLE OF ATTACK = 8°

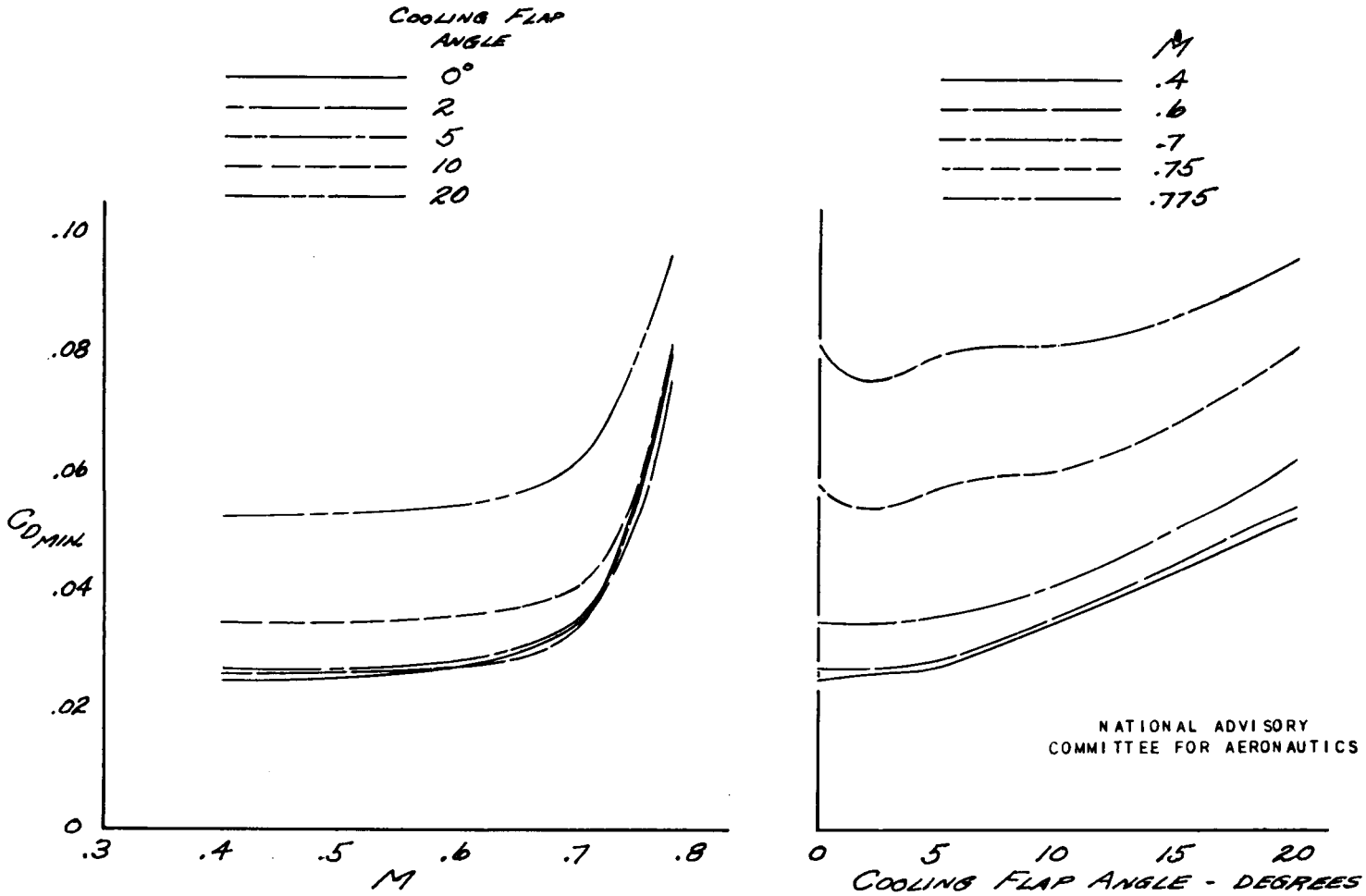

FIGURE 42.- EFFECT OF COOLING FLAPS ON MINIMUM DRAG COEFFICIENT.

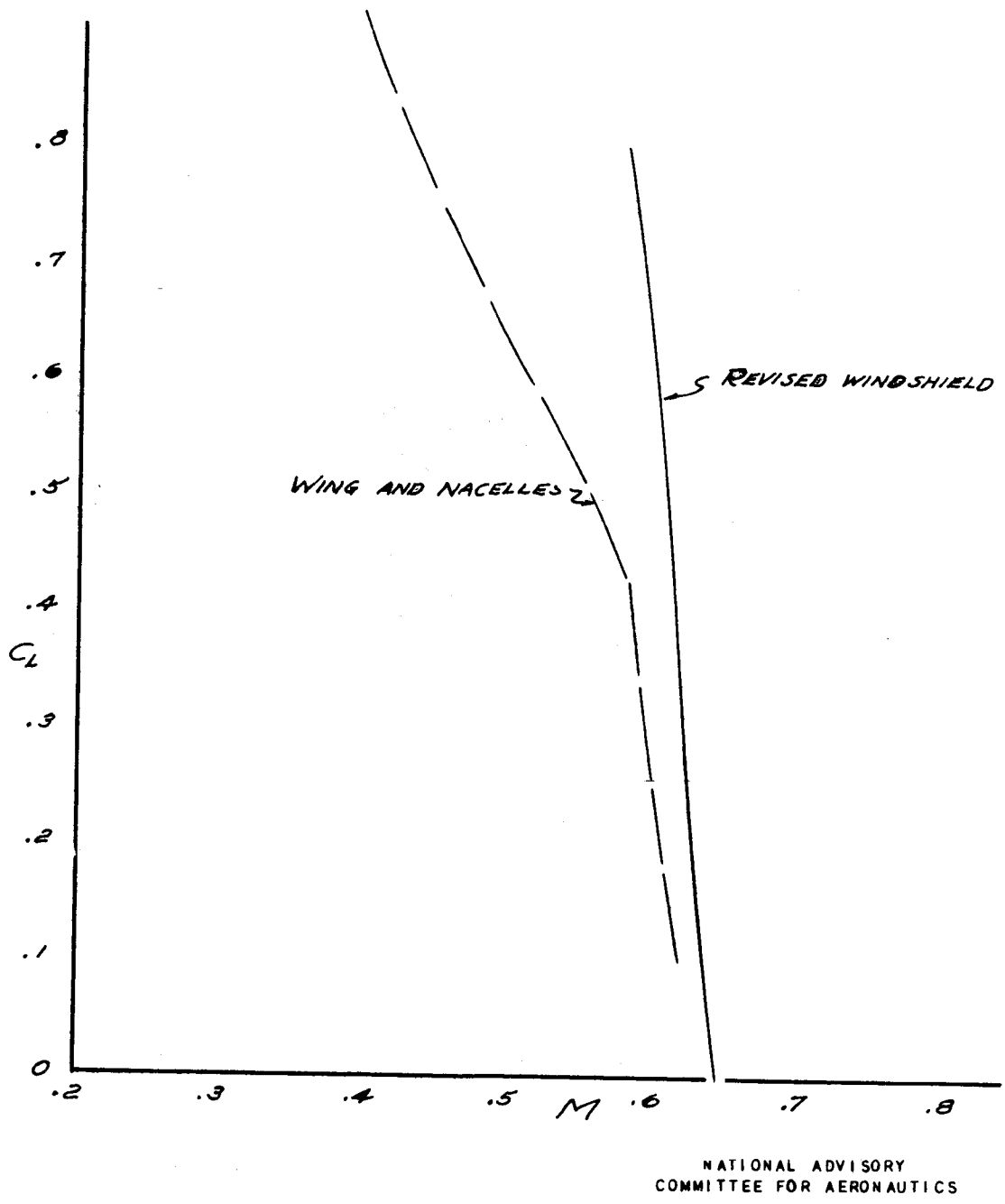

FIGURE 43. - CRITICAL SPEEDS OF WING - NACELLE COMBINATION AND REVISED WINDSHIELD.

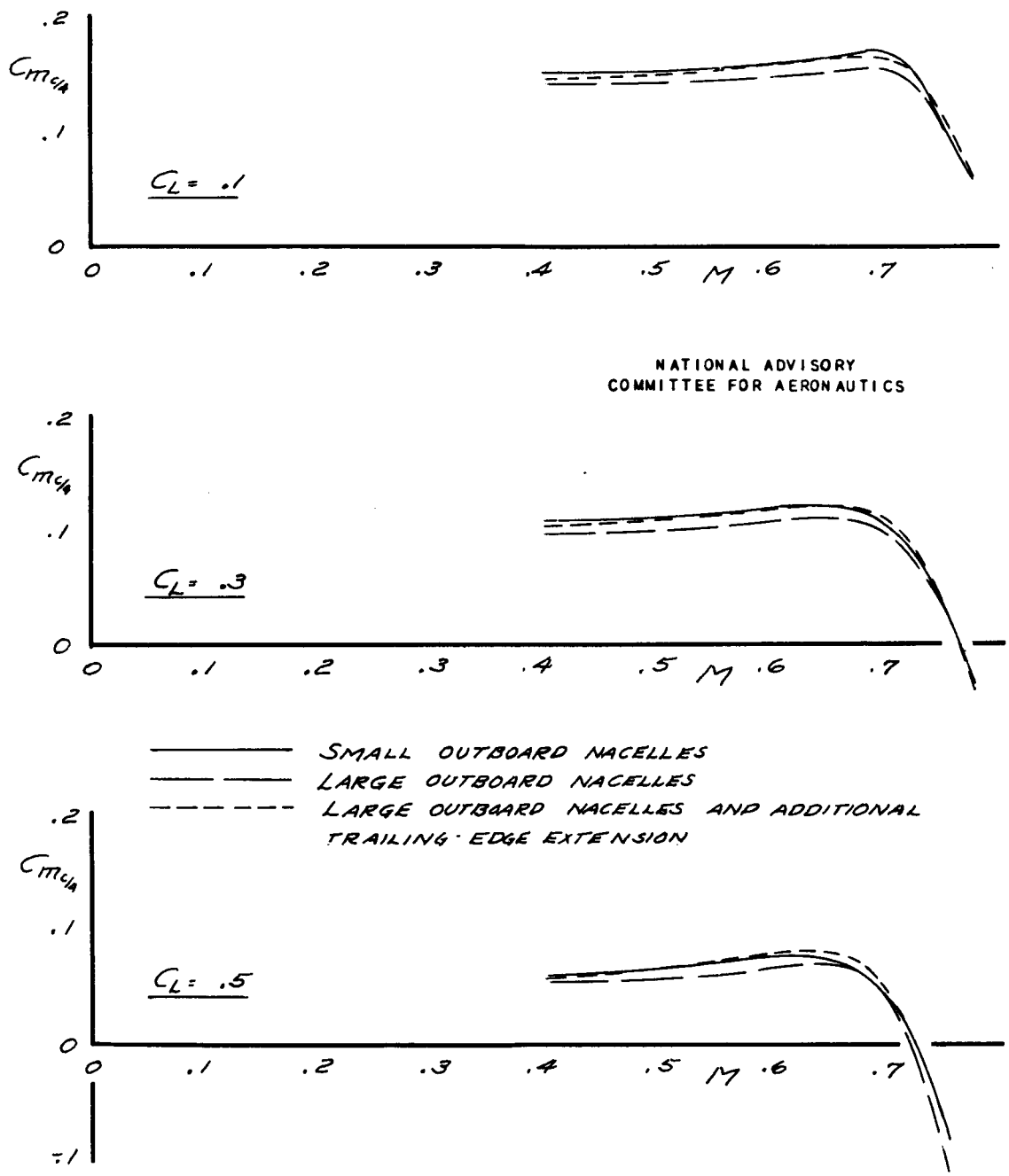

FIGURE 44. - PITCHING-MOMENT COEFFICIENTS WITH SMALL OUTBOARD NACELLES, LARGE OUTBOARD NACELLES, AND LARGE OUTBOARD NACELLES WITH ADDITIONAL TRAILING-EDGE EXTENSIONS.

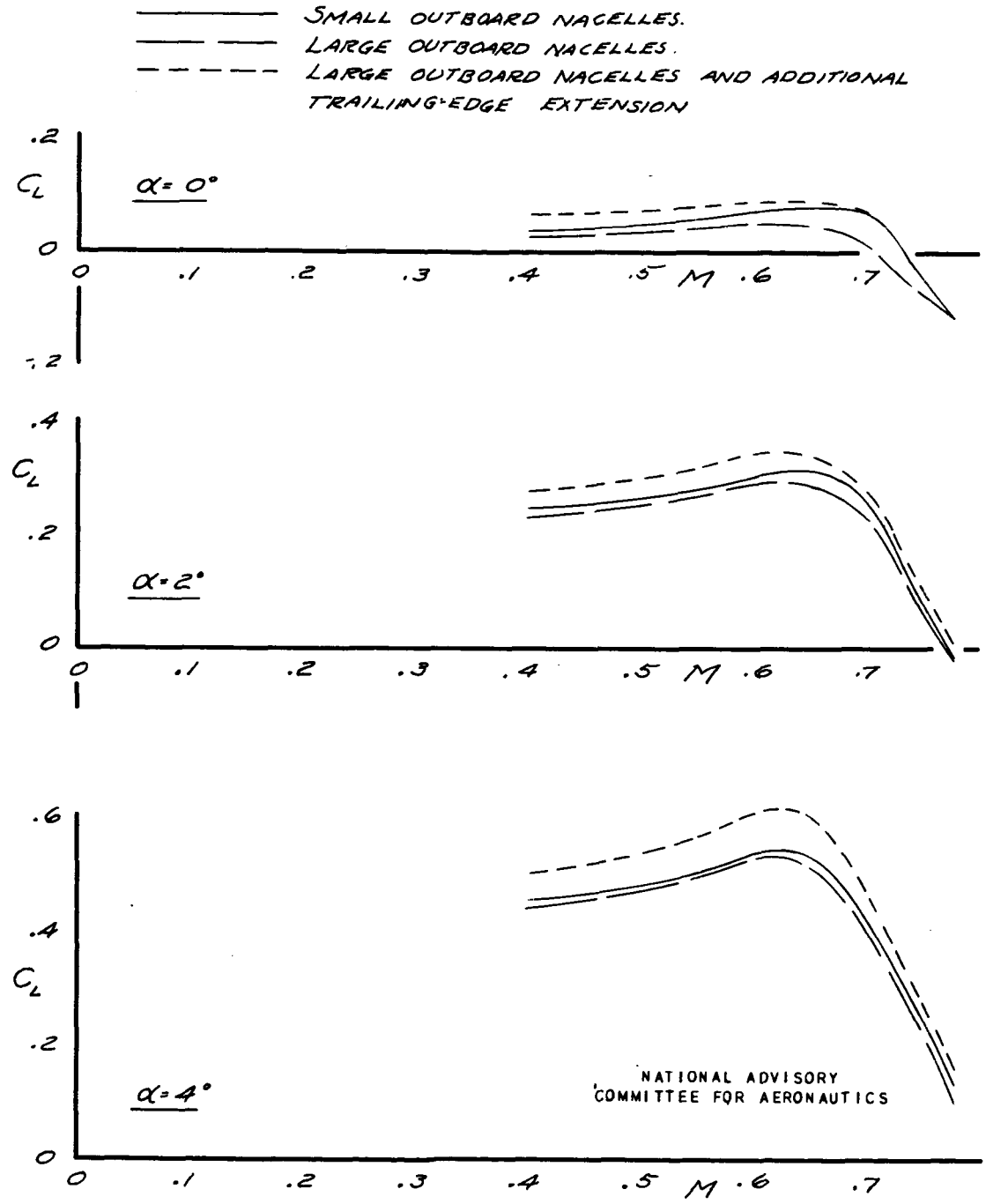

FIGURE 45. - LIFT COEFFICIENTS WITH SMALL OUTBOARD NACELLES, LARGE OUTBOARD NACELLES, AND LARGE OUTBOARD NACELLES WITH ADDITIONAL TRAILING-EDGE EXTENSIONS.

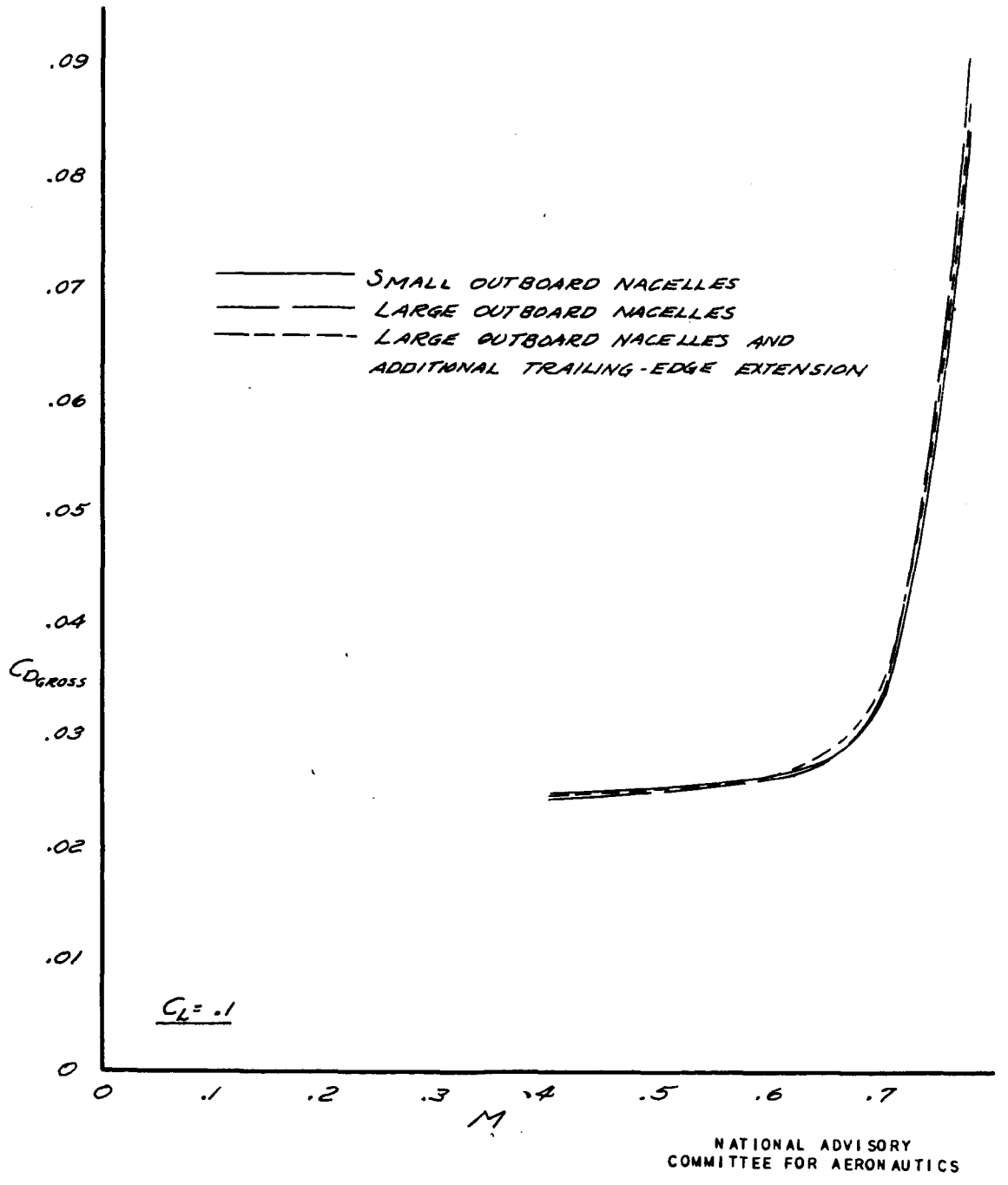

FIGURE 46(a).- DRAG COEFFICIENTS WITH SMALL OUTBOARD NACELLES, LARGE OUTBOARD NACELLES, AND LARGE OUTBOARD NACELLES WITH ADDITIONAL TRAILING-EDGE EXTENSIONS. LIFT COEFFICIENT = 0.1.

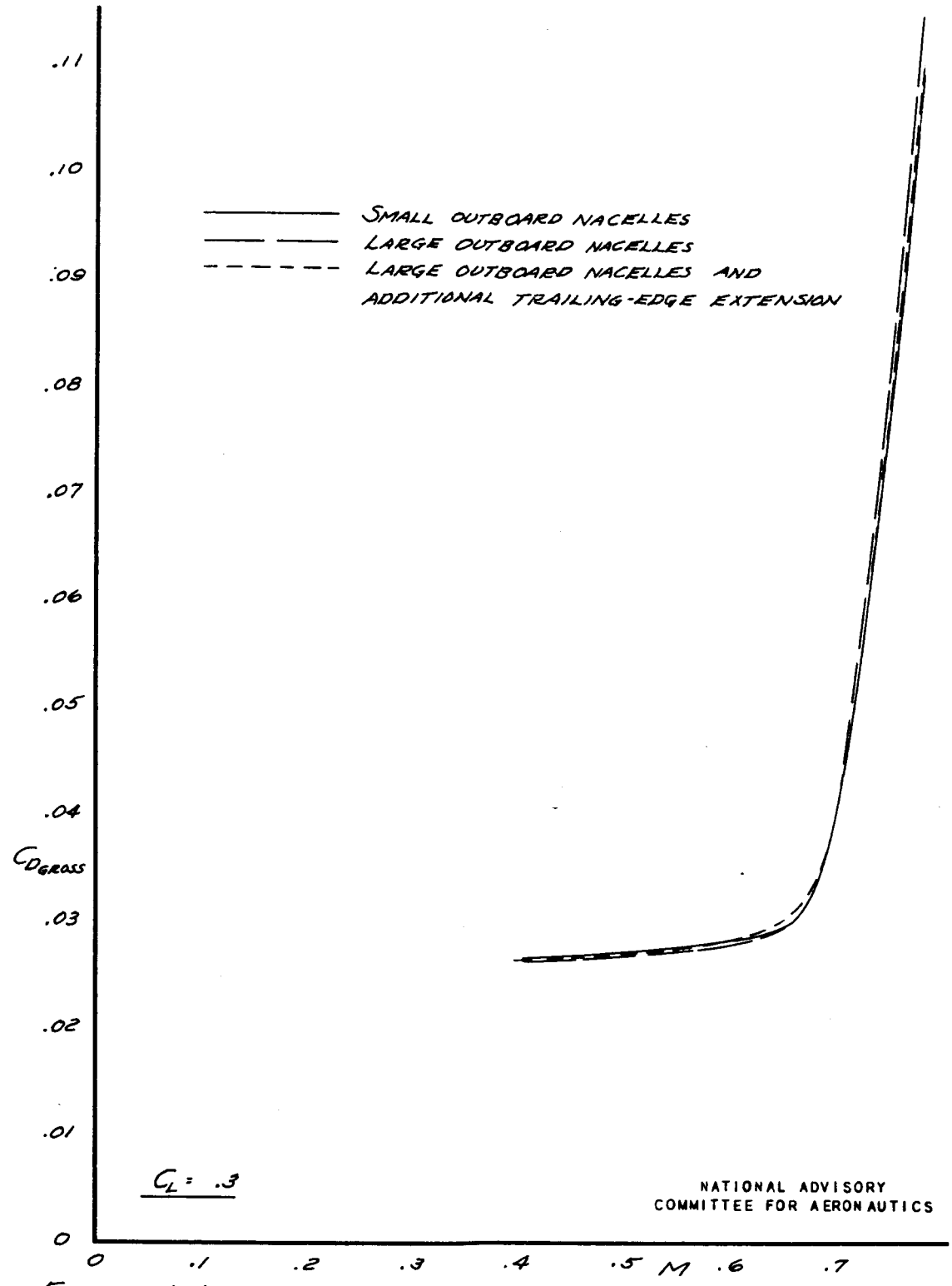

FIGURE 46(b).- DRAG COEFFICIENTS WITH SMALL OUTBOARD NACELLES, LARGE OUTBOARD NACELLES, AND LARGE OUTBOARD NACELLES WITH ADDITIONAL TRAILING-EDGE EXTENSIONS. LIFT COEFFICIENT = 0.3.

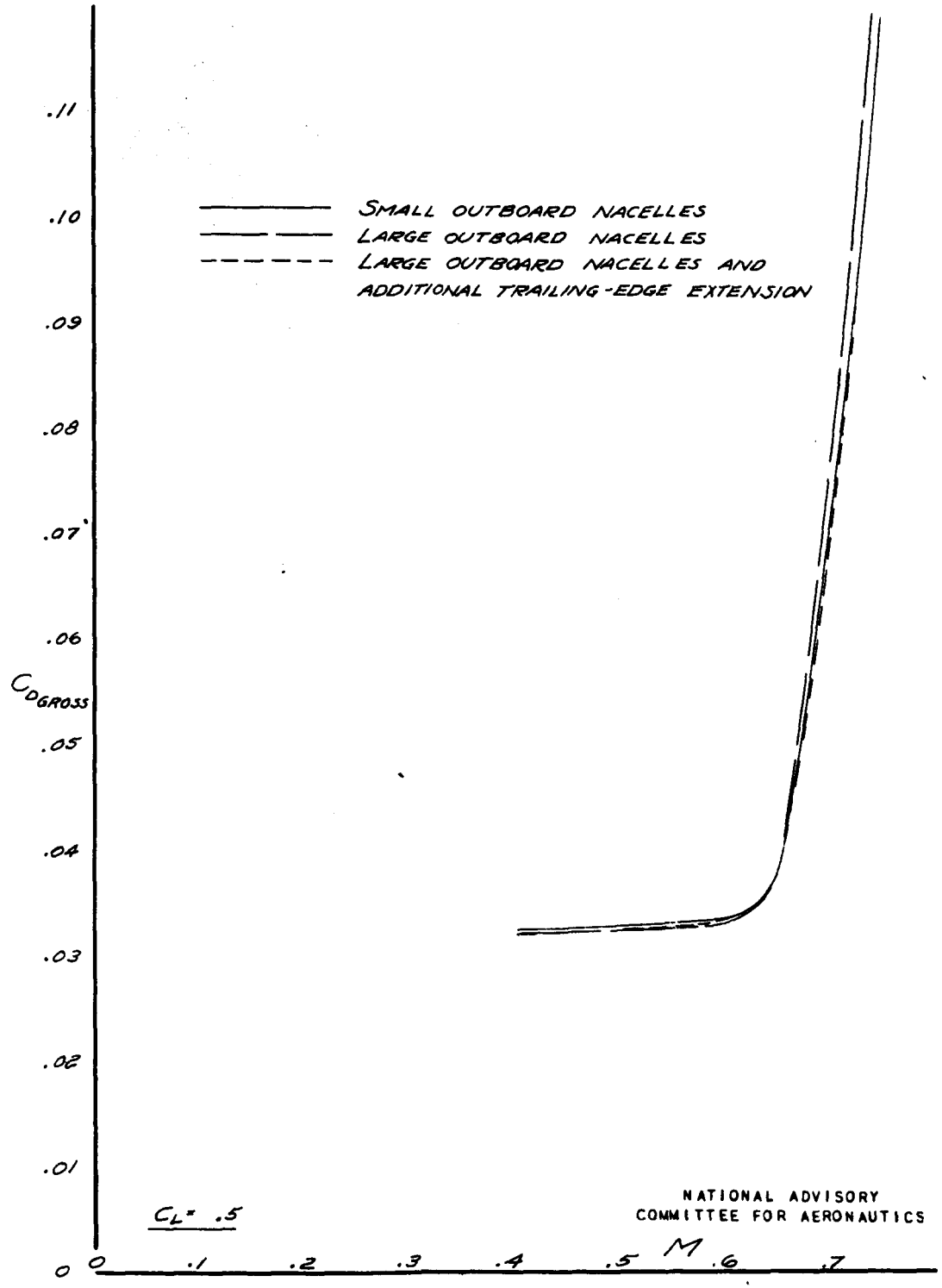

FIGURE 46 (a). - DRAG COEFFICIENTS WITH SMALL OUTBOARD NACELLES, LARGE OUTBOARD NACELLES, AND LARGE OUTBOARD NACELLES WITH ADDITIONAL TRAILING-EDGE EXTENSIONS. LIFT COEFFICIENT = 0.5.

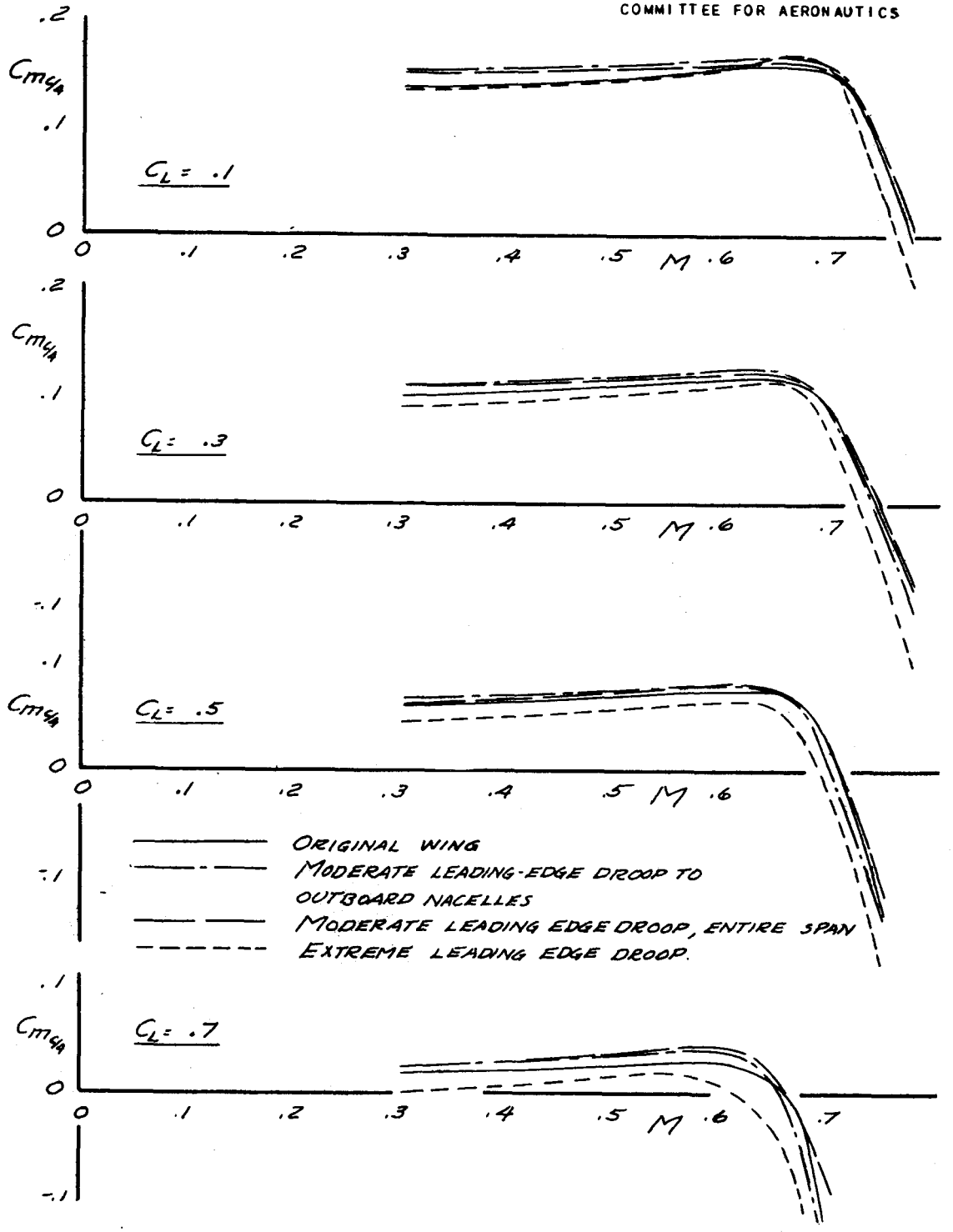

FIGURE 47. - EFFECT OF LEADING-EDGE MODIFICATIONS ON PITCHING-MOMENT COEFFICIENTS.

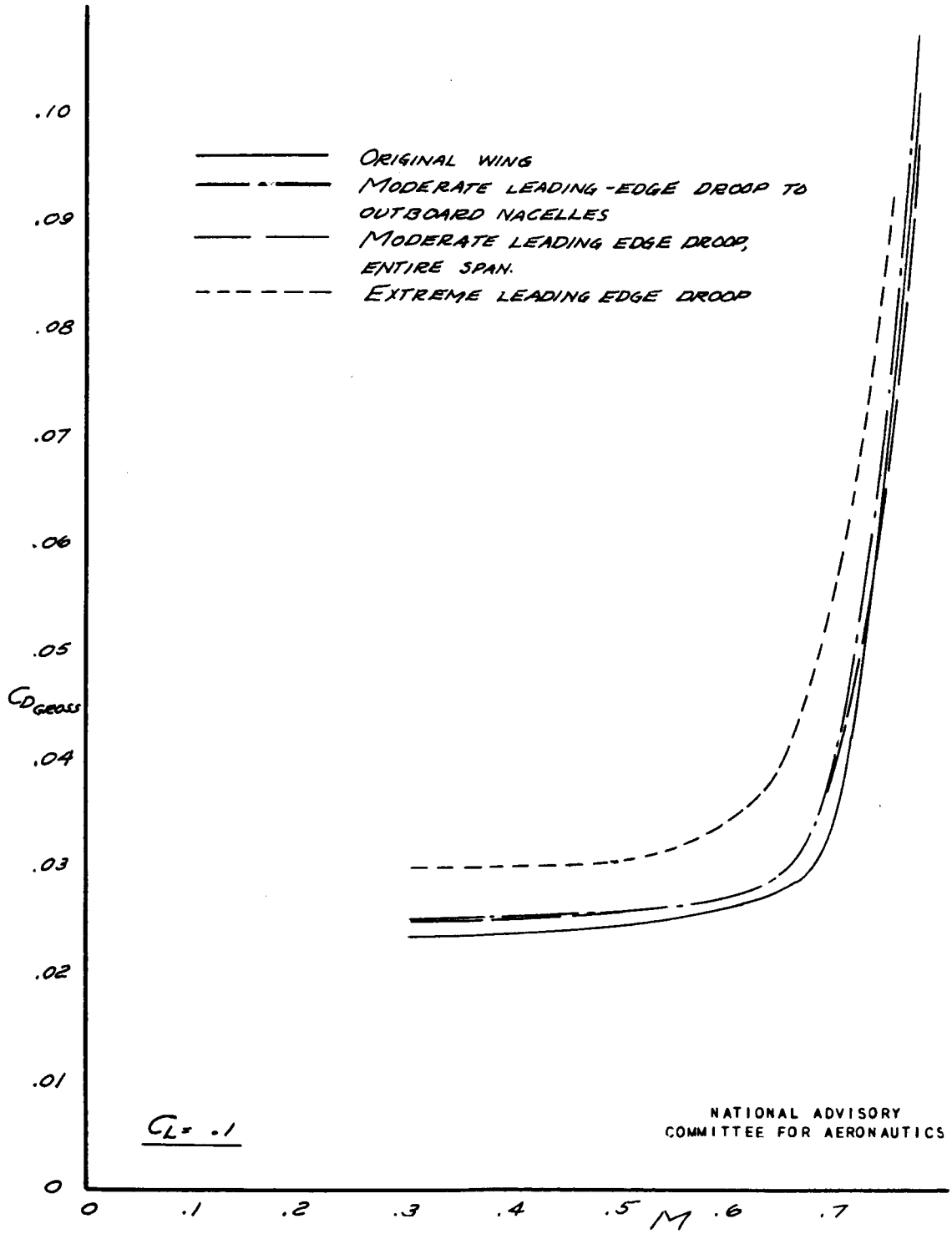

FIGURE 48(a).- EFFECT OF LEADING-EDGE MODIFICATIONS ON DRAG COEFFICIENTS. LIFT COEFFICIENT = 0.1.

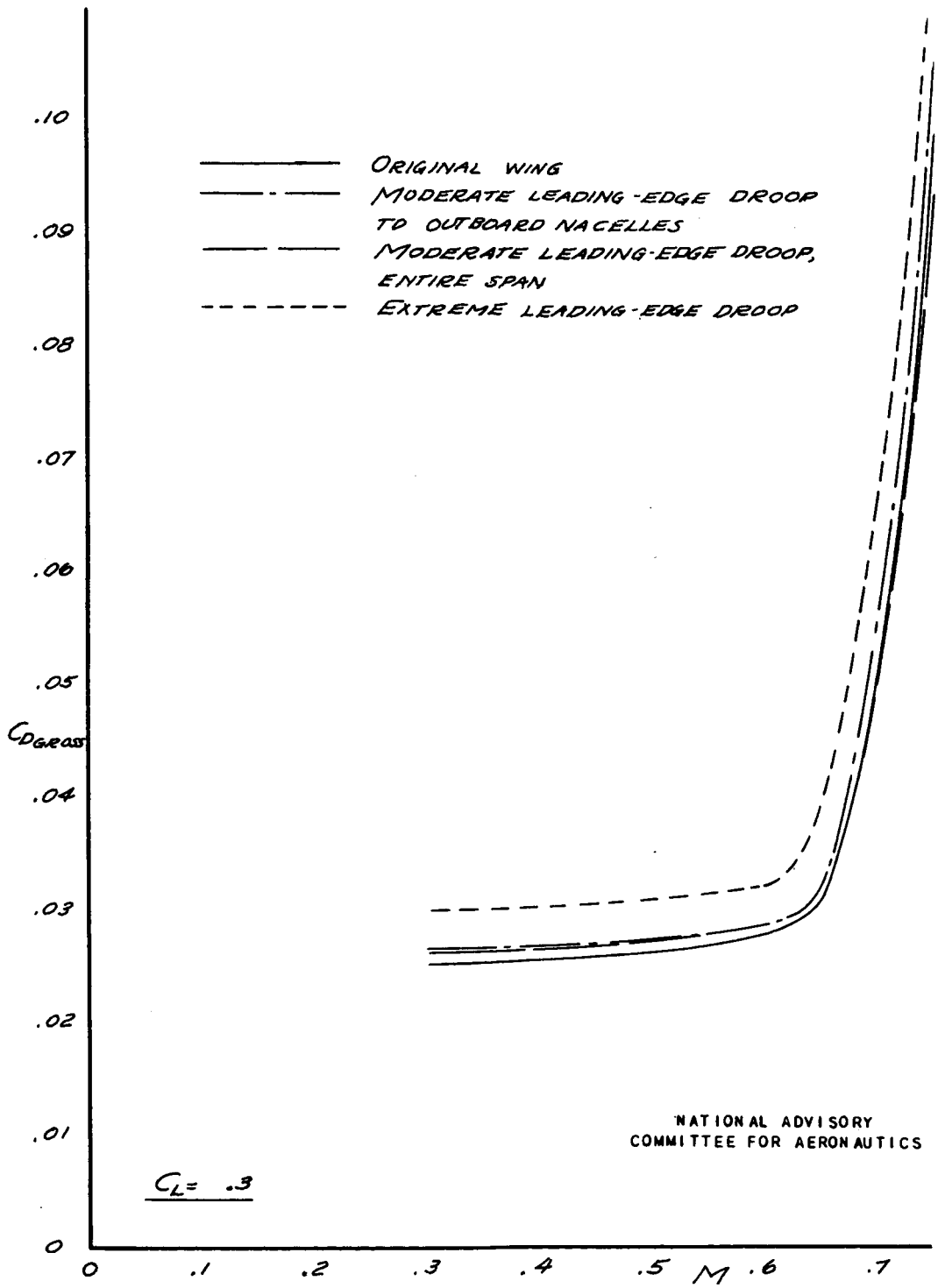

FIGURE 48(b).-EFFECT OF LEADING-EDGE MODIFICATIONS ON DRAG COEFFICIENTS. LIFT COEFFICIENT = 0.3.

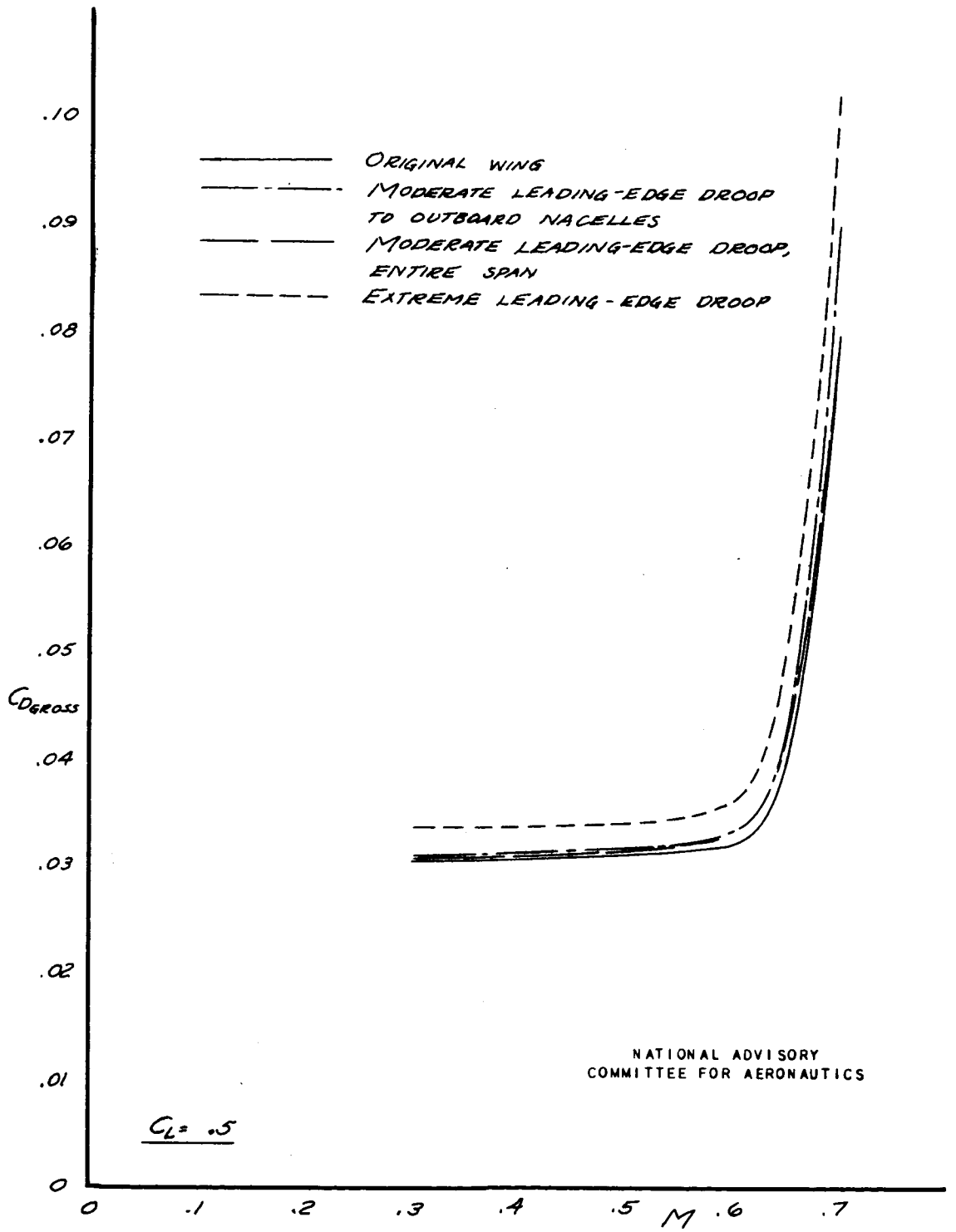

FIGURE 48(c). - EFFECT OF LEADING-EDGE MODIFICATIONS ON DRAG COEFFICIENTS. LIFT COEFFICIENT = 0.5.

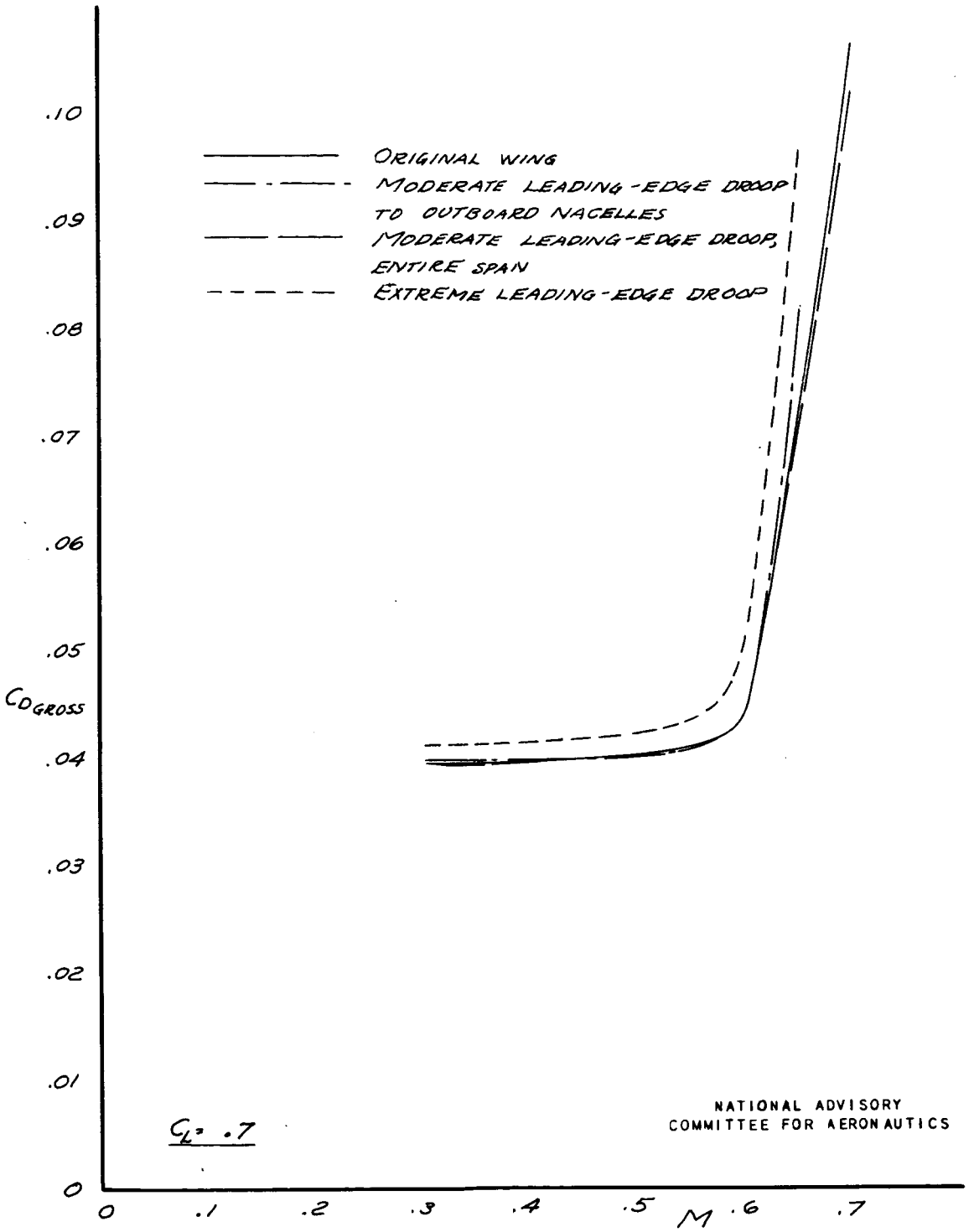

FIGURE 48 (d). - EFFECT OF LEADING-EDGE MODIFICATIONS ON DRAG COEFFICIENTS. LIFT COEFFICIENT = 0.7.

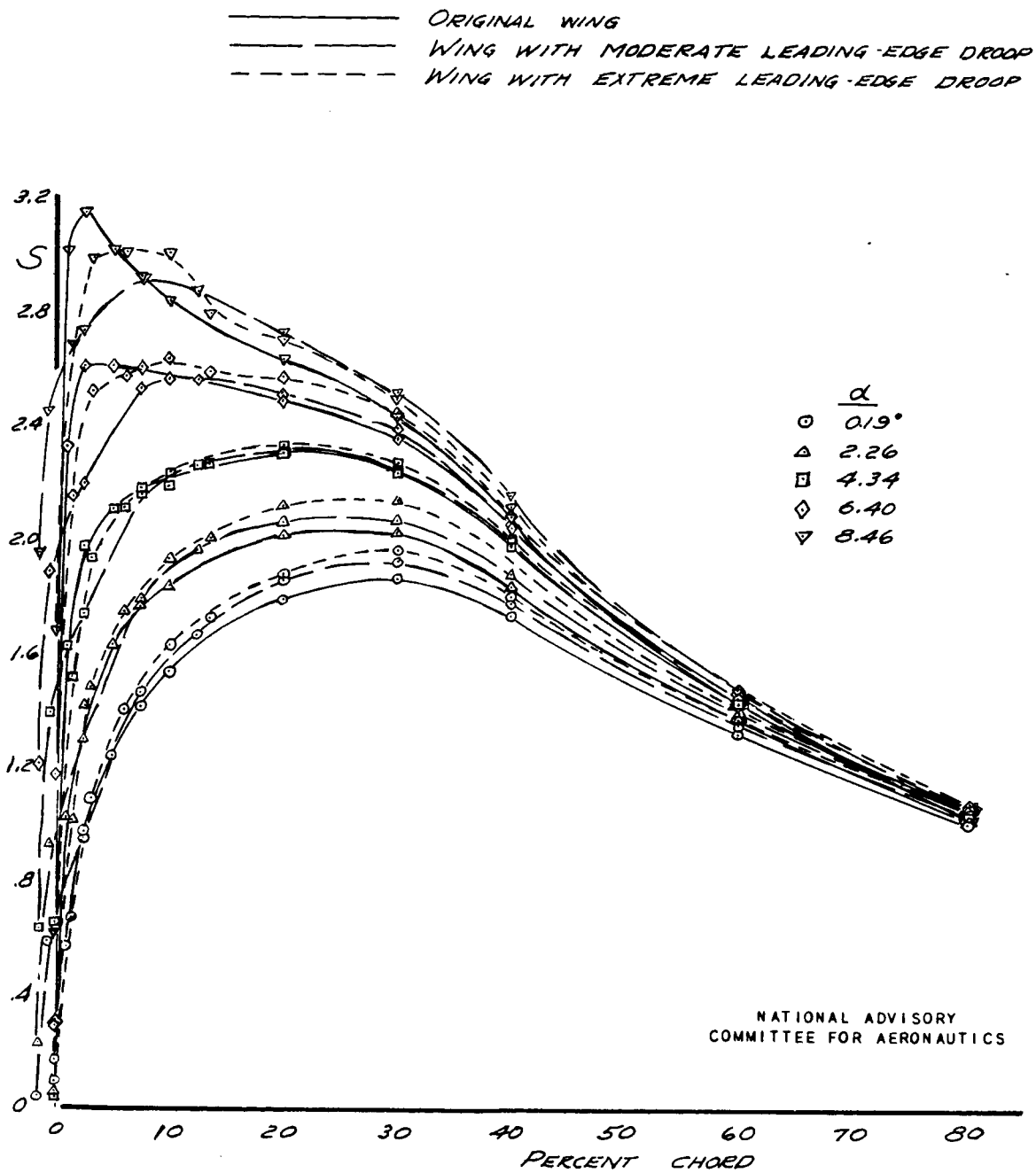

FIGURE 49.- EFFECT OF LEADING-EDGE MODIFICATIONS ON PRESSURE DISTRIBUTION ON UPPER SURFACE. WING STATION 35.638, M = 0.40.

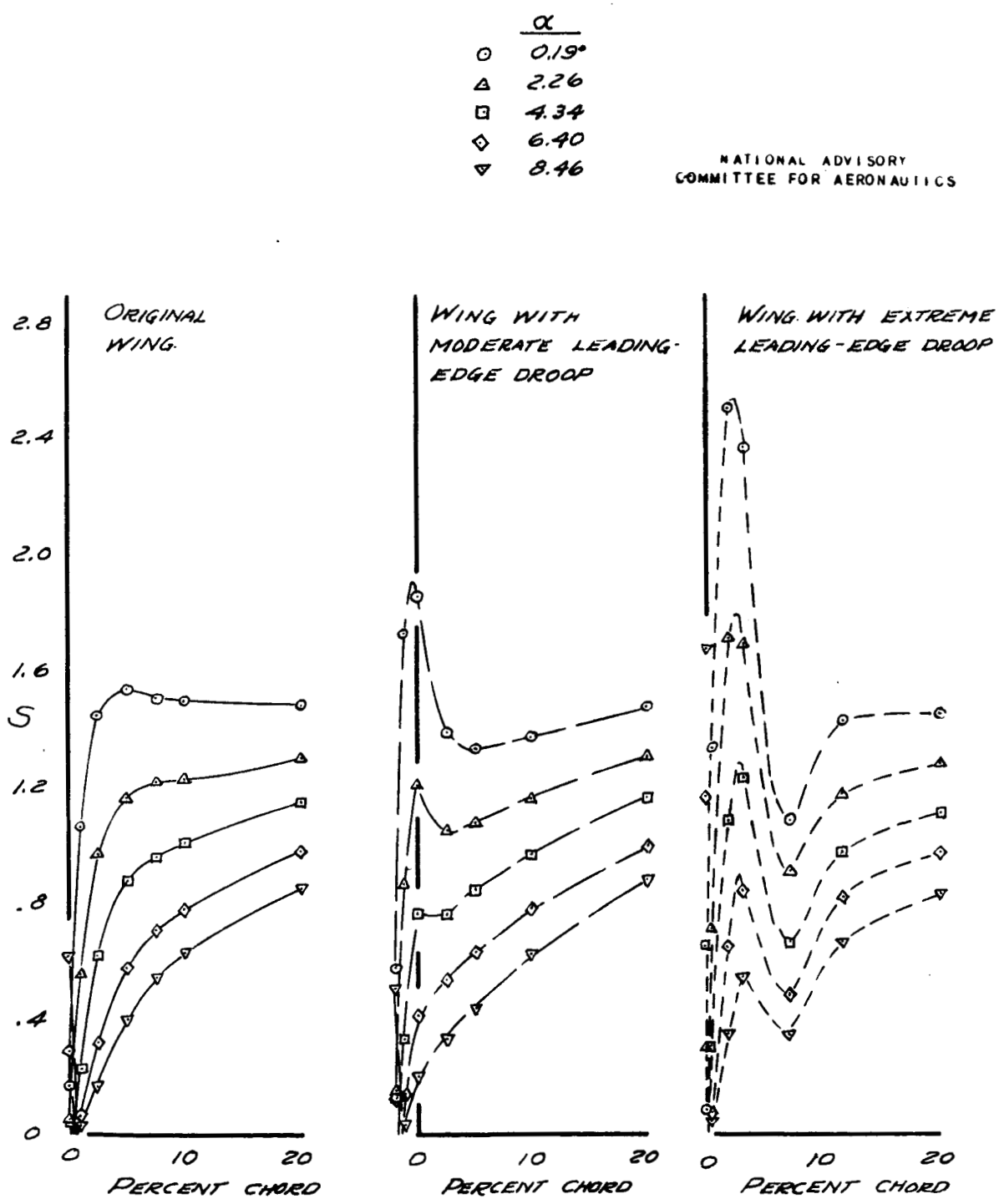

FIGURE 50.- EFFECT OF LEADING-EDGE MODIFICATIONS ON PRESSURE DISTRIBUTION ON LOWER SURFACE. WING STATION 35.638, M = 0.40

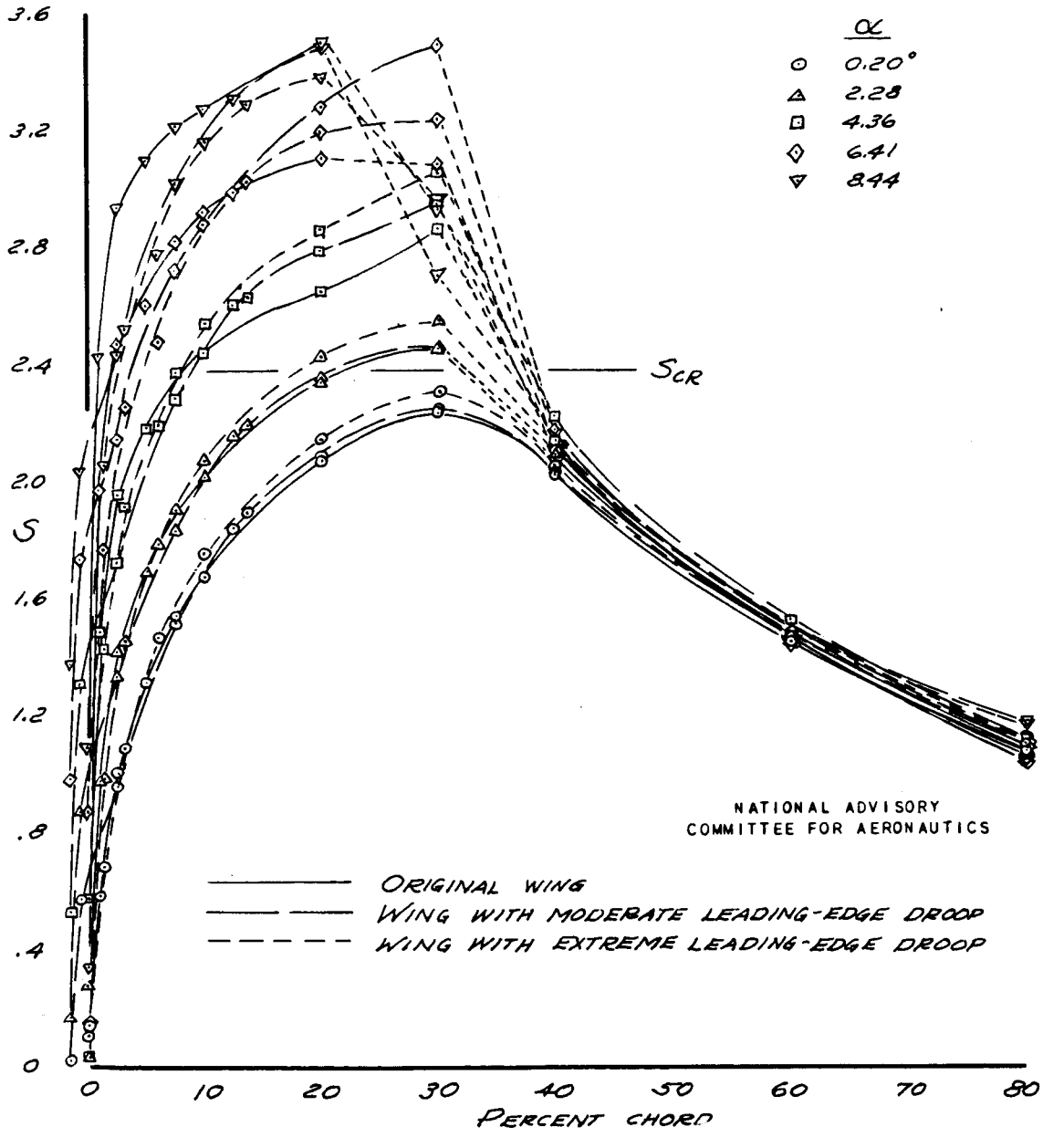

FIGURE 51.- EFFECT OF LEADING-EDGE MODIFICATIONS ON PRESSURE DISTRIBUTION ON UPPER SURFACE. WING STATION 35.638, $M = 0.60$.

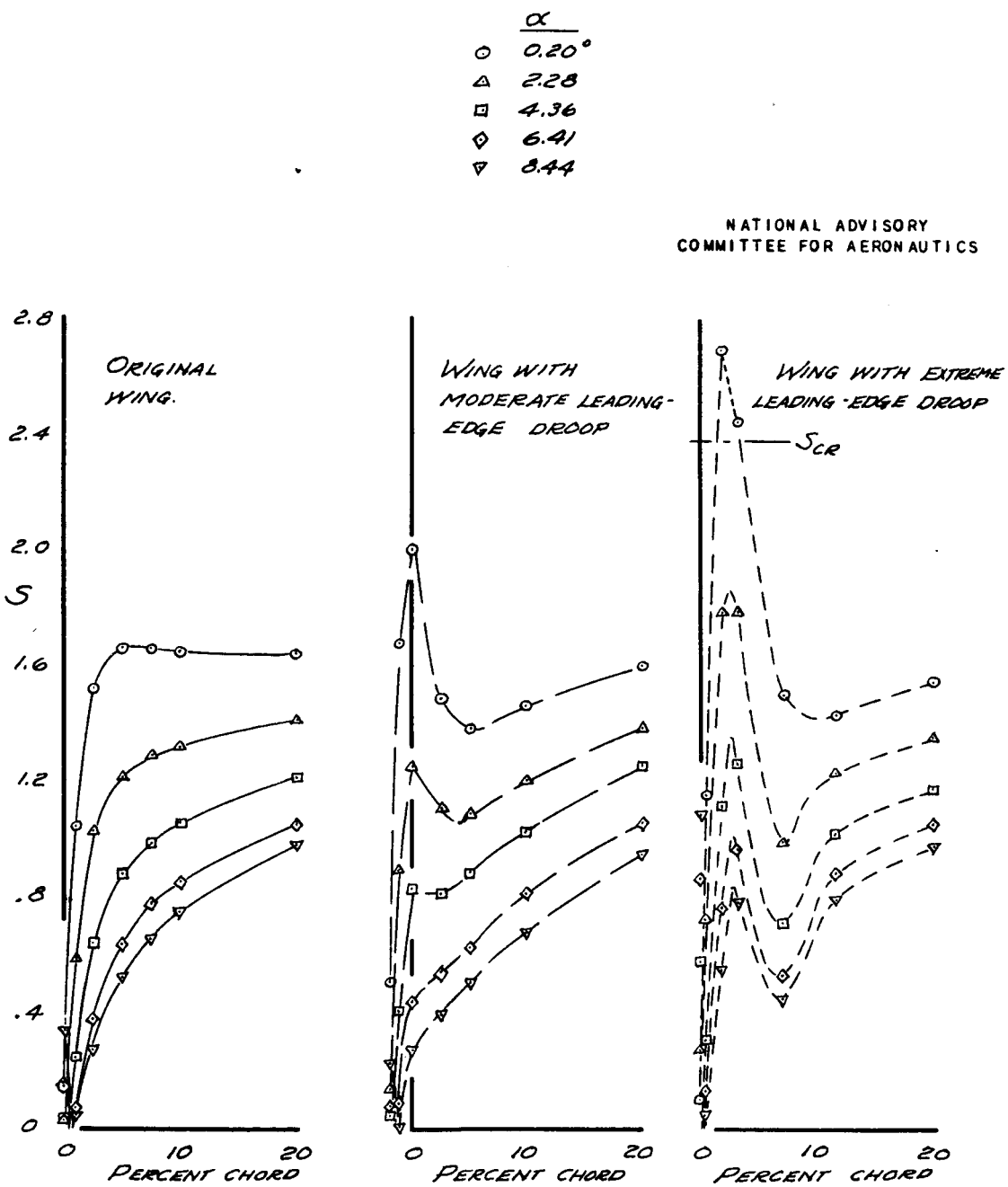

FIGURE 52.- EFFECT OF LEADING-EDGE MODIFICATIONS ON PRESSURE DISTRIBUTION ON LOWER SURFACE. WING STATION 35.638, M = 0.60.

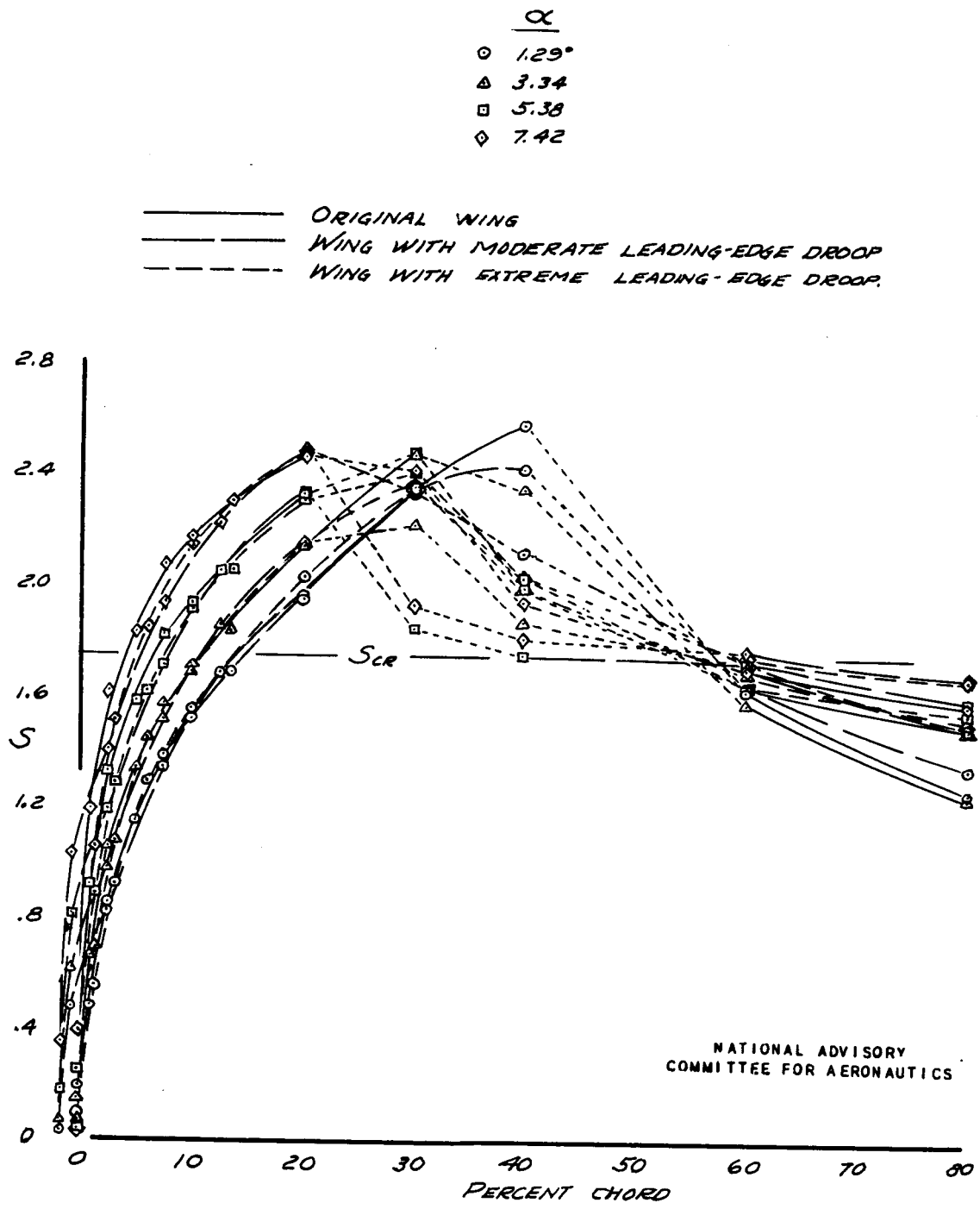

FIGURE 53. - EFFECT OF LEADING-EDGE MODIFICATIONS ON PRESSURE DISTRIBUTION ON UPPER SURFACE. WING STATION 35.638, $M = 0.75$.

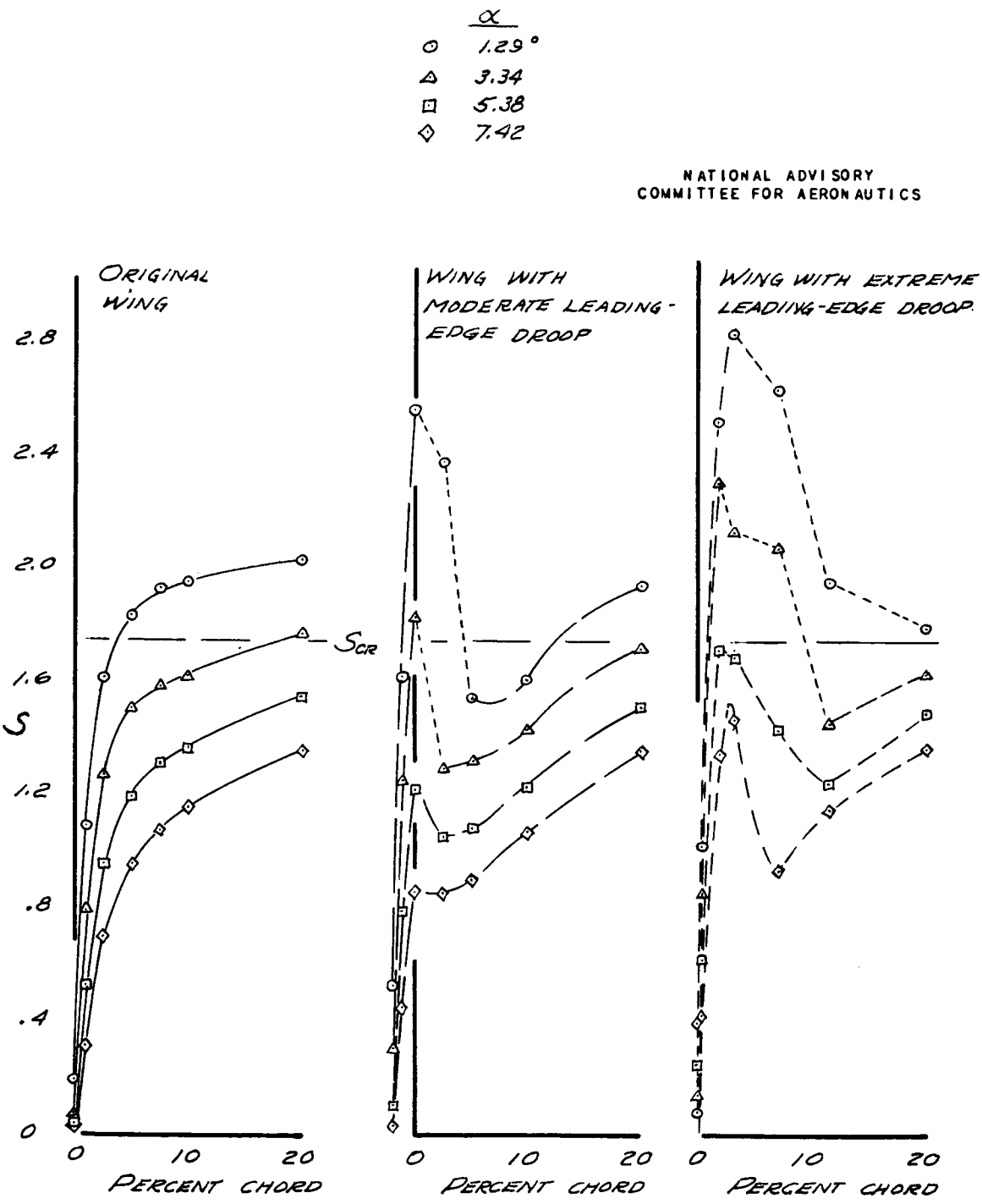

FIGURE 54. - EFFECT OF LEADING-EDGE MODIFICATIONS ON PRESSURE DISTRIBUTION ON LOWER SURFACE. WING STATION 35.638, M = 0.75.